Title
COMPRESSION IGNITION OF COAL SLURRY FUELS

Author
Brehob, D.D.

Publication Date
1985-11-01

Lawrence Berkeley Laboratory
UNIVERSITY OF CALIFORNIA

APPLIED SCIENCE DIVISION

COMPRESSION IGNITION OF COAL SLURRY FUELS

D.D. Brehob
(Ph.D. Thesis)

November 1985

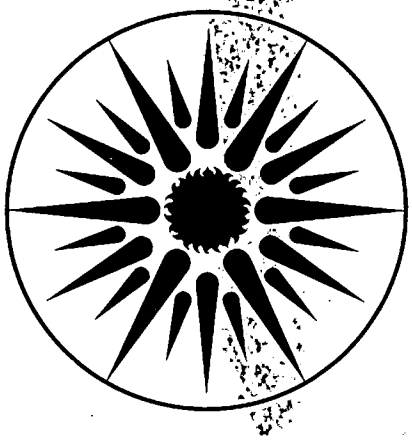

APPLIED SCIENCE
DIVISION

Prepared for the U.S. Department of Energy under Contract DE-AC03-76SF00098

DISCLAIMER

LBL-20710

COMPRESSION IGNITION OF COAL SLURRY FUELS*

Diana D. Brehob

Ph.D. Thesis

Lawrence Berkeley Laboratory
University of California
Berkeley, California 94720

November 1985

*This work was supported by the Assistant Secretary for Energy Technology, Heat Engines Section, U.S. Department of Energy under Contract Number DE-AC03-76SF00098.

TABLE OF CONTENTS

NOMENCLATURE

a	area, m^2.
A	pre-exponential factor, msec-$atm^{1.5}$.
ATDC	after top dead center.
BDC	bottom dead center.
C	specific heat of thermocouple bead, J/kg-K.
CAD	crank angle degree.
C_D	discharge coefficient.
CR	compression ratio.
C_p	specific heat of air at constant pressure, J/kg-K.
C_v	specific heat of air at constant volume, J/kg-K.
C_1-C_6	constants in polynomial fit for C_p.
D	cylinder diameter, mm.
E_a	activation energy, kJ/kg.
EVO	exhaust valve opening.
h	convective heat transfer coefficient, W/m^2-K.
H_R	enthalpy of reaction, MJ/kg.
ID	ignition delay, msec.
IL	integrated needle lift, mm-msec.
IVC	intake valve closing.
k	thermal conductivity, W/m-K.
K	adjustable leak rate coefficient.
L	connecting rod length, mm.
m	mass, gm.

M	measured static leak rate, gm/atm-sec.
Nu	Nusselt number.
P	pressure, atm.
Pr	Prandtl number.
Q	heat transferred, J.
r_c	crank radius, mm.
R	gas constant for air (universal gas constant divided by the molecular weight of air), J/kg-K.
$\overline{R}$	universal gas constant, J/kgmole-K.
t	time, sec.
T	temperature, K.
T_a	activation temperature, K.
U	internal energy, J.
V	volume in combustion chamber, m^3.
v_p	average piston velocity, m/sec.
W	work, J.
y	distance between head and piston top, mm.
γ	ratio of specific heats.
η	efficiency.
μ	dynamic viscosity, kg/m-sec.
ρ	density, kg/m^3.
τ	time constant, sec.
θ	crank angle rotation, deg.

Subscripts and Superscripts

c	combustion.
cr	crevice.
f	of fuel.
g	in gas.
n	(superscript) constant in ignition delay equation.
n	(subscript) nth calculation step.
t	at thermocouple.
w	at wall.
$'$	effect of heat transfer included.
$''$	effects of leakage and heat transfer included.

COMPRESSION IGNITION OF COAL SLURRY FUELS

Diana D. Brehob

ABSTRACT

About half the oil consumed in the United States must be imported. From an economic and national security viewpoint, it is desirable to replace petroleum usage with domestically available energy sources such as coal. Slow and medium speed compression ignition engines are devices with the potential for conversion to coal fueling. Severe injection, safety, and handling problems arise with coal dust. Consequently, recent work focusses on coal slurried in a liquid carrier. Engine studies on coal slurry to date have investigated the slurries' wear, thermal efficiency, and injection performance. Previously lacking information on the compression ignition characteristics of coal slurries, specifically, the ignition delay times and conditions for ignition of 45 mass % coal in methanol, oil, and water are compared to methanol and diesel No. 2.

The slurries are evaluated using a 900 rpm, direct injection, square piston engine simulator operating for one combustion cycle per experiment. Both 16:1 and 22:1 compression ratios are used with inlet air temperatures from ambient to 250 °C and 2 atm abs. supercharge. The square geometry accommodates windows on two opposite walls of the combustion chamber for complete optical access. High speed Schlieren, shadowgraphic, and direct cinematography show the qualitative features of the motoring and combusting cycles.

The pressure and luminosity defined ignition delay times are 0.7 to 10 msec for the conditions of the experiment. All of the test fuels except coal/water slurry ignited at the operating conditions attainable in the engine simulator. The temperature at time of injection required to obtain ignition is approximately 680 K for diesel No. 2 and coal/diesel slurry, 725 K for coal/methanol slurry, and 825 K for neat methanol. Activation temperature, $E_a/\bar{R}$, in the Arrhenius type expression relating temperature, pressure, and delay time, is found for the test fuels: 5559 K for diesel No. 2, 7685 K for methanol, 3541 K for coal/diesel, and 5330 K for coal/methanol by the pressure delay method and 4357 K for diesel No. 2, 3926 K for coal/diesel, and 5510 K for coal/methanol by the luminosity delay method. Neat methanol combustion emits about five times less radiation than the other fuels making determination of start of combustion by photodetector response unreliable. The results establish the compression ignitability of the coal/methanol and coal/diesel slurry fuels at conditions appropriate to medium speed diesel engines.

1. INTRODUCTION

1.1. PURPOSE

Presently the United States imports 45% of the petroleum products it consumes creating a trade deficit with oil producing nations. Thus, the U.S. economy and national security are highly vulnerable to fuel embargos. If petroleum burning systems could be converted to operate on coal, the situation would be eased. The U.S. energy consumption is about 2.5 X 10^{17} J/day according to Penner and Icerman's (1981) text. The major components of the supply are: oil at 47%, gas at 27%, and coal at 20%. Robben (1983) proposes that it may be technically feasible to burn coal for railroad and domestic marine transportation instead of petroleum products currently used. These consume about 2.7 X 10^{15} J/day, *i.e.*, approximately 1% of the U.S. daily energy consumption or 2% of the petroleum consumption. If a 2% reduction in petroleum usage is achieved, a 4% reduction in imported oil results.

The costs of diesel No. 2 and No. 6 fuels are $10.00 and $7.60, respectively, for 10^9 J compared to $1.70 for 10^9 J of coal according to Liddle, *et al.* (1981). Robben (1985) estimates that a stabilized, benificiated coal/water slurry may cost approximately $4.00 per 10^9 J. If realized, the coal/water slurry gives almost a 2 to 1 economic advantage over No. 6 oil based on fuel costs.

Most of the work on coal fired diesel engines before 1945 was conducted by German industry using coal dust. However since that time, the majority of the coal fueled diesels have used coal slurries: various percentages of coal in oil, water, methanol, ethanol, or mixtures of the liquid carriers. The existing fuel storage and

transportation infrastructure for diesel engines is designed for liquids. Thus, conversion to slurry usage would present fewer difficulties compared to pulverized coal. Other points of comparison outlined in Table 1.1 indicate that slurries give advantages in the areas of fuel handling safety and fuel injection control and reliability with slight cost disadvantages and an ignitability disadvantage for coal/water slurry only. Coal slurried with water, methanol, and oil are the test fuels for this study.

1.2. LITERATURE REVIEW

1.2.1. Coal Burning Compression Ignition Engines

Pre-WW II Work

The concept of a diesel engine which burns liquid and solid fuels was first described by Rudolph Diesel in his 1892 patent of a "self-ignition" internal combustion engine. Soehngen (1976) reports that Diesel quickly discontinued experiments on pulverized coal after finding heavy deposits of unburned coal in his engine after seven minutes of operation. The following account is based on Soehngen's comprehensive summary of available information on coal burning diesel experiments conducted in Germany before 1945.

A one time co-worker of Diesel's, Rudolf Pawlikowski, was instrumental in promoting the idea of a coal fired diesel engine. Pawlikowski's company, the Kosmos Machine Works, worked on coal buring internal combustion engines in 1911 and pronounced the idea ready for commercialization in 1923. Under Pawlikowski's stewardship, progress was made in the areas of fuel feeding and

Table 1.1 General Performance and Economic Comparisons of Three Coal Slurries and Pulverized Coal for Use in Compression Ignition Engines

	Coal/ water	Coal/ methanol	Coal/ diesel	Coal dust
Handling safety	VG	G	G	VP
Ease of transportation	F	F	G	VP
Ignitability	VP	F	G	VP
Low additive cost	F	F	F	G
Low total cost	G	G	G	VG
Ease of injection	P	P	P	VP

Key: VG - very good, G - good, F - fair, P - poor, VP - very poor.

control systems, seals, lubrication, and wear. His original engines used high pressure injection into the cylinder. Later designs employed a prechamber with low pressure fuel injection. Due to the longer residence time of the fuel in the prechamber compared to the direct injection system, the coal/air mixture is more reactive upon introduction into the main combustion chamber. Despite technological advances made by the Kosmos company, operation ended in the late 1930's with only one major sell: Hanomag in Hanover, Germany bought a license in 1934. The Hanomag Co. had a very modest program which met with difficulty providing reliable injection.

The I.G. Farben company worked on coal fired diesel through 1925-29. The Farben Co. concentrated more effort on the wear problem. They instituted several clever lubrication, piston, and piston ring schemes to reduce wear. But, the program was discontinued due to failure to realize the goal of developing an engine which could be readily commercialized and because of impending patent problems with Pawlikowski. The Farben Co. primarily burned lignite coal because of its higher volatility. Unfortunately, several severe accidents occurred in handling the explosive coal dust.

Significant accomplishments in the areas of engine wear and fuel feeding were made by Schichau Werk during the 1930-39 period. Selection of new materials for engine components was important in reducing wear rates by 90% (as claimed by Schichau). Schichau's economic evaluation of the coal-burning engine concluded that further work was not warranted. The program was subsequently terminated.

The highest level of achievement was made by the I. Bruenner Maschinenfabrikes - Ges. from 1930-45. The project was significantly aided by the Technical University at Dresden, Germany. In 1935 Prof. Jehlicka headed the development which was strengthened considerably by fundamental scientific research programs. Ignition, combustion, fluid mechanical, and wear problems were addressed on a more fundamental basis than other programs, i.e., theoretical and experimental work outside the engine were carried out. In cooperation with Schichau Werk, I. Bruenner developed materials which alledgedly gave comparable wear results with oil fired engines. Engine and combustion vessel experiments led to the result that pulverized coal may burn nearly as fast as oil droplets under optimization of combustion chamber geometry, fuel distribution, and turbulence. The project was terminated as a result of the end of World War II.

Both indirect injection and direct injection engines were successfully operated on coal dust. In addition to these accomplishments, fuel property requirements were defined:

- Ash number must be less than 140 to prevent abrasive and erosive wear from engine components. (The ash number is defined as gm ash per 10,000 kcal.)
- Coal particle size must be less than 75 μm mean diameter to keep burn out time reasonable.
- Moisture content must be kept low to prevent agglomeration in transport and in the fuel system.
- The softening temperature must be greater than 200 °C. Otherwise, softened coal tends to stick to engine components causing malfunctions.

- The volatility of the coal must be in a moderate range. High volatility is desirable for improving the coal's ignition characteristics and low volatility for preventing unwanted combustion in fuel handling.

The German's did not realize their goal of developing a commercial engine to operate on coal dust due to the remaining problems of engine wear, fuel induction, and engine speed control. However, new materials were developed which significantly reduced wear rates and patents were awarded for improved control over the fuel injection. Many hours of engine operation on coal dust were logged providing information on thermal efficiency and approximate engine conditions for coal dust combustion. In addition, fuel property requirements were specified.

Post-WW II Work

Many researchers have investigated using coal to fuel compression ignition engines since World War II. The majority of the fuels tested were coal slurries instead of the coal dust used by the German researchers. The advantages of slurries over neat coal is discussed in Section 1.1. A summary of these studies, partially taken from Tables 2 and 3 in Caton and Rosegay's (1983) review paper, is given in Table 1.2. The engine tests outlined in the table provide valuable information concerning engine modifications to enhance slurry combustion and engine and injection performance with slurries. However, more fundamental combustion information is contained in the work by Siebers and Dyer (1985) in a constant volume bomb. The pressures and temperatures necessary to simulate diesel engine conditions are achieved by inducting and burning a lean, premixed charge of H_2, O_2, and N_2 which is O_2 enriched. The fuel is injected into the hot combustion products. The 50 mass % coal in water slurry evaluated by Siebers

Table 1.2 Summary of Work on Coal Fired Diesel Engines from 1945 to Present

Investigators	Engine and Fuel	Conclusions
Hanse (1949) Univ. of North Carolina	4 cyl., 4 stroke, IDI, 800 cc, 1200 rpm Injection: Mechanical Fuel: 20% coal slurried in diesel oil Coal size: < 75 μm	Fuel injection operation was not reliable, injector nozzles seized; engine performance was erratic; engine efficiency continually decreased during slurry operation.
Tracy (1957) Southwest Research Institute	1 cyl., 4 stroke, DI, 3400 cc, 1000 rpm Injection: Mechanical Fuel: 30% coal in oil Coal size: > 20 μm	Fuel injection equipment repeatedly failed; severe engine wear; engine efficiency continually decreased during slurry operation.
Marshall and Selton (1959) Virginia Polytechnic Institute	1 cyl., 4 stroke, IDI, 1400 cc, 1750 rpm Injection: Diesel fuel injection plus coal dust induction Coal size: > 45 μm	Severe engine wear during 45 hr. test; exhaust valve seizures; engine oil became contaminated; engine efficiency decreased from 18 to 13%.
Rich and Walker (1969) Howard University	1 cyl, 4 stroke, IDI, 1400 cc, 1000 rpm Injection: Diesel fuel injection plus coal dust induction Coal size: < 75 μm	Engine operation for 100 hrs with three overhauls; severe engine oil contamination (even though oil capacity and filtration were increased); engine efficiency down to 11% from 27%.
Marshall and Walters (1977) Virginia Polytechnic Institute	1 cyl., 4 stroke, IDI, 1400 cc, 1000-1800 rpm Injection: Mechanical Fuel: 15% Solvent Refined Coal in diesel Coal size: 2 μm	Fuel injection equipment frequently seized; engine efficiency decreased from 21% to 17%; conventional fuel injection systems incompatible with slurry fuels.
Tataiah and Lestz (1979) Southwest Research Institute	1 cyl., 4 stroke, IDI, 600 cc, 1200-2400 rpm Injection: Mechanical Fuel: 10 and 20% coal in oil slurry Coal size: > 10 μm, 2 μm mean.	Engine and fuel injection system wear; reduced engine efficiency; increased emissions.

Table 1.2 (continued)

Investigators	Engine and Fuel	Conclusions
Tataiah and Wood (1980) Southwest Research Institute	4 cyl., 4 stroke, DI, 3800 cc, 1000 rpm Injection: Mechanical Fuel: up to 40% coal in diesel fuel Coal size: >10 μm, 2 μm mean.	Significant ring wear during 11 hrs of operation; engine efficiency decreased as percent coal increased; fuel injection was unreliable.
Dunlay, *et al.* (1980) Thermo Electron Corp. and Sulzer Bros., Ltd. Winterthur, Swit.	1 cyl., 4 stroke, DI, 703000 cc, 120 rpm Injection: Accumulator system for slurry compatibility Fuel: 31.6% coal in oil Coal size: < 10 μm, 2μm mean.	Conventional, unmodified, injection nozzle frequently failed; thermal efficiency decreased during 20 hrs of operation due to ring wear; brake thermal efficiency near 39%
Marshall, *et al.* (1981) Virginia Polytechnic Institute	1 cyl., 4 stroke, IDI, 1400 cc, 1400 rpm Injection: Mechanical Fuel: up to 40% coal in diesel fuel Coal size: 2-11 μm mean	Only 32 to 88% of diesel fuel performance was obtained; rapid piston ring wear; higher emissions; apparently no coal was burned.
Clingenpeel, *et al.* (1984) National Institute for Petroleum Research	1 cyl., 4 stroke, IDI, 2000 cc, 750-1200 rpm Injection: Mechanical Fuel: 45% coal slurried with oil, methanol, and water Coal size: 5 μm mean	Ignition assist (glowplug or pilot injection) required for low cetane carriers; thermal efficiency reduced by about 11% over diesel fuel; wear was 100 times higher with slurries than with diesel fuel.
Nelson, *et al.* (1984) Energy and Environmental Research Corp.	1 cyl., 4 stroke, DI, 2330 cc, 300-1200 rpm Injection: Mechanical and air blast atomizer Fuels: Coal/oil, coal/ methanol, coal/water, coal/methanol/water Coal size: , 20 μm, 5 μm mean.	No coal/water results because of injection problems; combustion efficiency drops off at speeds above 800 rpm; engine unstable on slurries; slurry atomization poor, improved with air blast atomizer.

Abbreviations: DI-direct injection, IDI-indirect injection.

and Dyer is identical to the slurry used in the present work. They conclude that the ignition delay is approximately five times longer for coal water slurry than diesel fuel. (This is the pressure recovery delay which is defined in Section 1.2.2.) Also, the minimum temperatures for significant coal slurry combustion is approximately 800 K. In addition, they report that the ignition delay time has Arrhenius type behavior as a function of temperature as well as inverse proportionality to pressure.

1.2.2. Fuel Performance Analyses in Compression Ignition Engines

Ignition Delay

A suitable fuel for diesel engines is one with a short autoignition delay under compression ignition conditions. Ignition delay is the time between fuel delivery into the combustion chamber and the start of combustion. (Definition for start of combustion and injection are discussed below.) Starkman (1946) postulates that the delay period is comprised of overlapping physical and chemical periods: vaporization and mixing for the physical delay and initiation reactions building a radical pool for the chemical delay. During the delay interval, the fuel becomes "prepared" for combustion, *i.e.*, vaporizes and comes in contact with sufficient air to be flammable, as discussed by Lyn (1969-70). At the onset of ignition the premixed fuel burns rapidly. If the ignition delay is too long, a large portion of the fuel is prepared for combustion before ignition and the pressure rise associated with the premixed combustion is excessive resulting in uncontrolled combustion and diesel knock. High cylinder pressures subject engine components to high stresses which is undesirable from an engine designer's point of view.

Due to the higher viscosity of coal slurries, the droplet size distribution issuing from the fuel injector nozzle is larger than for the liquid component alone. Nelson, *et al.* (1985) verify that coal/water slurry droplet sizes are larger than diesel fuel as measured by a Malvern laser diffraction analyzer at atmospheric pressure. Figs. 15 and 16 from their paper are replotted in Fig. 1.1. The droplet distributions are vastly different as 90% of the mass of diesel droplets are contained in droplets less than 100 μm. But, less than 20 mass % of the coal/water slurry spray is composed of drops less than 100 μm. Nelson and coworkers also report on high resolution shadowgraphs of diesel and coal/diesel fuels. The maximum droplets observed in the developed region of the spray are approximately 650 μm and 250 μm for coal/oil slurry and neat diesel fuel, respectively. Larger drop size distributions prolong the physical delay period. Nelson, *et al.* (1984) report that the ignition delay times for coal/oil and coal/methanol slurries are acceptably short, 0.5-2.0 msec. However, no information is provided comparing slurries to the neat fuels or on air temperatures in the engine. The slurry fuels may exhibit longer ignition delays than their corresponding reference fuels without coal due to the longer physical delays.

The ignition delay interval is dependent on many variables: air temperature, air pressure, turbulence levels, and fuel injection parameters such as spray formation, jet breakup, and impingement on combustion chamber surfaces, to name a few. For a given fuel, Lyn and Valdamis (1966-67) report that temperature is the dominant factor with pressure also playing a role. Henein and Bolt (1967) summarize the functional relationships historically used to relate ignition delay to

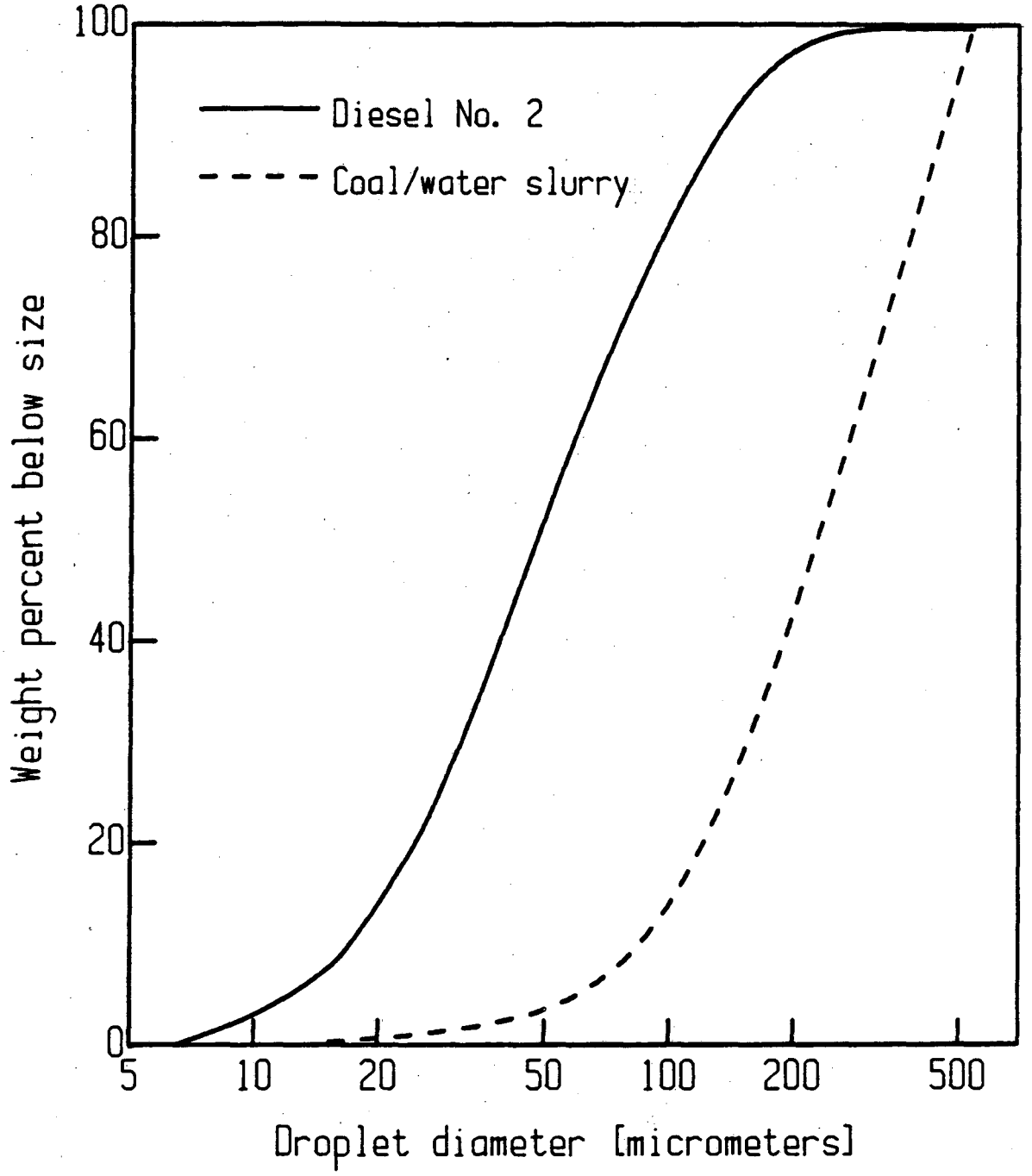

Figure 1.1. Fuel droplet size distributions for diesel No. 2 and coal/water slurry as reported by Nelson, *et al.* (1985).

pressure, temperature, and engine rpm. (Engine rpm is used in the correlation of Tsao, *et al.* (1962) only.) An Arrhenius type expression is the most widely used:

$$ID = \frac{A}{P^n} \exp(\frac{E_a}{\overline{R}T})$$

where ID is the ignition delay in msec, A the pre-exponential factor in msec-atm^n, P the pressure in atm, E_a the activation energy in J/kg, $\overline{R}$ the universal gas constant in J/kgmole-K, and T the temperature in K. The term activation energy strictly corresponds to an elementary reaction. For this system, the Arrhenius type expression is used to describe an extremely complex set of reactions. To emphasize the empirical nature of the activation energy concept applied to compression ignition of high molecular weight fuels, Parker, *et al.* (1985) define $E_a/\overline{R}$ as an activation temperature. From constant volume bomb studies with induced turbulence, Wolfer (1938) in an early study proposed the following constants for diesel fuel:

$$ID = \frac{0.44}{P^{1.19}} \exp(\frac{4650}{T}) .$$

The value of the constant, n is not believed to be a fuel dependent parameter. There is, however, considerable disagreement concerning the value of n:

Reference	System	n
Wolfer (1938)	Heated constant volume bomb	1.19
Mullins (1953)	Flow reactor	1.0
Henein and Bolt (1969)	Indirect injection engine	1.46-1.78
Kuniyoshi, *et al.* (1980)	Heated constant volume bomb	0-1
Spadaccini and TeVelde (1982)	Flow reactor	2.0
Parker, *et al.* (1985)	Heated constant volume bomb	0

Kuniyoshi, *et al.* report that n is 0 for pressures above 40 atm. Also, they find that n is 0.62 for pressure delay and about one for luminosity delay. Henein and Bolt report that n increases with increasing turbulence levels, *i.e.*, engine rpm. Thus, they found n is 1.46 at 600 rpm and 1.78 at 1000 rpm. For this work at 900 rpm with relatively low turbulence levels, n of 1.5 is assumed:

$$ID = \frac{A}{P^{1.5}} \exp(\frac{T_a}{T}) \, . \tag{1.1}$$

The ignition delay characteristics of the fuels, described by A and T_a are found for the coal slurry fuels in this study. Also, the values for the reference fuels are compared to published results.

Two definitions are used for the beginning of injection: needle lift and optical determination of fuel injection into the engine. The latter method requires optical access perpendicular to the fuel jet at the injector orifice. A parallel light beam

aimed across the orifice outlet to a photodetector is broken during injection. This technique provides a more direct measure than needle lift of fuel flow into the engine. However, because of experimental complications, most researchers define start of injection as the time when the injector needle leaves the seat. The needle lift technique is also used in this study.

The start of combustion (end of ignition delay interval) is defined in a number of ways:

- pressure recovery delay--point in the cycle where the pressure history with combustion recovers to noncombustion pressure history after reduced pressure from enthalpy absorption of fuel.
- pressure delay--the point in the combusting cycle where the slope of the pressure-time curve exceeds that of a corresponding noncombusting case.
- illumination delay--significant light emission is detected by a photodetector
- temperature delay--temperature rise due to combustion is measurable
- fuel consumption delay--a small percentage of the energy content of the injected fuel is released.

The pressure recovery delay is primarily used in constant volume studies, *eg.*, Siebers and Dyer (1985). The start of combustion is rarely defined by the temperature delay due to the experimental difficulties in accurately measuring highly transient temperatures in the range encountered in firing engines. For the purposes of this work, both the illumination and pressure delays are measured.

The final measurements necessary for insertion into the ignition delay relation are the air temperature and pressure. (The measurement techniques employed are

discussed in Chapters 2 and 3.) The temperature and pressure change significantly throughout the delay interval. Tsao and coworkers (1962) use the temperature and pressure at the time of first injection; whereas, Henein and Bolt (1967, 1969) use the mean temperature and pressure during the delay period. Using a linear formula to compute mean quantities is only an approximation to the true case which has nonlinear dependencies:

$$\ln (ID) \sim 1/T \quad \text{and} \quad \ln (ID) \sim -n \ln (P).$$

Tsao, *et al.* (1962) argue that temperature measurements during the delay interval are of questionable accuracy. In addition, the temperature is nonuniform due to the latent enthalpy of vaporization of the fuel causing temperature decreases in the fuel cloud. Thus, an average bulk gas temperature may not accurately describe the temperature at the ignition sites in the fuel cloud. In the present work, the injection timing is held nearly constant for the majority of the tests. Therefore, for experiments with different inlet temperatures, the temperature histories during the delay interval are nearly parallel, but offset. Computing an average value for the quantities is more important under a wide variety of injection timings: fuel injected very early experiences rapid heating; whereas, the temperature profile is nearly flat or decreasing slightly for late fuel injection (near TDC). The ignition delay is less sensitive to the pressure than to the temperature. The additional accuracy obtained by computing an average pressure throughout the delay period is unwarranted because it is a second order effect. The temperature and pressure at the start of injection is the quantity inserted into the Arrhenius type relation in the present work.

Combustion Performance

The pressure-volume indicator diagram is a useful tool to compare engine operating variables such as fuel type according to Taylor (1977). By integration over the cycle, the work is computed:

$$W = \int P dV .$$

The thermal efficiency, η, is evaluated from the work, W, the mass of fuel injected, m_f, and H_R, the enthalpy of reaction of the fuel:

$$\eta = \frac{W}{m_f H_R} .$$

Thermal efficiency is an important engine performance criterion as it relates to the economics of operating an engine. The majority of the investigators testing coal slurries evaluated thermal efficiency (summarized in Table 1.2).

Information about the combustion progress is obtained via calculation of the energy release rate. It is based on a first law analysis:

$$Q = U + W = mC_vT + PV ,$$

where Q is the energy release during combustion, U is the internal energy of the system, and W is the work performed on the system boundaries. Differentiating with respect to engine rotation, θ:

$$\frac{dQ}{d\theta} = \frac{d}{d\theta} (mC_vT) + P \frac{dV}{d\theta} .$$

Using the ideal gas relation,

$$\frac{dQ}{d\theta} = \frac{C_v}{R}\frac{d(PV)}{d\theta} + \frac{PV}{R}\frac{dC_v}{d\theta} + P\frac{dV}{d\theta} .$$

But, $R = C_p - C_v$ and $\gamma = C_p/C_v$.

$$\frac{dQ}{d\theta} = \left(\frac{\gamma}{\gamma-1}\right) P\frac{dV}{d\theta} + \left(\frac{V}{\gamma-1}\right)\frac{dP}{d\theta} - \frac{PV}{(\gamma-1)^2}\frac{d\gamma}{d\theta} .$$

So, Miyamoto and Muryama (1979) conducted analyses on the sensitivity of the energy release rate on the calculation technique. They argue that $d\gamma/d\theta$ is much smaller than $dP/d\theta$ or $dV/d\theta$ and can be neglected. Also, the complication introduced by computing the time varying value of γ is not warranted because of the small error from using an average value for k. Using γ equal to 1.32:

$$\frac{dQ}{d\theta} = 4.13\ P\frac{dV}{d\theta} + 3.13\ V\frac{dP}{d\theta} .$$

By integrating $dQ/d\theta$, the total energy released over the cycle is computed.

For combustion of low quality fuels such as coal slurries, combustion efficiency is a measure of the fraction of the chemical energy input of fuel consumed. Combustion efficiency, η_c, is defined as the energy released, Q, divided by the fuel enthalpy injected:

$$\eta_c = \frac{Q}{m_f H_R} .$$

From the combustion efficiency, the percentage of coal burned in the slurry fuels is estimated.

1.3. OBJECTIVES

Most of the engine researchers burning coal report experiences with engine and fuel injection equipment wear problems. It is not, however, in the scope of this work to cover the wear characteristics of the coal slurries. In addition to the wear difficulties, reduced thermal efficiencies and unreliable ignition are reported. Detailed information about the combustion characteristics of coal slurries in diesel engines is not available currently. Therefore, it is the objective of this study to provide the following information on the test fuels:

- qualitative analysis of combustion by high speed cinematography.
- igniton delay characteristics of the three coal slurries tested.
- engine conditions required for slurry combustion.

These measurements are used to evaluate slurry performance compared to diesel No. 2 as the reference fuel. Also, the coal slurry ignition data are compared with measurements made in a constant volume bomb.

2. EXPERIMENTAL APPARATUS AND TECHNIQUE

2.1. ENGINE TEST FACILITY

2.1.1. History and Purpose

Direct photographs of the combustion radiation have been taken in conventional engines fitted with quartz windows in the cylinder head starting with Rasweiler and Withrow (1938). The method provides information about the flame location in spark ignition engines and area inflamed and intensity of radiation for compression ignition engines. However, to elucidate the details of the flow and density fields through the engine cycle, the Schlieren technique must be employed. Optical access on opposite sides of the combustion chamber or access on one side with a mirrored opposite surface is required for observation of the Schlieren effect.

Taylor, *et al.* (1950) presented frames from Schlieren movies of a rapid compression machine fitted with a quartz cylinder head (no poppet valves) and a mirror on the piston head. This provides a view parallel to the cylinder axis. Oppenheim, *et al.* (1976) made the first Schlieren high speed movies in a square piston rapid compression and expansion machine with a view perpendicular to the cylinder axis. The piston trajectory, the fluid motion induced by the piston travel, and the density gradients caused by the combustion were filmed using a square engine simulator geometry. These experiments did not, however, simulate the intake and exhaust processes of a conventional engine. Thus, two laboratories have built square piston engines incorporating conventional poppet valves, bore and stroke dimensions, and piston trajectory. Namazian, *et al.* (1980) obtained

Schlieren data from a square piston engine built on top of a CFR (Cooperative Fuel Research) test engine. Edwards, *et al.* (1985) reported on Schlieren motion pictures from a square piston engine built on a CLR (Coordinated Lubrication Research) test engine. The following details about the engine's fluid mechanics are resolved by the Schlieren movies: jet flow through the intake valve, large scale rotation in the cylinder during the intake and compression strokes, flow out of the crevices, and the thermal boundary layer thickness.

2.1.2. Engine Simulator

A single cylinder, CLR engine, commonly used for evaluation of engine lubricants is used as the base for the square piston engine simulator. The CLR's cylinder head is removed and replaced with a square "cylinder" and piston. The square and CLR pistons are attached by an adjustable connecting rod which permits compression ratios of 4.75:1 to 24:1 to be attained. Lateral or thrust forces are absorbed by the CLR piston acting as a crosshead. The cross-sectional area of the two pistons are identical: D = 97 mm for the round piston and L = 86 mm for the square piston.

A square geometry is chosen to provide large flat surfaces for mounting windows for optical access. Two of the "cylinder" walls and the head are made of stainless steel. Quartz windows or aluminum flats (24.9 cm X 8.5 cm X 5.1 cm) are installed in the other two walls depending on the experimental techniques employed. One quartz window and adjacent stainless steel wall are shown in Fig. 2.1.

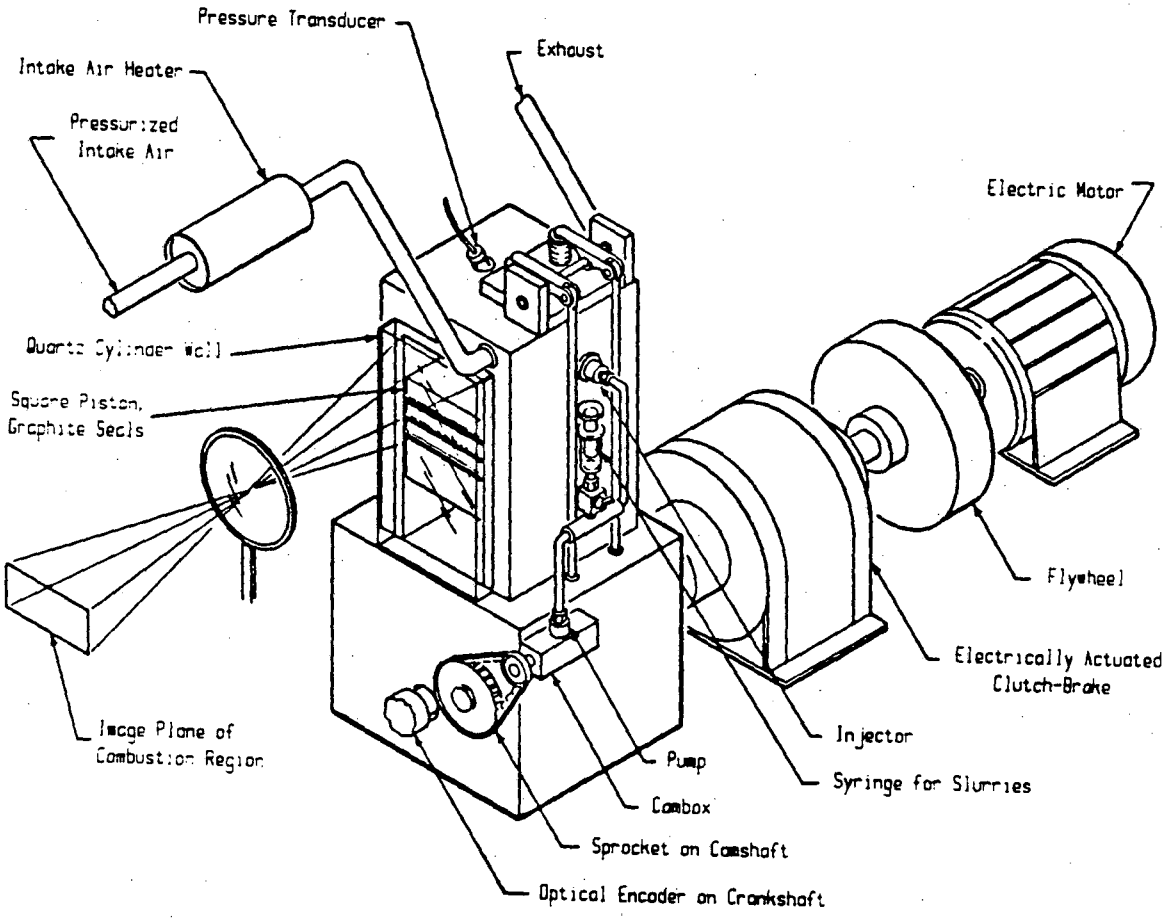

Figure 2.1. Sketch of square piston engine simulator.

The square piston engine simulator is a 4-stroke, direct injection engine scavenged by the CLR inlet and exhaust valves installed in the square head. The valves are opened and closed in the conventional manner: opened by the camshaft on the CLR engine (with extended push rods) and held closed by valve springs.

The square piston design is similar to the piston described by Namazian, *et al.* (1980). A sketch of the piston and sealing rings is shown in Fig. 2.2. Each of the three grooves contain four piston ring sections which overlap in the corners. Copper leaf springs placed behind the piston rings at the back of the grooves force the rings against the cylinder walls.

Both the piston top and cylinder head are flat except for the the valves and pressure transducer located in the head. Therefore, the clearance volume is nearly a parallelpiped, i.e., the piston area times the clearance height. Most of the tests are conducted with a 16:1 compression ratio. With a swept volume of 700 cm^3 and a piston cross-sectional area of 73.3 cm^2, a clearance height of 6.35 mm is required for 16:1 CR. However, the volume between the piston crown land and the cylinder walls is 4.0 cm^3. Since this space must be considered part of the clearance volume, the clearance height to achieve 16:1 compression ratio is 5.80 mm. Other crevices present in the head cannot be measured. So they are disregarded for purposes of setting the compression ratio. The clearance height for 22:1 compression ratio is 4.00 mm. A summary of the salient features of the square piston engine simulator is contained in Table 2.1.

As indicated in Section 1.1, a slow or medium-speed compression ignition engine is preferred over high-speed engines for burning coal fuels because of the

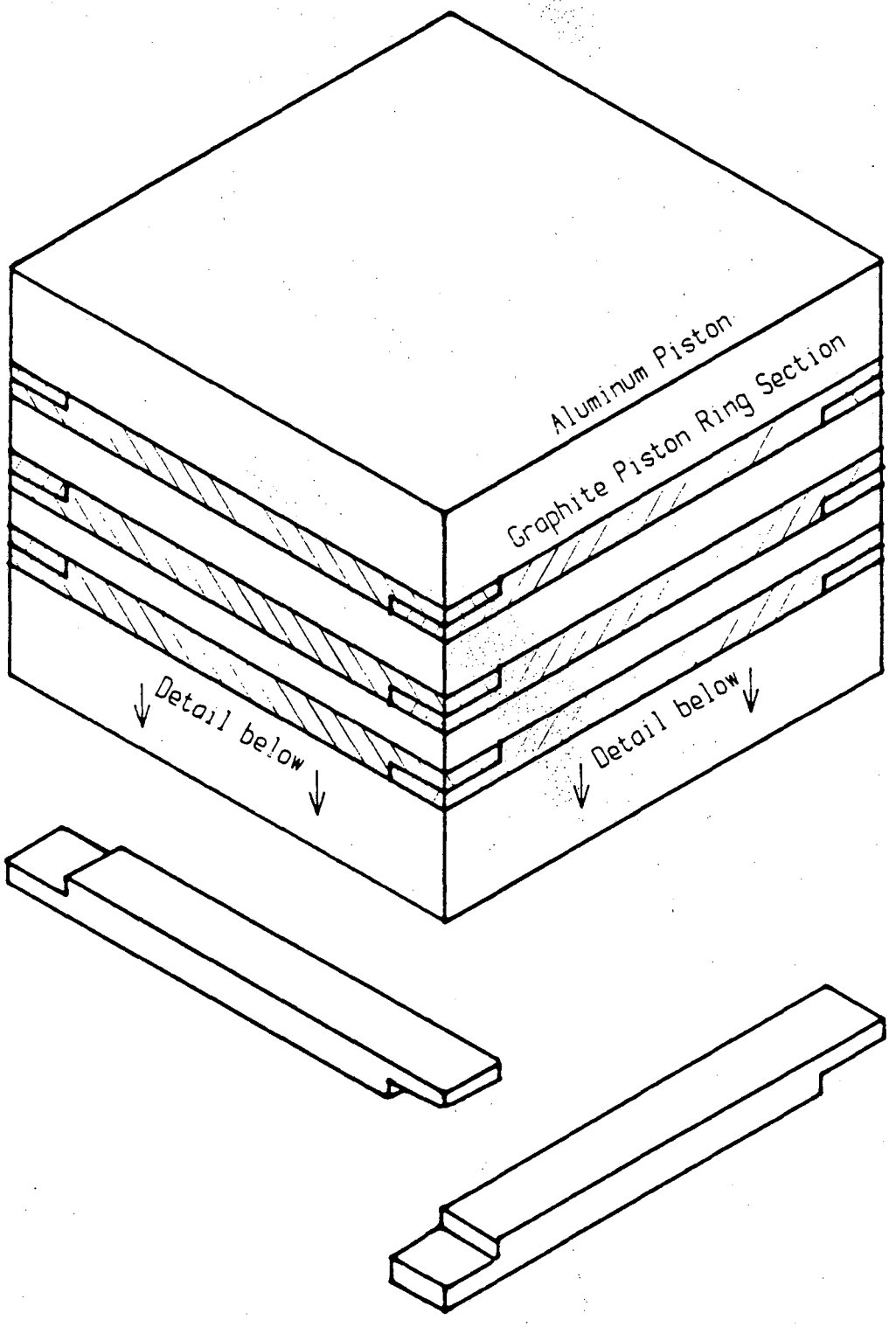

Figure 2.2. Isometric sketch of square piston and graphite ring pack.

Table 2.1 Description of Square Piston Engine Simulator

Single cylinder
Direct injection into parallelpiped shaped combustion chamber
86 mm X 86 mm square cross-section piston
94.5 mm stroke
700 cm^3 displacement
900 rpm
2 atm supercharge
16:1 and 22:1 compression ratio

longer residence time for more complete coal burnout. The vast majority of these engines are supercharged or turbocharged which raises the inlet air pressure and temperature. Thus, the square piston engine facility is equipped with a 12 kW air heater which is connected to compressed air. A pressure of 2 atm abs at the heater is maintained for all the experiments. Air temperatures of ambient to 375 ° C can be delivered to the inlet of the engine. The heater and associated equipment are shown in Fig. 2.3. In most of the experiments the engine block is unheated. Even when the block is preheated (maximum temperature of 150 ° C), the cylinder temperatures are below normal operating temperatures in a conventional engine. Georgi (1950) gives temperature ranges for engine components: 100-375 ° C for the cylinder head and upper portion of the wall and 425-825 ° C for the exhaust valve. The temperature maps for three piston shapes plotted by Roehrle (1978) show maximum piston top temperatures are between 300 and 400 ° C. In this experiment the inlet air is heated to compensate for heat transfer losses to the cold block so that the peak compression temperature is comparable to conventional engines. Two typical values are 850 K reported by Tsao, *et al.* (1962) and 1000 K reported by Lyn and Valdmanis (1966-67).

Each experiment consists of approximately ten revolutions with data collected during two revolutions (one firing event). The synchronous electric motor shown in Fig. 2.1 rotates at 1800 rpm. For the purposes of simulating slower speed diesel engines, a speed of 900 rpm is chosen. The electric motor is turned off after the flywheel and motor are rotating at 1800 rpm. The flywheel and motor speed reduces to 1200 rpm within one minute. The clutch is rapidly engaged bringing the

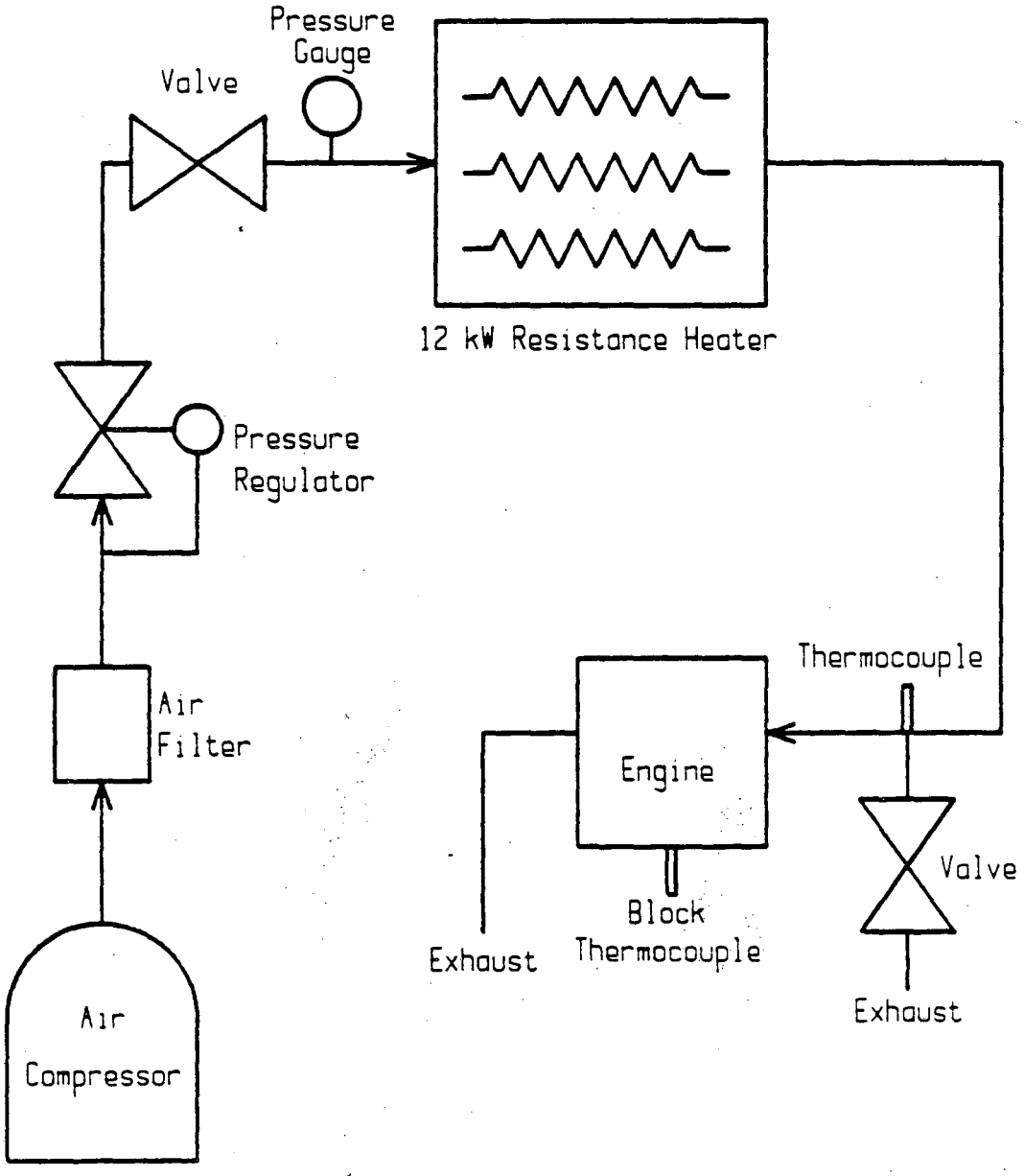

Figure 2.3. Schematic diagram of square piston engine air supply providing pressurized and heated inlet air to engine.

engine to 900 rpm within one revolution. After approximately 0.7 sec the clutch is disengaged and the brake is applied.

2.1.3. Data Acquisition and Control

A schematic of the engine simulator control electronics is shown in Fig. 2.4. Two time bases are used to manage the engine facility: real time and engine time or CAD. Real time events are controlled by a programmable 6 channel Xanadu UP-Timer (model M78-100) containing reed relays. The engine is equipped with an optical shaft encoder which gives two signals: one at every TDC crossing and one at each one-half CAD. Data collection of other events are clocked based on engine time using a digital counter.

The data are collected via a LSI-11 microcomputer. The LSI-11 and interfacing electronics are shown in Fig. 2.5. The measuring equipment and the computer communicate via a Data Translation DT2872 direct memory access analog-digital (A/D) board, a Digital Equipment Corporation (DEC) KWV-11C clock board, and a DEC DRV-11 parallel port.

Before data taking commences, the computer measures flywheel speed and reports it to the user via the terminal. An inductive pickup is situated slightly above a hole in the flywheel surface. The proximity of the pickup is adjusted to give a maximum signal of 5 volts at 1800 rpm. (As the flywheel slows the pickup's signal strength is reduced.) The raw signal from the pickup is nearly symmetrical with positive and negative going spikes. The flywheel pulses are detected by the parallel input port. Because the parallel port requires signals in the 0 to +5 volt range, the signal's negative spike is clipped by placing a diode in parallel with the

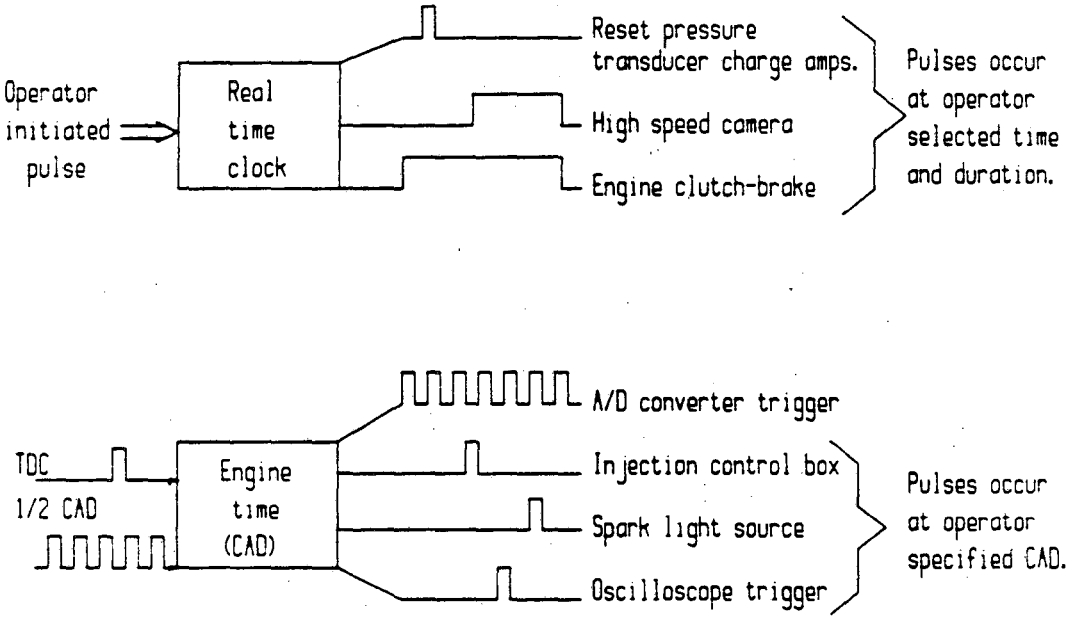

Figure 2.4. Diagram of two timers used for data taking and engine control of square piston engine test facility.

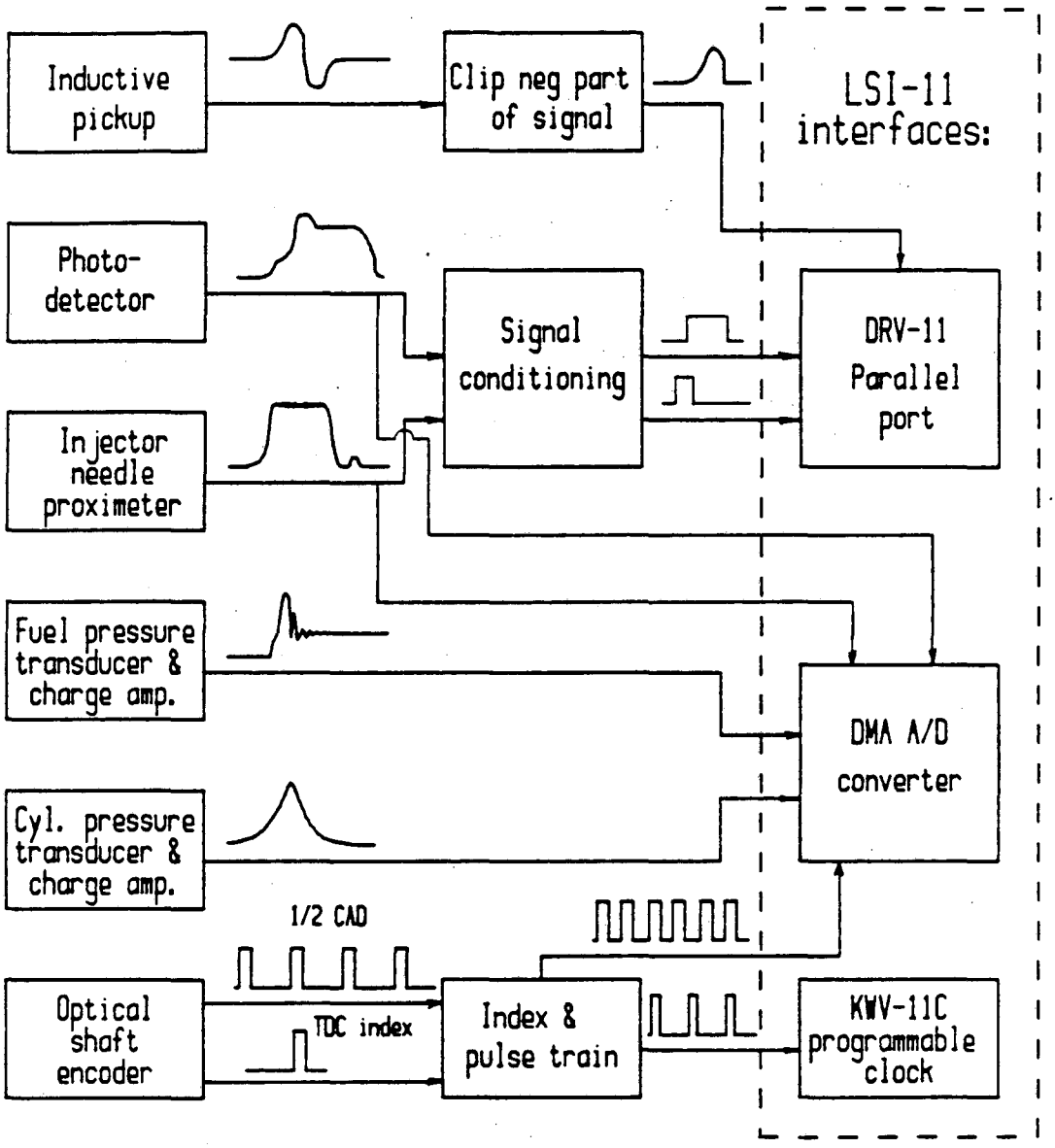

Figure 2.5. Diagram of LSI-11 microcomputer and the interfacing to the square piston engine simulator data taking electronics.

parallel port. Flywheel rpm is computed from the number of clock ticks counted (10 kHz clock rate) between the one flywheel pulse per revolution coming in to the parallel port. When the desired speed is reached (1200 rpm flywheel speed to give 900 rpm engine speed), the operator initiates the data taking by starting the UP timer program.

The digital counter (designated index and pulse train in Fig. 2.5) has two functions. First, the number of TDC crossings is counted. Data collection does not begin until TDC has been reached a preselected number of times. At TDC of the desired revolution, the counter enables the A/D clock, *i.e.*, the one-half CAD pulses from the shaft encoder are sent to the A/D clock. If the A/D clock on the counter is connected to the A/D board RTC trigger, each one-half CAD triggers an A/D conversion. Switches inside the counter allow for one, two, three, or four pulses per one-half CAD to be sent. This is useful for multichannel data collection. Secondly, a LED counter on the front panel of the counter unit displays the number of CAD elapsed from the occurrence of TDC of the revolution set point. Four independently adjustable trigger outputs rise from ground to 5 volts at the selected CAD. The output stays at 5 volts until manually reset.

An 8 channel, direct memory access A/D convertor is operated in the autoincrement mode, *i.e.*, sampling channels 0 through 7 in order, wrapping from 7 to 0, and repeating. For two channel operation, the output from the cylinder pressure charge amplifier is connected to channels 0, 2, 4, and 6 and the differential amplifier output from the cylinder thermocouple to odd channels. Similarily, cylinder pressure, injection line pressure, injector needle lift, and combustion

luminosity are connected to every fourth channel for four channel operation. Data is collected on four channels at one sample per CAD on each channel or on two channels at one-half CAD intervals. The subroutines in the four channel program are:

m2ch4.c	-send operation to subroutines.
mkst4.c	-set or change input parameters such as data file name calibration factors of transducers, etc.
input.c	-routine for inputting data into mkst4.c.
fwrpm.mac	-assembly language routine for measuring the flywheel rpm.
ad2ch4.mac	-assembly language routine overseeing A/D conversions.
draw4.c	-plot the data on the screen for viewing.
bxtik4.c	-draw box and ticks.
wr4.c	-write data to a file.

A listing of the subroutines is contained in Appendix A.

The cylinder pressure is measured using an AVL piezoelectric pressure transducer (model 12QP505clk) installed in the spark plug hole in the cylinder head. A Kistler 5004 charge amplifier is used to increase the signal to the 0 to 5 volt range for maximum sensitivity of the A/D converter.

Combustion luminosity is detected by an Applied Solar Energy Corp. photodiode (model 33PV05M) with an active area of 4 mm^2 placed behind a plexiglas plug in the wall. The axis of the photodiode is perpendicular to the axis of the injector to provide an unobstructed view of the fuel cloud. The plexiglas plug is 6.4 mm in diameter by 12.7 mm in length subtending a solid angle of

0.186 steradians (sr). The luminous combustion occurs along the axis where the fuel is injected. The cylinder head reduces the actual view angle of the detector to 0.120 sr. Likewise, the angle is further reduced when the piston is at TDC, *eg.*, 0.062 sr with 16:1 compression ratio. The photodiode's position allows for 25 mm of the 89 mm across the piston to be detected. This does not limit the ability to detect start of combustion because of the high reflectance of the internal combustion chamber surfaces. The photodector responsivity as shown in Fig. 2.6 shows high infrared and low UV sensitivities. Infrared radiation is emitted well into the expansion stroke even after the combustion ceases due to CO_2 emission. Therefore, the measurement of the end of combustion is not accurately measured with the photodiode. However, the compressed air, injected fuel, and internal combustion chamber surfaces are expected to emit insignificant radiation before ignition. Thus, a precise measure of the start of combustion is detected by the photodiode.

Amplification of the photodiode's signal is accomplished by the signal conditioning circuit in Fig. 2.5. The amplified signal is sent to the A/D converter. In addition, it is compared to an adjustable threshold voltage. When the signal is greater than the threshold, a 5 volt signal is sent to the parallel port. Similarily, a ground is sent to the parallel port when the photodiode's signal falls below the threshold. The same circuit exists for the injector needle lift transducer in the signal conditioning module. When the parallel input ports are sampled, the beginning and end of the needle opening and combustion luminosity can be

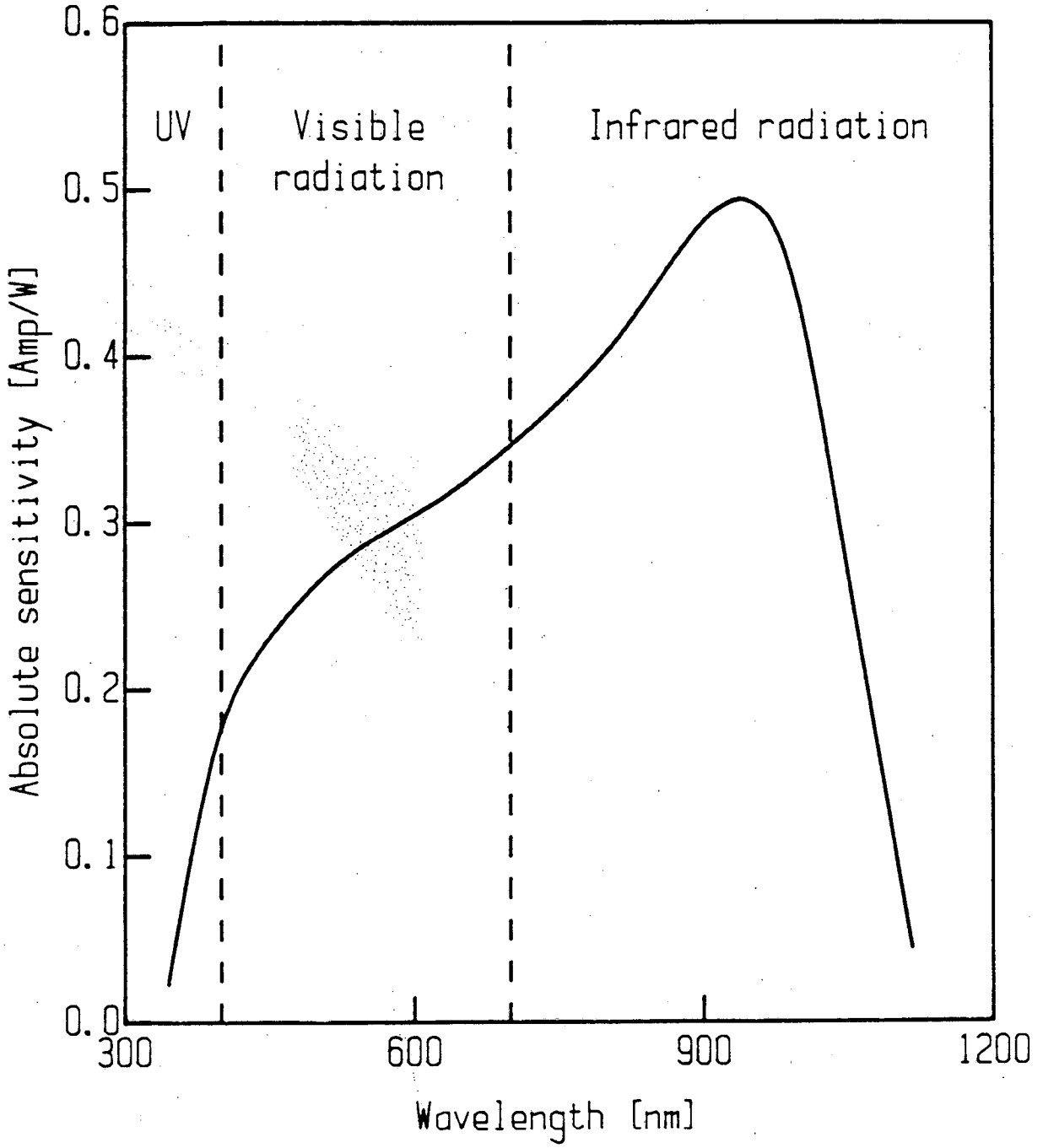

Figure 2.6. Photodiode responsivity to incident radiation.

detected. Since the fuel injection system and measuring equipment are discussed in Sections 2.2.2 and 2.2.3, the descriptions are omitted here.

2.1.4. High Speed Cinematography

Three photographic techniques are employed in the square piston engine simulator to visualize the injection, fluid motion, and combustion processes. Air motion during scavenging and compression in a motored engine is observed with the aid of Schlieren cinematography. A shadowgraphic technique is used to observe the injection and combustion in the engine simulator. And, direct photographs of the combustion process result from emission from the combustion event.

The Schlieren setup is shown in Fig. 2.7. The point light source, a xenon arc lamp, is placed one focal length (3.95 m focal length mirror) from the spherical mirror. The collimated light from the mirror passes through the test section and is collected by another spherical mirror. An iris is placed at the focal point of the second mirror. Local density gradients in the engine combustion chamber change the gases' index of refraction causing the collimated light to be bent. The Schlieren stop or iris will not pass bent light rays making a pattern of light and dark on the image plane. The diameter of the iris opening determines the Schlieren sensitivity. The image is focussed onto the film plane of a Hycam motion picture camera operating at 5000 frames per second. Films of fluid motion in a motored engine with ambient inlet conditions, preheated inlet air, and 2 atm inlet pressure were taken. Because the Schlieren images are monochrome, Kodak's 7278 Tri-X reversal black and white film of tungsten ASA 160 is used.

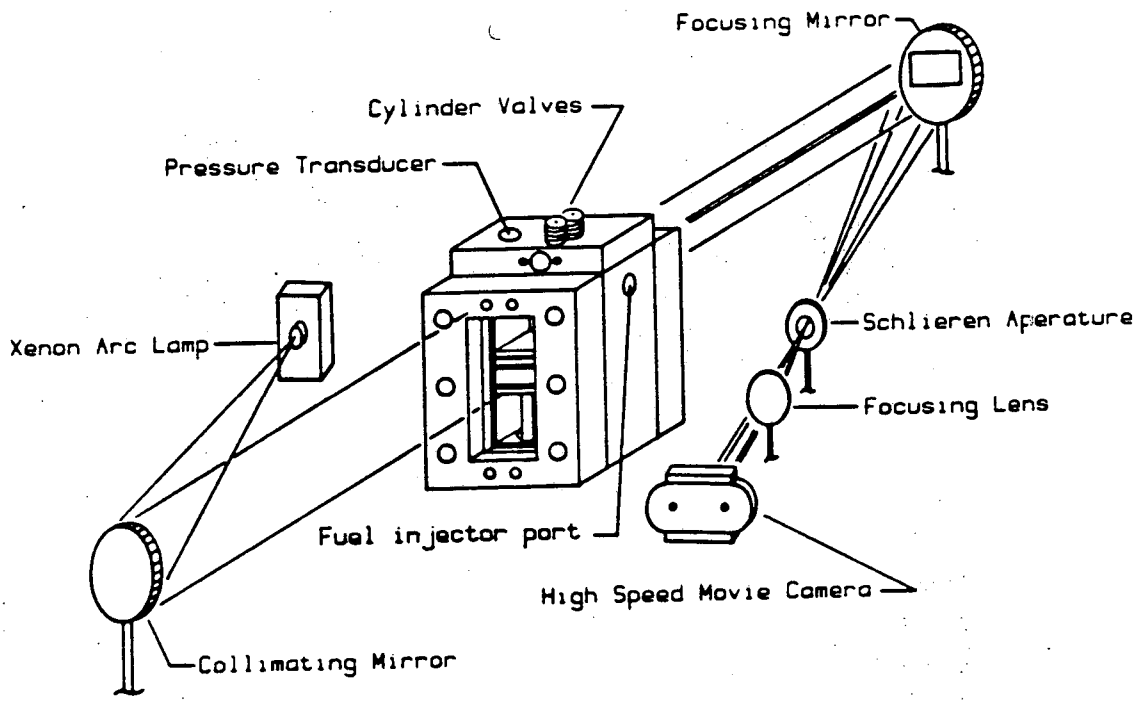

Figure 2.7. Schematic diagram of square piston engine simulator test section with associated optical equipment for Schlieren cinematography.

To take high speed shadowgraphs, the equipment is identical to that described above except that the Schlieren stop is removed. High speed shadowgraphs of the injection and combustion of diesel No. 2, methanol, coal/diesel, and coal/methanol slurries have been taken. When injection occurs the high density of the fuel completely blocks out the light source. During the combustion interval, the visible radiation is collected onto the film plane directly. The light source provides white light which is distinguishable from the orange light of the radiating fuel particles during combustion. Thus, Kodak 7251 color film with tungsten 100 ASA film is used.

Direct cinematography of the combustion event is filmed with the Hycam camera placed at the image plane shown in Fig. 2.1. The engine is illuminated with two flood lamps so that the piston motion can be observed before and after the combustion. The light emitted from the combusting fuel is focussed directly on the film plane are recorded at at 5000 frames per second. Movies using both the black and white and color films described above are taken.

2.2. INJECTION SYSTEM

2.2.1. Test Fuels

The performance of coal/water, coal/diesel, and coal/methanol slurry fuels is compared to two reference fuels: diesel No. 2 and pure methanol. The fuel industry standard engine test for evaluating ignition and combustion performance of diesel fuels yields a cetane rating. Roughly speaking, the lower cetane numbers indicate longer ignition delays and poorer engine performance. The cetane number for

diesel No. 2 is 40; and Ullman, *et al.* (1982) report that methanol has a cetane number of 3. Cetane ratings of coal slurry fuels are not available in the literature.

The coal slurries used in this work were prepared by the Department of Energy's Bartlesville Energy Technology Center (now National Institute for Petroleum and Energy Research). They are 45 mass % subbituminous, pulverized coal (Pittsburgh seam HVA) suspended in water, diesel No. 2, and methanol. The 0.7 mass % ash coal is cleaned by the Otisca process, a hot acid wash. The coal is ground by conventional technology to approximately 70 μm. Further grinding of the coal to 5 μm mean diameter is accomplished by a ball mill after the dry coal has been added to the liquid carrier. The largest coal particles, as observed under 300 power stereo microscope, are 40 μm. The elemental composition for this low ash coal is given in Table 2 of a paper by Gurney, *et al.* (1984): 79.7% C, 5.9% H, 12.9% O and N, 0.6% S, and the remainder is ash. The coal contains 40.7% volatiles, 55.9% fixed carbon, 2.7% moisture, and 0.7% ash.

In addition to the coal and liquid carrier, the fuels contain additives. Surfactants, dispersants, viscosity improvers, and lubricants with a maximum total dosage of 5 mass % are added to the fuels. The surfactants and dispersants maintain the coal suspension. However, these agents thicken the slurry making viscosity improvers necessary. Lubricant is added to the water and methanol slurries to provide lubricity for improving the injection equipment performance with slurries.

The calculated enthalpies of reaction and the specific gravity of the test fuels are:

Fuel	Enthalpy of reaction [MJ/kg]	Specific gravity
Diesel No. 2	43.3	0.82
Methanol	19.9	0.80
Coal	32.5	1.80
45% Coal/55% Oil	38.4	1.09
45% Coal/55% Methanol	25.6	1.07
45% Coal/55% Water	14.6	1.25

The slurry supplier can not reveal the details concerning the dosage level and chemistry of the additives by agreement with the additive manufacturers. Thus, the slurry properties listed above are derived mathematically from the fuel components without taking account of the fuel additives.

2.2.2. Injection Equipment

A Stanadyne pencil type injector (model 20071) is used for injecting the coal and reference fuels. The injector nozzle as received from Stanadyne has one orifice of 0.71 mm diameter. This injector is made for indirect engines where high velocity, high atomization sprays are of lesser importance than in direct injection engines. For the purposes of research in a direct injection engine, the nozzle tip is removed and replaced with a single orifice made of hardenable steel. A range of orifices, 0.25-0.76 mm diameter, were fabricated to determine the optimum size for providing a suitable compromise between good atomization and minimal plugging with coal slurries.

The high pressures required to open the fuel injector and to maintain a high velocity spray during the injection interval is provided by a 6 mm Bryce (A size, model 99-65010) jerk pump. The pump is actuated by a cambox driven off the engine crankshaft sprocket as shown in Fig. 2.1. Normally on a 4-stroke engine the fuel injection rate is one-half engine speed, *eg.*, 450 injections/min for a 900 rpm engine. However, since the square piston engine is a single combustion cycle device and the highest pumping pressures are desired, the sprocket ratio between the engine's camshaft sprocket ratio between the engine's camshaft and the cambox is 2:1 making the pump frequency 900 injections/min. It is necessary to avoid injection during the scavenging stroke before combustion as this is a form of pilot injection which Obert (1973) reports is an ignition aid. Therefore, solenoids on each end of the rack pull it open and closed for one stroke only. The solenoid timing sequence is set by the solenoid control module. The detail necessary to show the solenoids and control box is not feasible in Fig. 2.1. However, they are shown in Fig. 2.8 in a schematic of the injection equipment on a bench test rig.

2.2.3. Injection Testing Outside Engine

Before attempting to compression ignite the test fuels in the square piston engine simulator, the injection equipment performance is evaluated on a bench rig outside the engine. A schematic of the system except the computer interface is shown in Fig. 2.8. The LSI-11 microcomputer and electronic control and measurement equipment are shown in Fig 2.9.

The motor rotates the cambox at 900 rpm as on the square piston engine. The 6 mm injection pump rack is pulled open and closed by solenoids timed

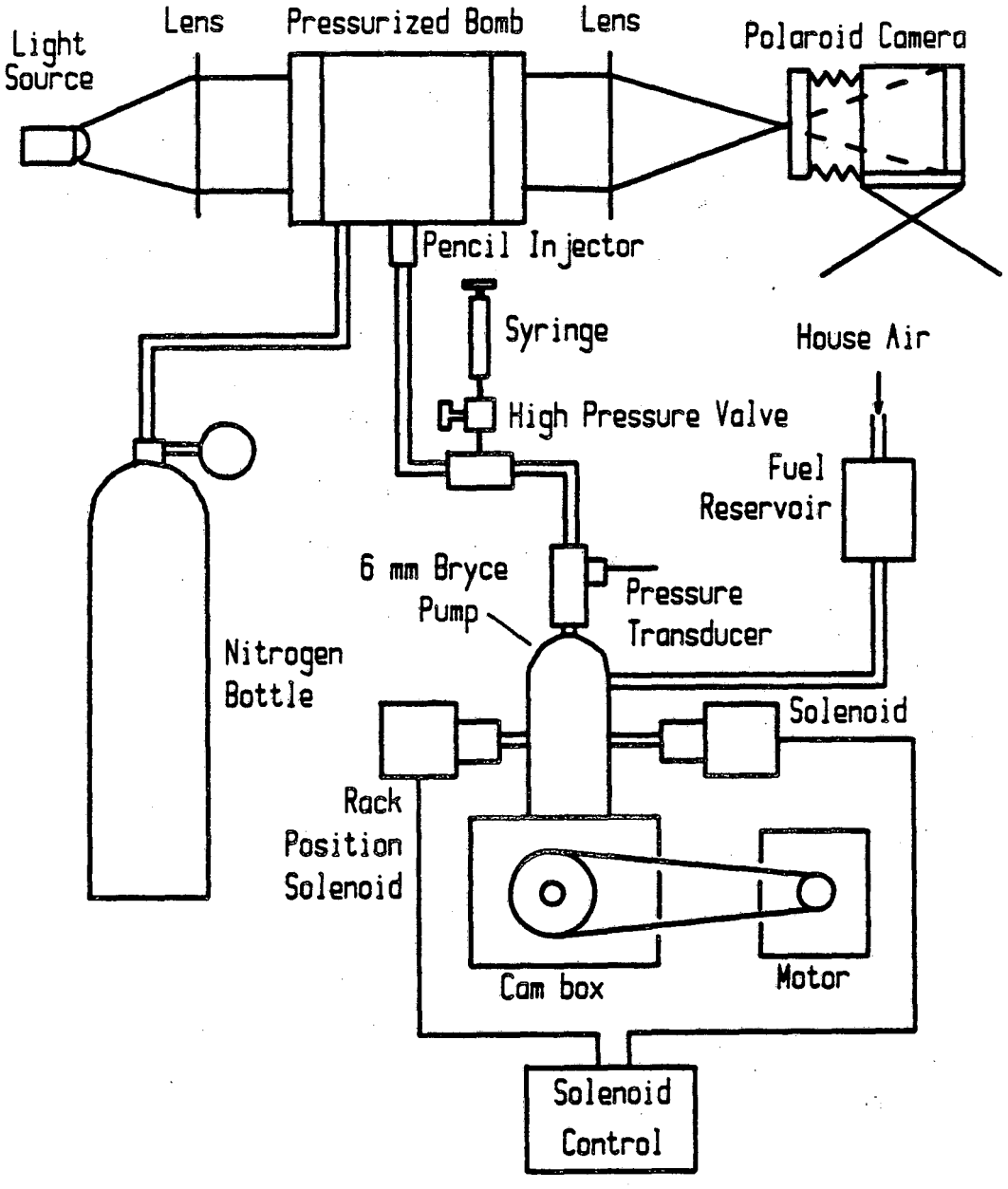

Figure 2.8. Schematic diagram of injection bench test (including apparatus for taking shadowgraphs) for evaluating injection performance outside the engine.

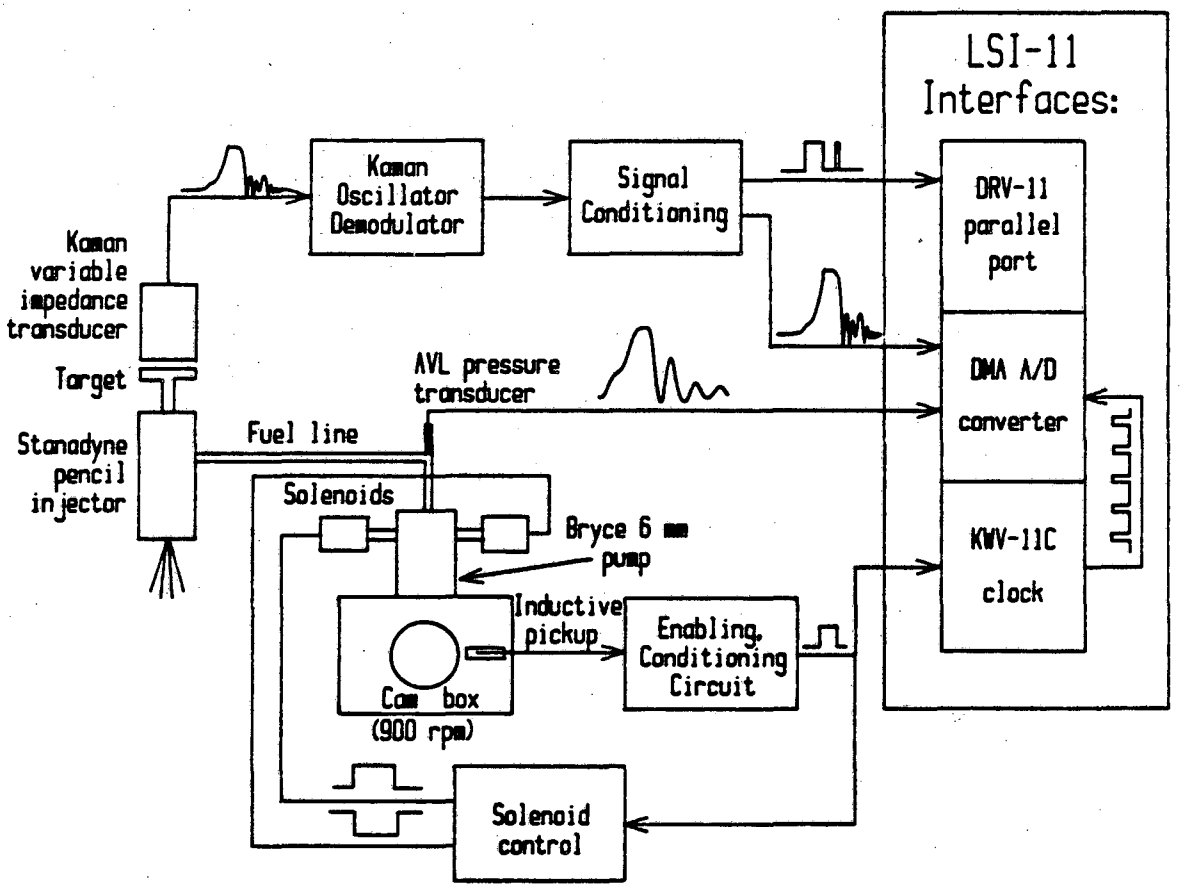

Figure 2.9. LSI-11 microcomputer interfaces to injection bench test.

externally by the the solenoid control module. The rack opening sequence is coordinated with the cambox rotation angle via pulses from an inductive pickup sensing a bolt on the cambox pulley. The enabling, conditioning circuit in Fig. 2.9 is reset by the operator. Immediately afterwards one inductive pickup pulse is sent to the solenoid control module and to the KWV-11C clock. From the trigger to the injection control box, the solenoids open the rack within 25 msec. After the rack is open for approximately 75 msec, the rack is closed.

The inductive pickup pulse comes in on the number 2 Schmitt trigger on the clock panel. The injection stroke begins approximately 60 msec after this inductive pickup pulse. Therefore, a delay loop of 55 msec is imposed before sampling by the direct memory access A/D converter commences. After the delay, the KWV-11C is programmed to provide a 40 kHz pulse train to the A/D RTC trigger. The needle lift and injection line pressures are sampled by the A/D converter at 20 kHz samples/channel. The signal conditioning circuit in Fig. 2.9 (same as in Fig 2.5) receives the raw signal from the needle lift transducer oscillator demodulator. The signal is amplified to the 0 to 5 volt range required by the A/D converter. An adjustable threshold voltage in the conditioning circuit is compared to the amplified oscillator demodulator signal. When the needle lift voltage exceeds the threshold voltage, the comparator circuit output gives 5 volt. The output returns to ground when the needle lift signal falls below the threshold. In this way the square wave signal which goes to the parallel input port is produced. By checking the parallel input port continually and storing the occurences of high and low inputs, the times of needle opening and closing are stored in memory.

The injection line pressure is sensed by a 10 mm AVL piezoelectric pressure transducer (model 8QP500C) with a Kistler 5004 charge amplifier. The fuel injection interval is detected by measuring the position of the injector needle. The needle is forced against the orifice by a spring. Injection begins when the pressure acting to open the needle exceeds the spring force. The injector body is modified to hold an aluminum target which moves with the needle. A Kaman KD-2300-1SM proximity detector located approximately two millimeters from the target provides a signal proportional to the needle position.

A listing of the data acquisition software is contained in Appendix B. The program consists of three parts: the main program (inject.c) which communicates to the user and sends control to the subroutines, the assembly routine (inj.mac) which provides a delay interval and collects the data, and several subroutines for drawing the data on the terminal screen.

3. DATA ANALYSIS AND DISCUSSION

3.1. MOTORING CYCLE

3.1.1. Temperature Measurements

The ignition delay characteristics of fuels are important comparison parameters to evaluate fuel performance. The Arrhenius expression relates the fuel properties (activation temperature and pre-exponential factor) with the ignition delay, air temperature and pressure. The ignition delay and cylinder pressure are measured directly on the engine simulator. However, the temperature is not measured directly. Because the exponential of the temperature appears in the Arrhenius relation, it is the most critical parameter to determine accurately. Information concerning air temperatures for conventional engines is obtained from the literature or is estimated from simple cycle calculations. However, the engine simulator suffers from higher leak and heat transfer rates than the engines covered in the literature due to the square cross-section and unheated combustion chamber surfaces. Thus, the temperature is estimated in two ways: computer modelling of motoring cycle (discussed in Section 3.1.2) and inference from fine wire thermocouple measurements which is discussed here.

A 0.013 mm chromel-alumel thermocouple is installed in the east combustion chamber port as shown in Fig. 2.3. The thermocouple leads are threaded through a ceramic insulator. The thermocouple junction protrudes from the ceramic plug approximately 10 mm which protrudes from the cylinder wall approximately 5 mm.

Therefore, the thermocouple bead is exposed to the bulk gas rather than the boundary layer.

Cylinder gas temperatures are measured for the following conditions:

Air temperature at IVC [°C]	Air pressure [atm]	Cylinder temperature [°C]
Ambient	1	Ambient
Ambient	2	Ambient
100	2	Ambient
125	2	Ambient
170	2	Ambient
195	2	Ambient
245	2	150

A two channel data acquisition routine is used for collecting temperature and pressure measurements at one-half CAD intervals. Measurements are made only at 16:1 compression ratio as cylinder clearance does not accommodate the thermocouple probe at 22:1 compression ratio. Figures 3.1 and 3.2 show both cylinder pressure and thermocouple temperature as a function of CAD. The cylinder pressure peaks well before the thermocouple temperature due to the heat transfer time lag for the thermocouple to attain the gas temperature. The gas temperature peak occurs before the pressure peak because both quantities drop linearily with heat loss, but pressure is rising with the volume ratio to the 1.4 power whereas temperature rises with volume ratio to the 0.4 power. (The values of 1.4 and 0.4 are approximate values for air.) Thus, as the rate of volume change

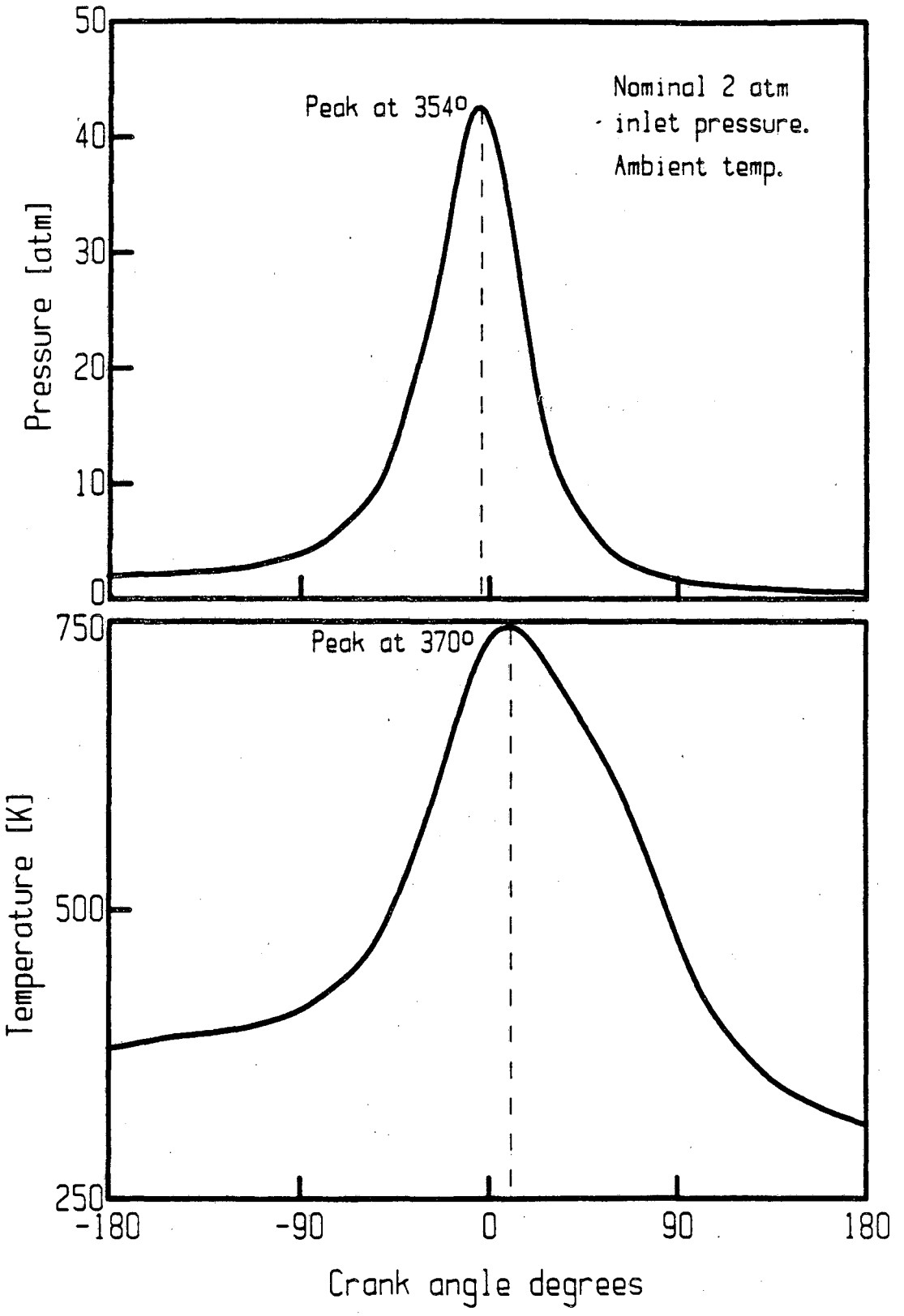

Figure 3.1. Thermocouple temperature and cylinder pressure for ambient inlet temperature and nominal 2 atm abs inlet pressure motoring cycle on the square piston engine simulator at 900 rpm and 16:1 CR.

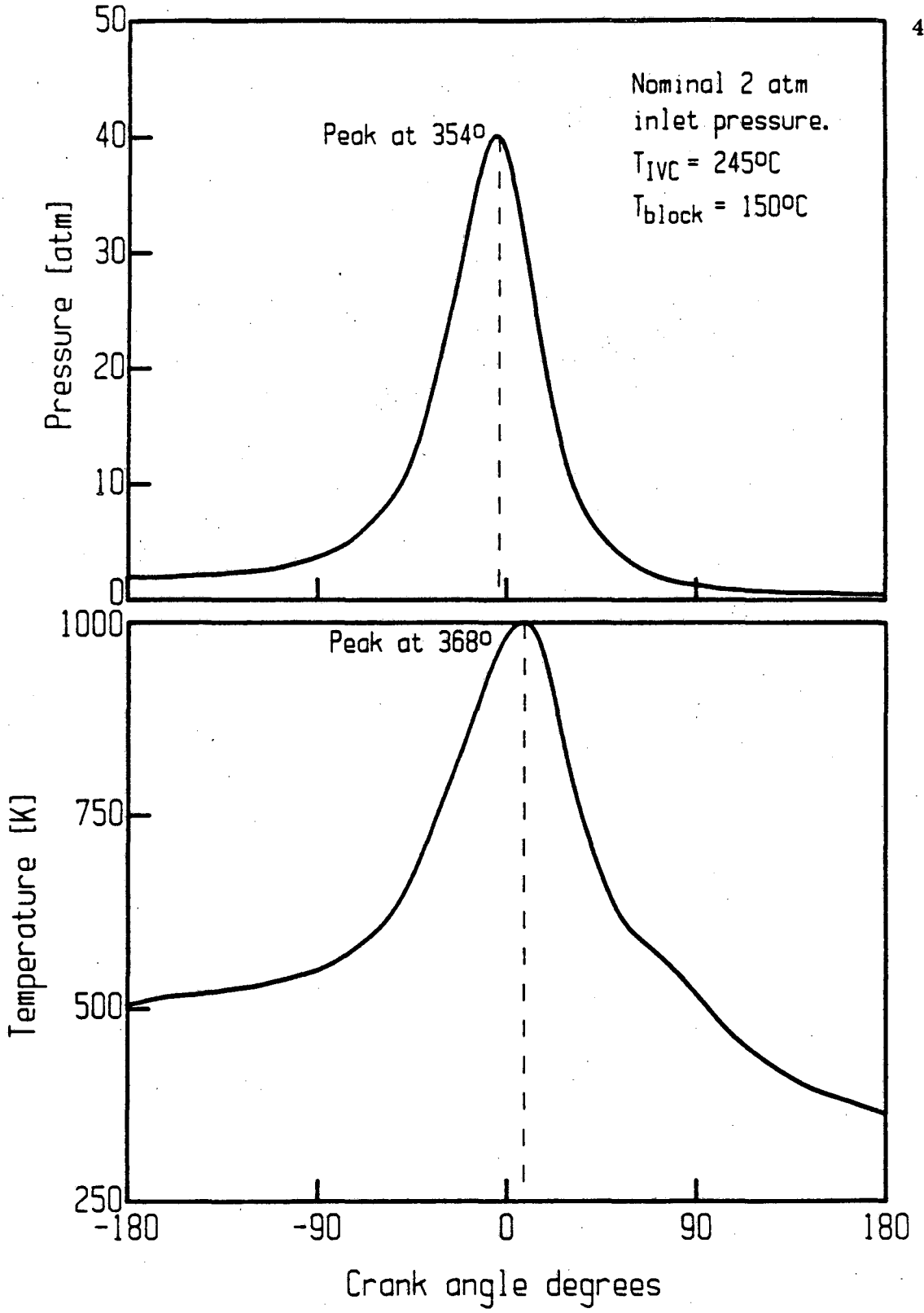

Figure 3.2. Thermocouple temperature and cylinder pressure for the square piston engine simulator motoring cycle at 900 rpm and 16:1 CR. The block temperature, inlet temperature and pressure are: 150 ° C, 245 ° C, and 2 atm abs, respectively.

decreases on compression, the losses due to heat transfer outweigh the gains due to volume change earlier for the temperature. In Fig. 2 of Henein and Bolts' (1969) paper, the peak temperature precedes the peak pressure in a motored engine. The thermocouple temperature lags behind the bulk gas temperature due to the finite thermal capacity of the bead.

The magnitude of the thermocouple's time delay is estimatable from a heat transfer analysis. Writing a first law energy balance:

$$\frac{dQ_t}{dt} = \frac{dU_t}{dt}$$

or, in words, the heat transfer rate to the thermocouple is equal to the rate of internal energy gain. The mode of heat transfer is by convection. Gaseous radiation from air at the temperatures attained in the cylinder is negligible. Conduction down the the thermocouple wires is insignificant for a wire diameter of 0.013 mm and lead length more than 3 mm according to Bradley and Matthew (1968).

The convection to the thermocouple is described by:

$$\frac{dQ_t}{dt} = hA(T_g - T_t) .$$

The rate of internal energy gain is:

$$\frac{dU_t}{dt} = C_t \rho_t V \frac{dT_t}{dt} .$$

So,

$$hA(T_g - T_t) = C_t \rho_t V \frac{dT_t}{dt} .$$

Rearranging,

$$T_g = \frac{C_t \rho_t V}{hA} \frac{dT_t}{dt} + T_t$$

or

$$T_g = \tau \frac{dT_t}{dt} + T_t \tag{3.1}$$

where the factor

$$\frac{C_t \rho_t V}{hA} = \tau .$$

The constant, τ (units of time), varies throughout the cycle because h is a function of piston velocity, gas density, gas temperature, etc. However, since several heat transfer parameters are not known accurately, computing a time varying value of h is not warranted. Instead, an average value for h is found.

The thermocouple supplier claims the bead is nearly spherical with diameter approximately three times the wire diameter, 0.038 mm. Standard tables do not contain properties for chromel-alumel. Thus, average values for specific heat and density of metals are used:

$$C_t = 200 \text{ J/kg-K and } \rho_t = 8000 \text{ kg/m}^3.$$

The heat transfer coefficient, h, is related to the Nusselt number:

$$h = \frac{Nu\ k_g}{D} .$$

For forced convection over a sphere,

$$Nu = 2.0 + 0.236\ Re^{0.606}\ Pr^{0.33} ,$$

according to Raithby and Eckert's (1968) correlation. The Prandtl number is about 0.69 for air. The Reynold's number is:

$$Re = \frac{v_p\ D\ \rho_g}{\mu_g} .$$

It is not well understood how the gas velocity relates to the driving force, the piston motion. In addition to this uncertainty, the piston velocity is not constant throughout the cycle. For simplicity, the gas velocity is taken to be the average piston velocity. At 900 rpm with a piston linear displacement of approximately 0.1 m, the average piston velocity is 3 m/sec. The gas density varies between twice ambient density to about 20 times ambient density. An average value of 10 times ambient density is used, 12 kg/m^3. Gas properties at an average temperature, 500 K, are used:

$$\mu_g = 2.8\ X\ 10^{-5}\ kg/m\text{-}sec \quad and \quad k_g = 43\ mW/m\text{-}K.$$

With the foregoing assumptions, h = 4.7 kW/m^2-K. Thus, the time constant is approximately 2.2 msec.

The bulk gas temperature is inferred from the thermocouple temperature records through Eqn. 3.1. The computation of the derivative of temperature in Eqn. 3.1 is extremely sensitive to digitizing error or other system noise. Thus, the

raw data are smoothed using an allowable rms error of 5 inserted into Reinsch's (1967) spline smoothing routine. Because of the high degree of uncertainty in estimating the time constant, a range of values are tested. In Figs. 3.3 and 3.4, two thermocouple temperature records are shown with time constant corrections of 2, 4, 5, 6, and 8 msec. To satisfy the condition that temperature peaks before the pressure, the time constant is evidently greater than 4 msec. As the time constant becomes large, as for 8 msec in Figs. 3.3 and 3.4, the correction is exaggerated and exhibits unexpected behavior on the expansion stroke, *eg.*, the temperature at 90 CAD is lower than the temperature at 180 CAD indicating that an 8 msecec time constant overcorrects. After evaluating several temperature records, a compromise of 5 msec for the time constant is found to be most suitable. The computed data for a variety of inlet conditions are shown in Fig. 3.5. The data are displayed for the injection and delay interval, 45 ° BTDC to 15 ° ATDC.

The air temperature at the elbow directly upstream of the intake valve (Fig. 2.3) is recorded before each experiment. The temperature of the air introduced into the engine is different from the measured elbow temperature for two reasons. The intake passages and cylinder walls are at ambient temperatures (less than inlet air temperature when preheating the block) allowing for heat transfer losses before compression begins at IVC. Secondarily, the air temperature is increased due to induction work as discussed by Tsao, *et al.* (1962). This effect is distinguishable only in the case with ambient inlet air temperature.

The temperature at IVC is read directly from the raw thermocouple temperature record. This temperature need not be corrected as the intake process

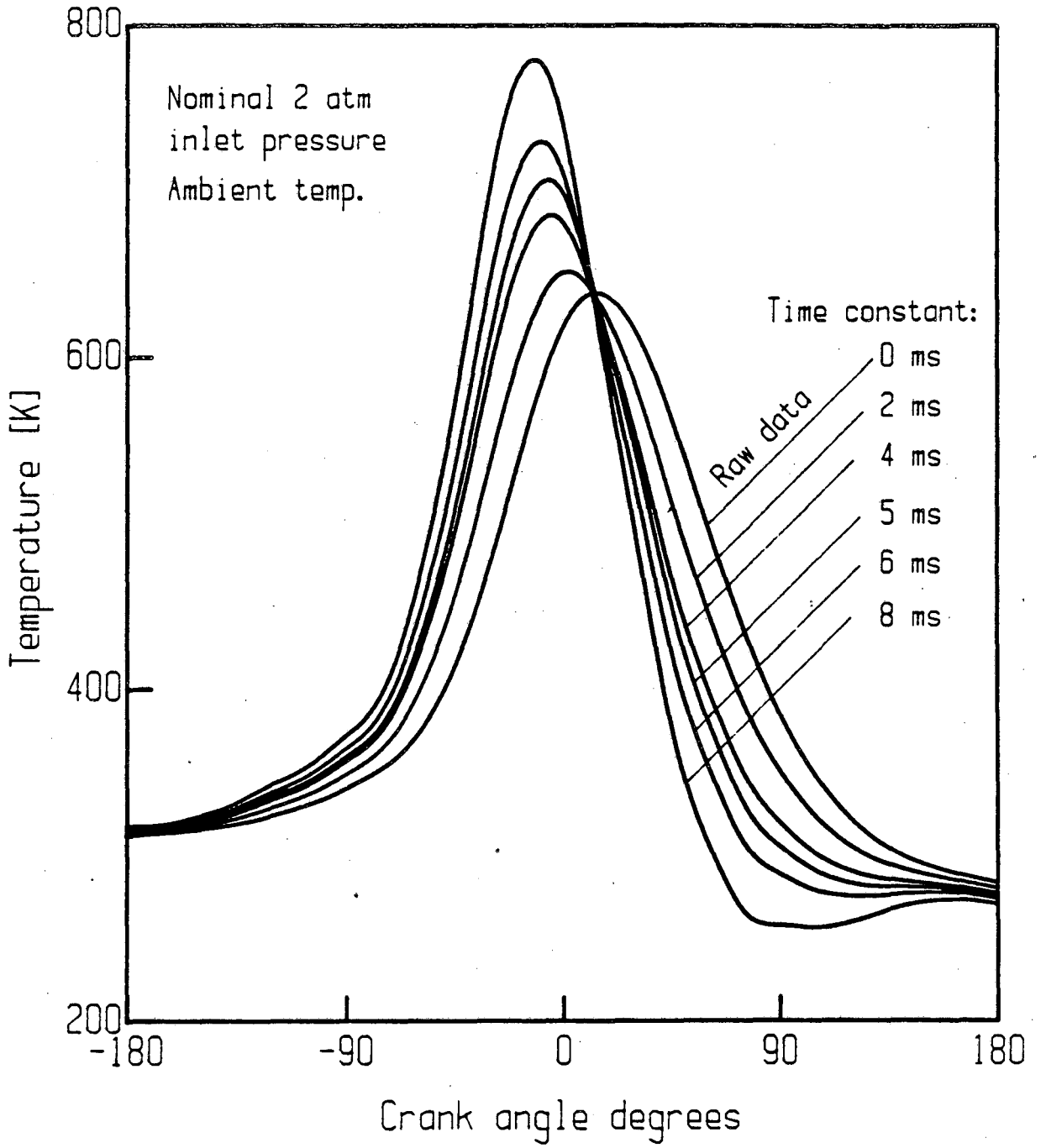

Figure 3.3. Thermocouple temperature for a motoring cycle in the square piston engine simulator (16:1 CR, 900 rpm) with ambient inlet temperature and 2 atm abs inlet pressure is plotted with five estimates (time constant corrections) of cylinder gas temperature.

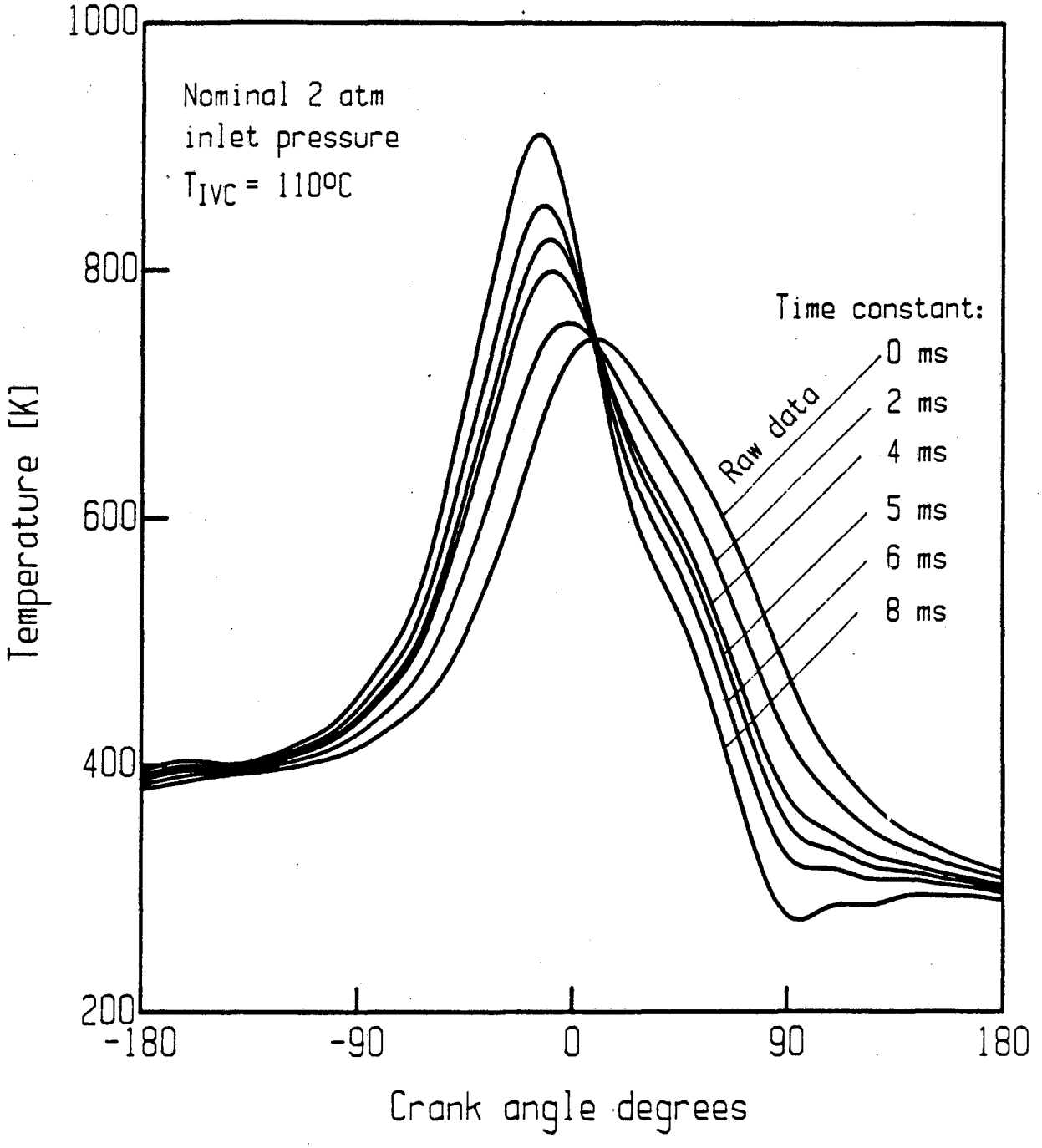

Figure 3.4. Thermocouple temperature and five estimates of cylinder gas temperature for the square piston engine with 110 °C inlet air temperature and 2 atm abs inlet pressure.

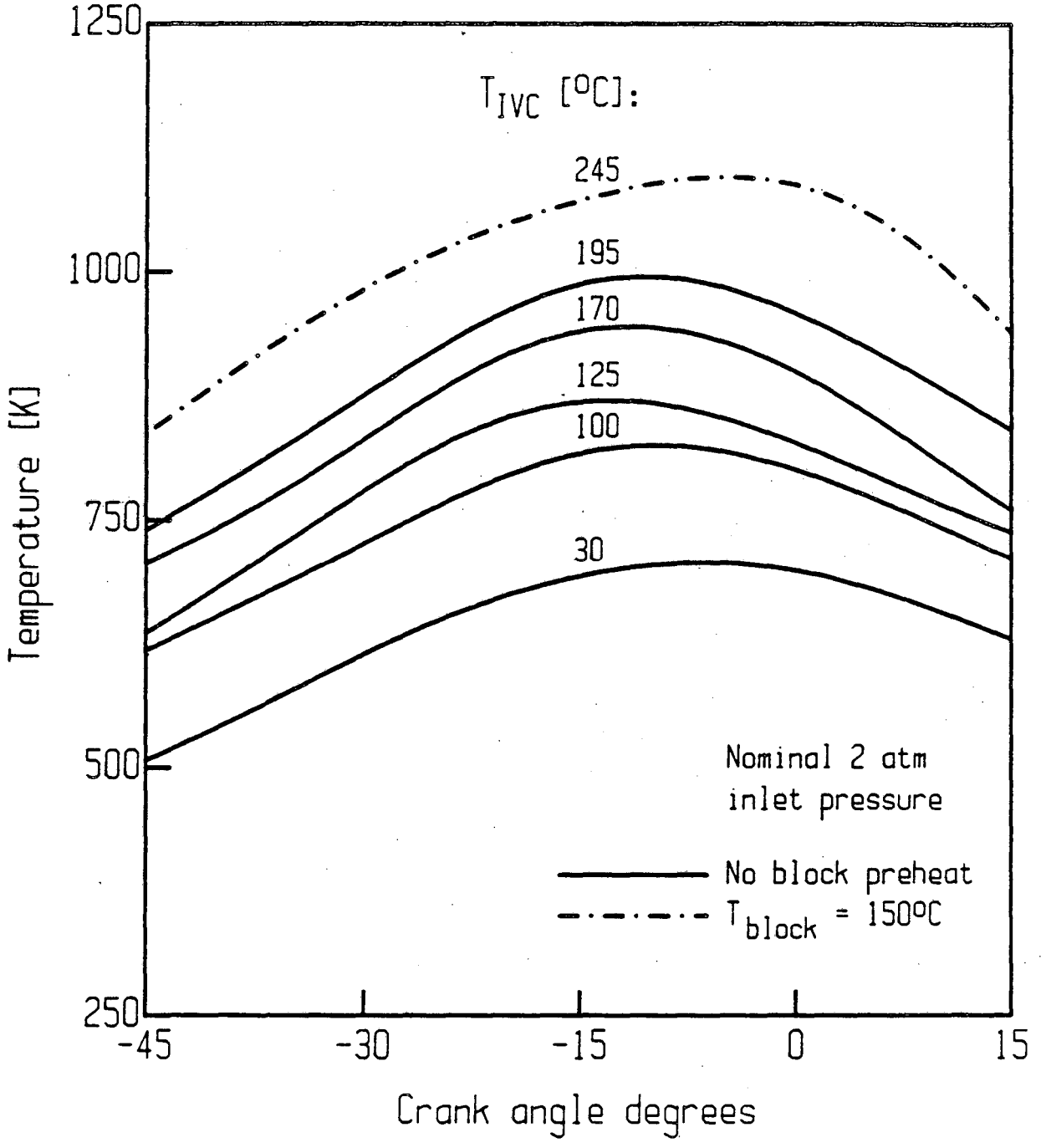

Figure 3.5. Cylinder gas temperature for the motored square piston engine simulator for six temperature conditions and 2 atm inlet pressure from 5 msec thermocouple delay time correction.

takes 25 msec, sufficient time for thermocouple response. The relation between the elbow temperature and IVC temperature is shown in Fig. 3.6. A least squares fit of the data indicates a temperature rise at IVC of about one-half degree for each degree the inlet temperature is raised.

The peak compression temperature as a function of the inlet temperature is shown in Fig. 3.7. A least squares analysis shows that each additional degree of temperature preheat corresponds to about 0.86 degree higher peak compression temperature. The variation of the data from the least squares correlation in Fig. 3.7 indicates the limitations of the correction technique. Any temperature nonuniformities due to large scale structures are magnified in the temperature correction routine. The uncertainty is reduced by averaging the temperature for several runs at the same temperature. However, the uncertainty in the measurement is on the order of $\pm$ 25 K.

In addition to uncertainties in the cylinder gas temperatures due to measurement/correction problems, the temperature is not uniform throughout the combustion chamber. From the Schlieren movies two examples of the nonuniformaties are evident:

- thermal boundary layer on combustion chamber surfaces.
- large scale vortical structures with density gradients within the vortex indicating large scale turbulence and limited mixing on a fine scale.

Fuel injected into hot pockets ignite more rapidly than an overall temperature measure would indicate. On the other hand, fuel droplets in cold pockets or near the combustion chamber surfaces experience a longer ignition delay or do not ignite

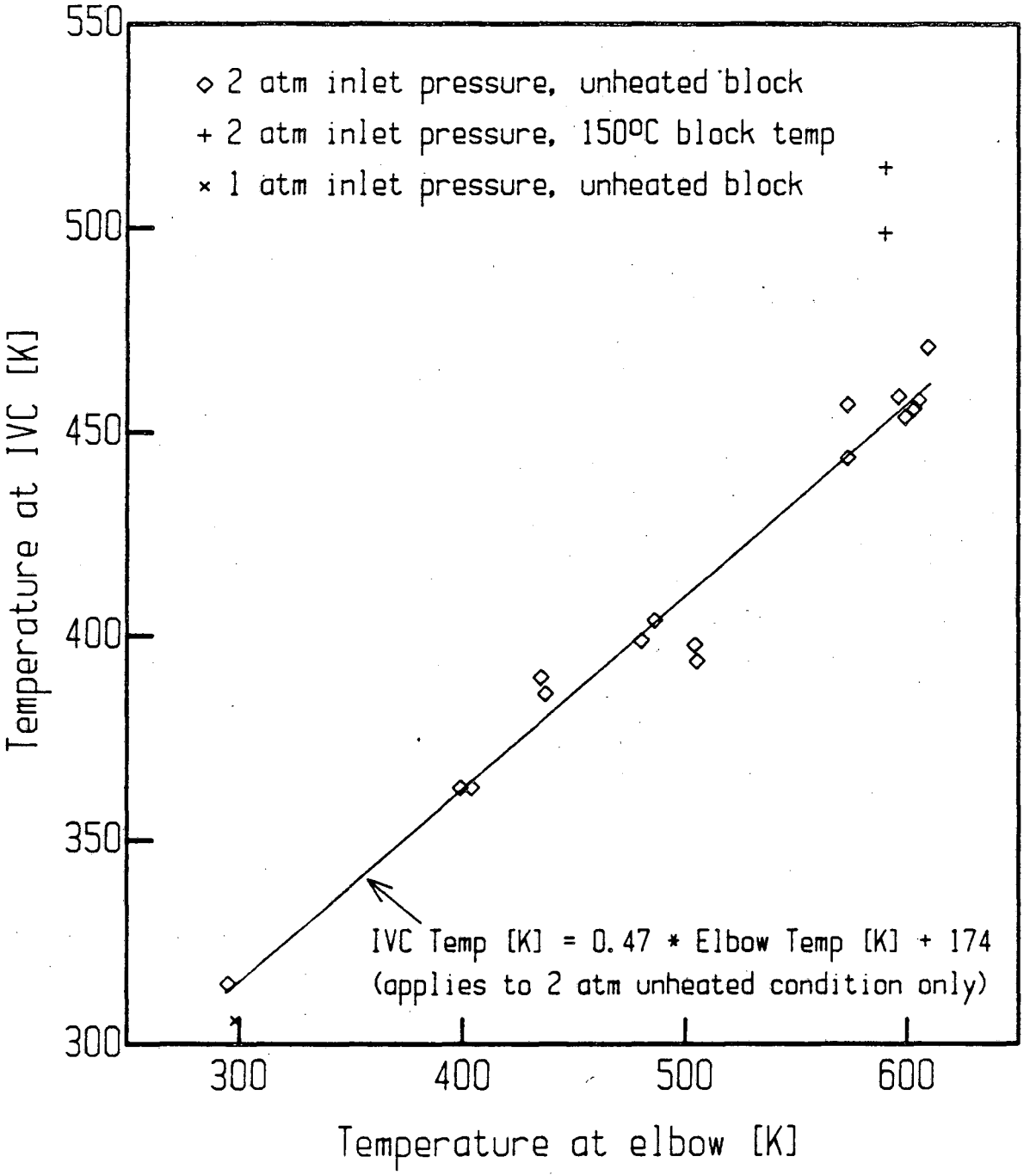

Figure 3.6. Correlation between inlet temperature measured upstream of the inlet valve and that measured at IVC in the cylinder for the square piston engine simulator at 900 rpm.

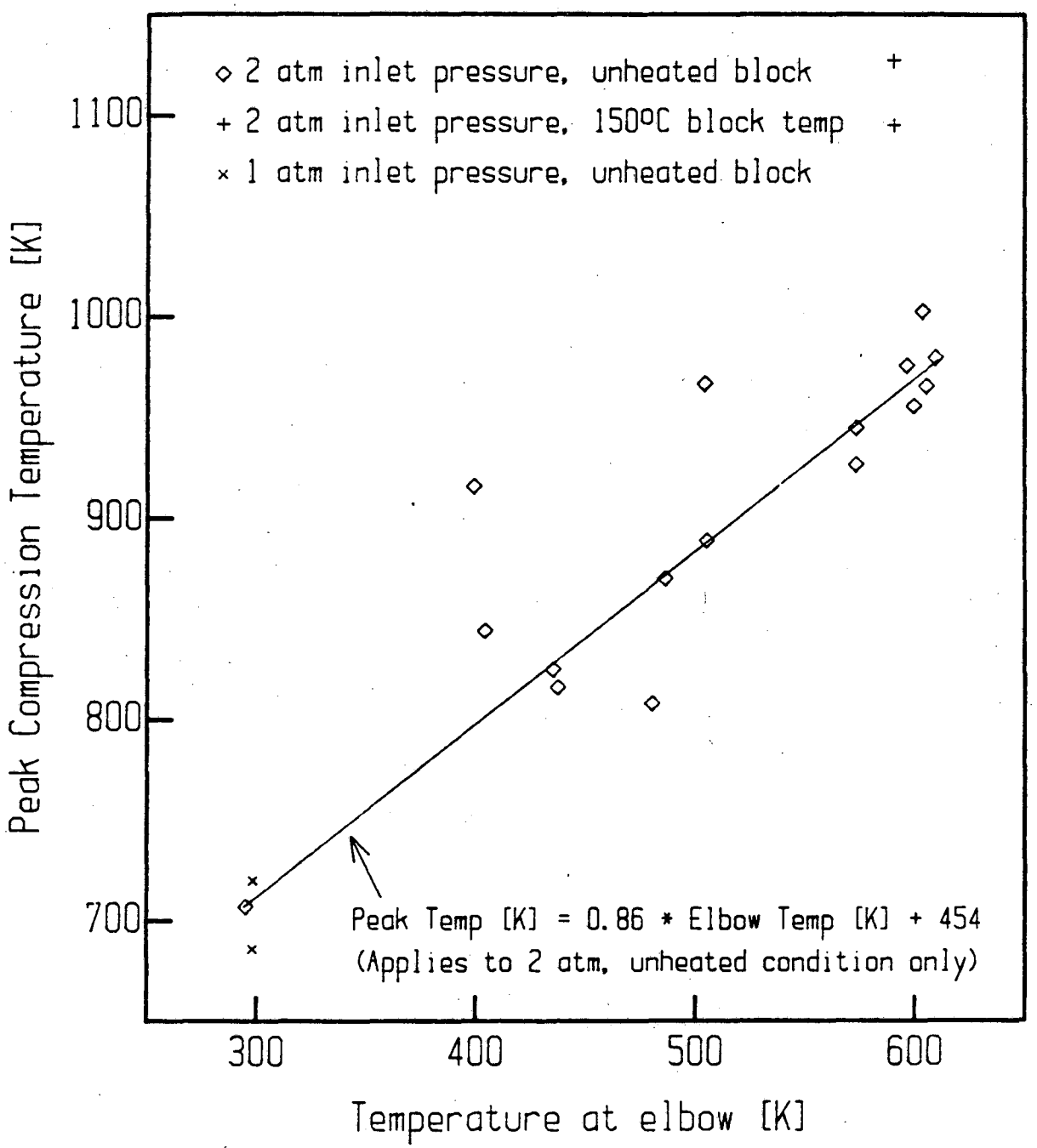

Figure 3.7. Correlation between the peak motoring temperature in the square piston engine and the temperature upstream of the inlet valve for 900 rpm, 16:1 compression ratio operation.

in the time available even though the bulk gas temperature may be high enough for shorter ignition delays.

The air temperature used in the Arrhenius correlation is the temperature at the time of fuel injection. Thermocouple measurements are available for several inlet temperatures only. But, the combusting tests are run at any temperature in the range. Thus, the temperature is interpolated linearly between two cases with the nearest inlet temperatue.

3.1.2. ENGINE MODELLING

Introduction

In the previous section the importance of estimating the gas temperature at the time of injection is discussed. Temperature measurements are available for the 16:1 compression ratio motoring cycle. But, it is impossible with the current piston and combustion chamber head configuration and the measuring equipment described in Section 3.1.1 to measure the temperature at 22:1 compression ratio. A model of the motoring cycle is developed to provide a check of the thermocouple temperature corrections and to provide estimates for the cylinder conditions for the higher compression ratio cycle.

Information available in the literature about bulk gas temperature in a motored engine does not apply to the engine simulator. The square cross-section of the piston does not allow the use of conventional piston rings thereby allowing significant leakage past the ring pack. The piston sealing is accomplished with four graphite sections in each ring groove which overlap at the corners. Figure 2.2 shows a sketch of the piston and ring pack. Behind each of the four graphite

sections is a copper leaf spring which forces a seal against the "cylinder" wall surfaces. Due to the lack of lubrication and the sealing difficulties at the corners, the leakage is much higher than a conventional engine: approximately one-third mass loss in one compression-expansion stroke in the square piston engine compared to mass loss of a few percent in a circular piston engine. Begeman (1962) reports 1-1.5% minimum blowby for spark ignition engines. Georgi (1950) indicates that blowby is approximately 1000 cm^3/sec in a diesel engine, roughly the same percentage as a spark ignition engine.

Description of Model

Injection occurs just before TDC on the compression stroke. Thus, computations commence when the inlet process is complete and cease before exhaust blowdown. The cylinder is cut off from the inlet line at IVC (intake valve closing) on the compression stroke, 150° BTDC. The expansion ceases at EVO, 135° ATDC, on the following revolution. Therefore, the computer simulation covers 285 CAD or 570 one-half CAD steps.

The temperature, pressure, mass, and volume are related by the ideal gas law. The volume above the piston is known from engine geometry. The combustion chamber of the engine simulator is a parallelpiped with a fixed cross-sectional area. Therefore, volume above the piston is the cross-sectional area times the distance between the piston top and the head, y. Engine CAD is related to piston position through the crank radius (r_c) and the connecting rod length (L), 47.6 mm and 165 mm, respectively.

$$y = L + r_c - (L^2 - r_c^2 \sin^2\theta)^{0.5} - r_c\cos\theta + \frac{2r_c}{CR - 1},$$

where θ is the crank angle, r_c is the crank radius, and CR is the compression ratio. All experiments in the compression expansion apparatus and the computer simulation use 16:1 CR.

The initial temperature (at IVC) is measured by a thermocouple in the cylinder. The initial pressure is assumed. (Determination of initial conditions will be discussed in detail later.) From these initial conditions and the volume, the mass is computed using the ideal gas law. The adiabatic temperature and pressure are found from the volume through the isentropic relations:

$$P_n = P_{n-1}\left(\frac{V_{n-1}}{V_n}\right)^{\gamma} \quad \text{and} \quad T_n = T_{n-1}\left(\frac{V_{n-1}}{V_n}\right)^{\gamma - 1}.$$

The ratio of specific heats is a weak function of temperature in the temperature range of the motoring test. However, because the volume ratio is raised to a power of the ratio of specific heats, this slight variation has a large effect on the resulting values for the isentropic temperature and pressure. The ratio of specific heats is calculated by the following:

$$\gamma = \frac{C_p}{C_v} = \frac{C_p}{C_p - R}$$

where C_p is a polynomial in temperature.

The compressed air supply to the compression expansion apparatus is wet. By assumption, the air is composed of 2 mass % water vapor in air. McBride, *et al.* (1963) provide polynomial relations for C_p as a function of temperature for several

pure gases. The relation for C_p of the mixture is the summation (over N_2, O_2, and water) of the mass % of the component times the polynomial expression for the pure component. The resulting form of the equation is:

$$C_p = C_0 + C_1T^{0.25} + C_2T^{0.5} + C_3T + C_4T^{1.5} + C_5T^{-2} + C_6T^{-3} .$$

The amount of heat transferred per calculation step is found using the Woschni (1967) correlation:

$$Q = K\, D^{-0.2}\, P^{0.8}\, T^{-0.53}\, v_p^{0.8}\, a\, (T_g - T_w)\, \Delta t .$$

One of the terms in Woschni's correlation is deleted here because it only applies to a combusting cycle. Benson and Whitehouse (1979) report that K = 26.6 for a four-stroke, medium-speed diesel engine. Kays and Crawford (1980) define a hydraulic diameter to use for geometries other than circular. The hydraulic diameter is four times the flow area divided by the perimeter. For the square piston engine the hydraulic diameter for use in the above equation is the piston side dimension.

The Woschni heat transfer correlation yields a steady state result, *i.e.*, averaged over the cycle. The heat transfer from the gas to the cylinder occurs primarily during the compression and expansion strokes near TDC. The compression-expansion period is less than one-third of two revolutions for each power stroke, the heat transfer rate in the model is increased over the Woschni correlation by a factor of four. The temperature at the wall, T_w, is assumed constant throughout the computation. The corrected values of temperature and

pressure are:

$$T_n' = T_n - \frac{Q_n}{m_n C_p} \text{ and } P_n' = P_n \frac{T_n'}{T_n} .$$

Mass leakage is assumed to be sonic, *i.e.*, leakage is proportional to the pressure in the cylinder. The flow is not sonic below a critical pressure which depends on the downstream pressure (atmospheric pressure in this case). However, the mass leak rate is estimated to be proportional to the cylinder pressure at all pressures for convenience. Because the leakage is insignificant at low pressures, this assumption introduces negligible error. The leak rate is:

$$\frac{dm}{dt} = M K \frac{dP'}{dt} .$$

The coefficient M is the static leak rate measured on the engine with the piston stationary. At pressures between 2 and 6 atm gauge, M was approximately 0.5 gm/atm-sec. The leak rate varies depending on the condition and fit of the piston and rings. Because the static value may be significantly different from the dynamic value, a second constant, K, is introduced which is adjusted to match experimental results. The effect that leakage has on the cylinder content properties is that of an isentropic expansion:

$$P_n'' = P_n' \left(\frac{m_n''}{m_n'}\right)^{\gamma} .$$

Similarly, temperature including leakage effects is computed.

The one zone model described above is found to be unsatisfactory when comparing model and experimental temperatures. The model predicts higher

temperatures than those measured as demonstrated in Figs. 3.8 and 3.9. In addition, the modelled pressure curve closely matches the experimental curve only at the beginning and end of the compression-expansion cycle and at the peak where it is forced to fit.

High speed Schlieren movies of the motoring cycle indicate that there are small crevice areas around the head. They fill during compression and are observed emptying during the expansion. From the inconsistency between experimental and model temperatures and the suggestion of crevices in the head, a two zone model is developed.

The two zone model consists of the bulk gas at uniform conditions as described above and an additional crevice zone containing air at cylinder wall temperature and bulk gas pressure. The volume in the crevices is a parameter varied in the calculation; but, it is constrained by matching the experimental temperature.

The two zone model differs from the one zone model in two ways. The volume above the piston is enlarged by the amount of the crevice volume. Thus, pressure is calculated as follows:

$$P_n = P_{n-1}\left[\frac{(V_{n-1} + V_{cr})}{(V_n + V_{cr})}\right]^{\gamma}.$$

Similarly, temperature is computed. Secondly, heat transfer from the bulk gas to the walls is greater because all the gas compressed into the crevices attains wall

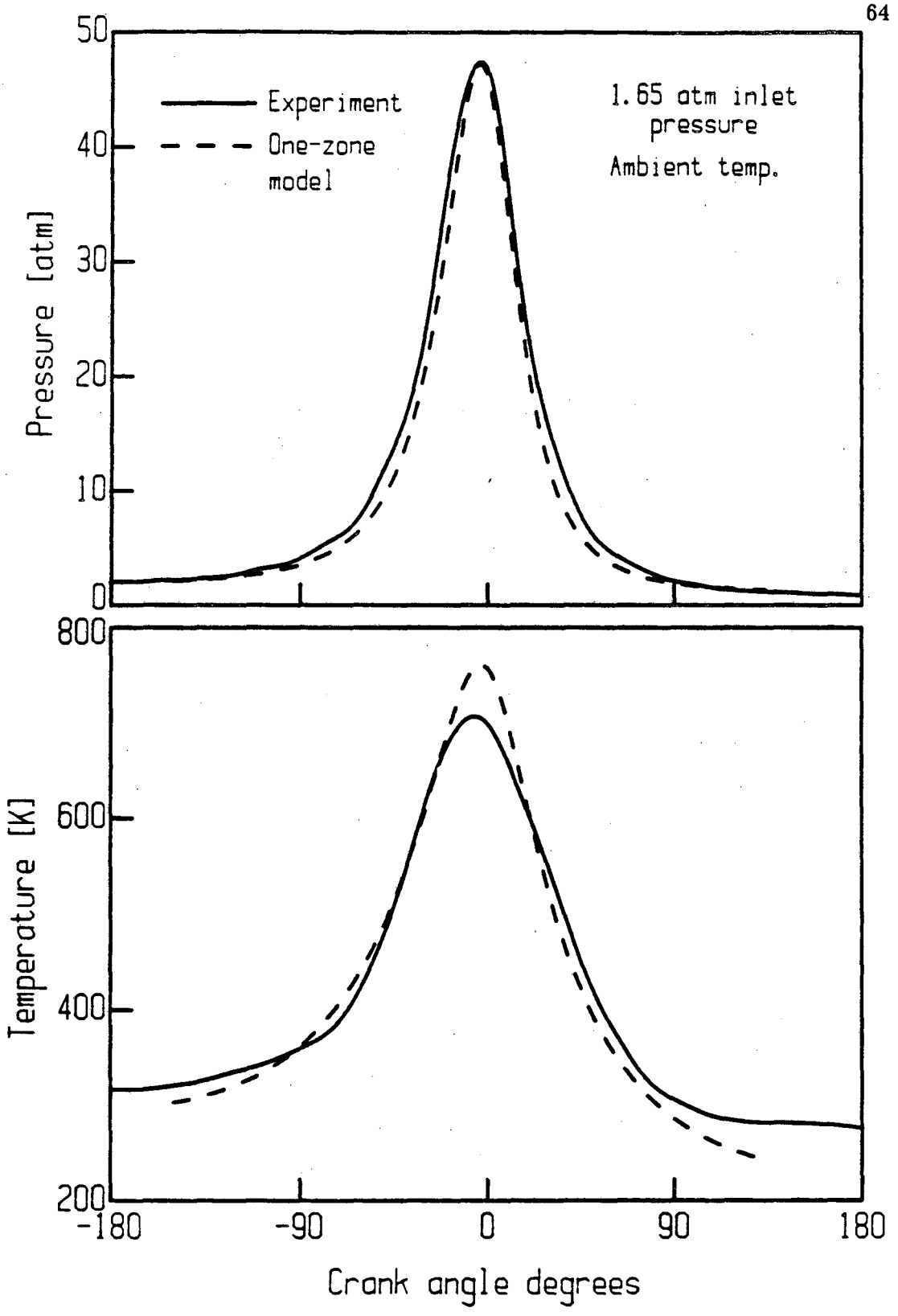

Figure 3.8. Air temperatures and pressures as measured and modelled (one-zone) for 16:1 CR, 900 rpm square piston engine for a motoring cycle with ambient inlet temperature and 1.65 atm abs actual pressure at IVC.

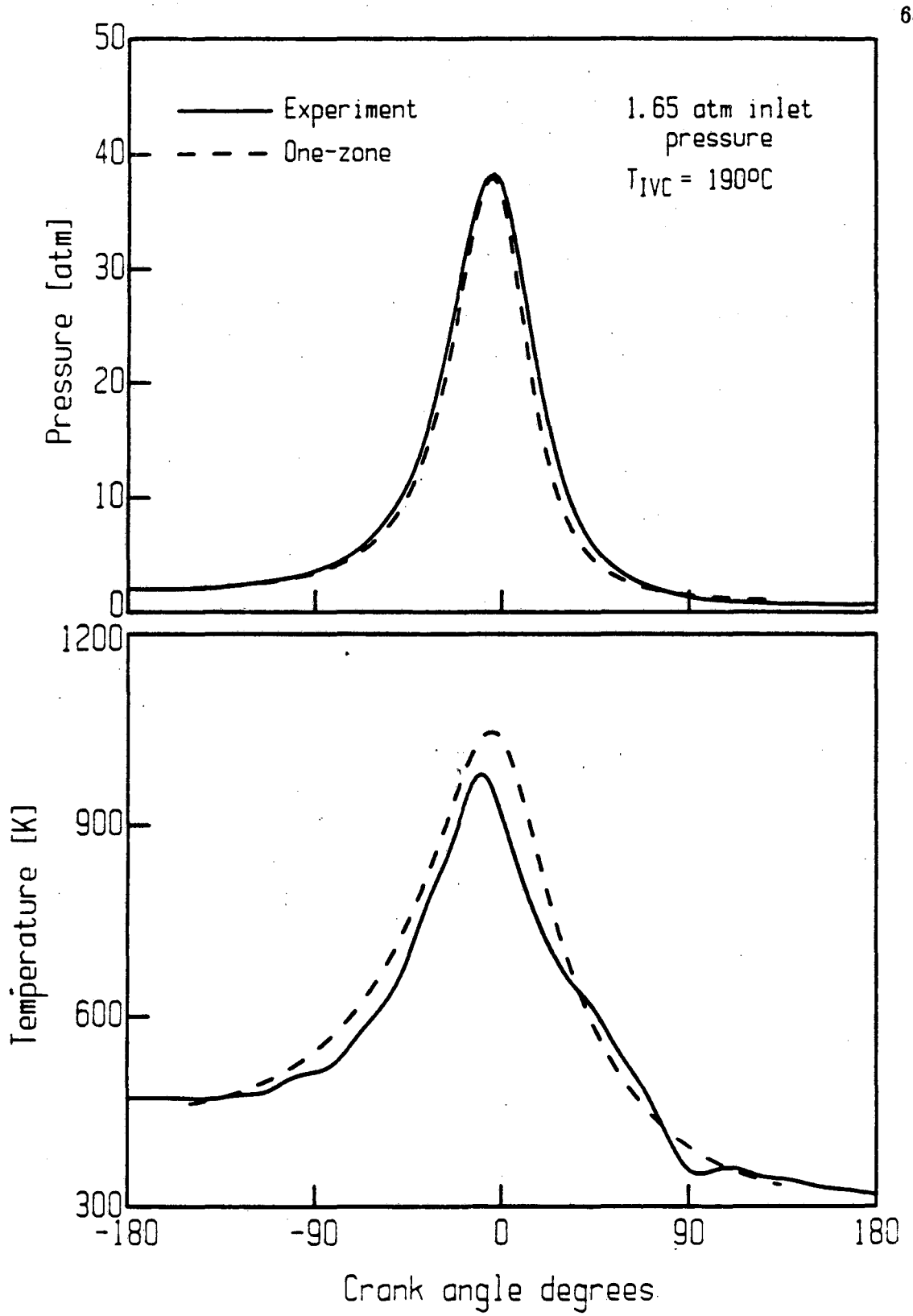

Figure 3.9. Air temperatures and pressures as measured and modelled (one-zone) for 16:1 CR, 900 rpm square piston engine for a motoring cycle with temperature of 190 ° C and 1.65 atm abs actual pressure at IVC.

temperature:

$$Q_{cr} = m_{cf}\, C_p\, (T_n'' - T_w)$$

where

$$m_{cr} = V_{cr}\, \frac{P_n''}{RT_n''}\,.$$

Results

The computation interval is one-half CAD to match the experimental data taking interval. Test cases of the simulation at one-quarter, one-half, and one CAD step size give identical results. Thus, one-half CAD is sufficiently small.

The input parameters which are varied are inlet pressure (discussed below), mass leakage factor, crevice volume, and block temperature. The crevice between the piston crown and cylinder wall is discussed in Section 2.1.2. The crevices discussed here are gaps between the head and walls from which outgassing is observed in the Schlieren movies during the expansion stroke. In the case of no supercharge and no air preheating, the two unconstrained input parameters are crevice volume and leakage factor, K. The independent variables are the temperature and pressure. K is varied from 0 to 3 and V_{cr} from 0 to 3 cm^3. The resulting peak pressures and temperatures are plotted in Fig. 3.10. Many combinations of K and V_{cr} satisfy either temperature or pressure. The solutions are plotted in Fig. 3.11. A value of K = 1.65 and V_{cr} = 2.4 cm^3 satisfies both temperature and pressure requirements. These values for K and V_{cr} are used for all

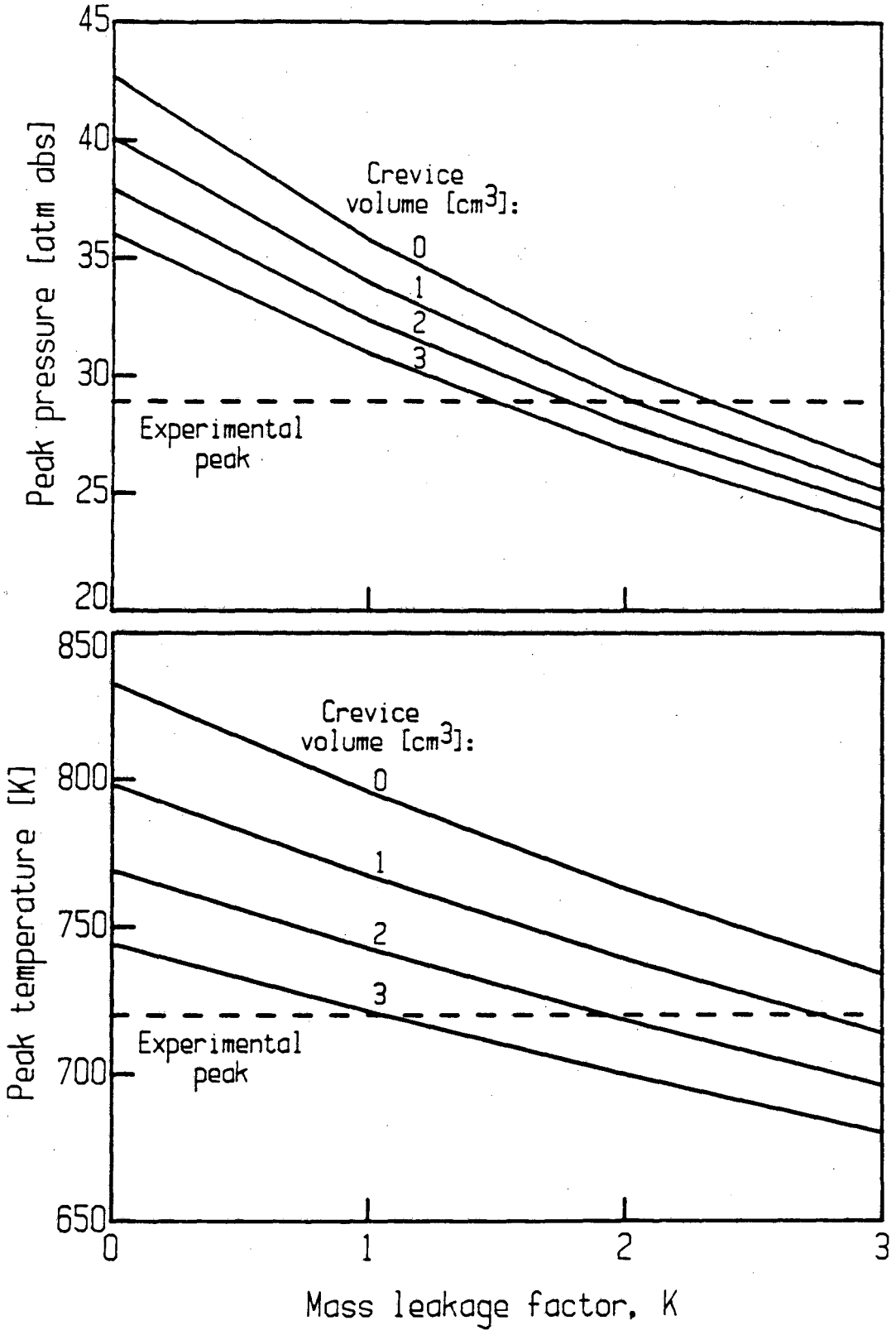

Figure 3.10. Experimental peak motoring pressure and temperature for ambient inlet condition compared to model peaks with crevice volume and mass leak factor as parameters: varied between 0-3 cm^3 and 0-3, respectively.

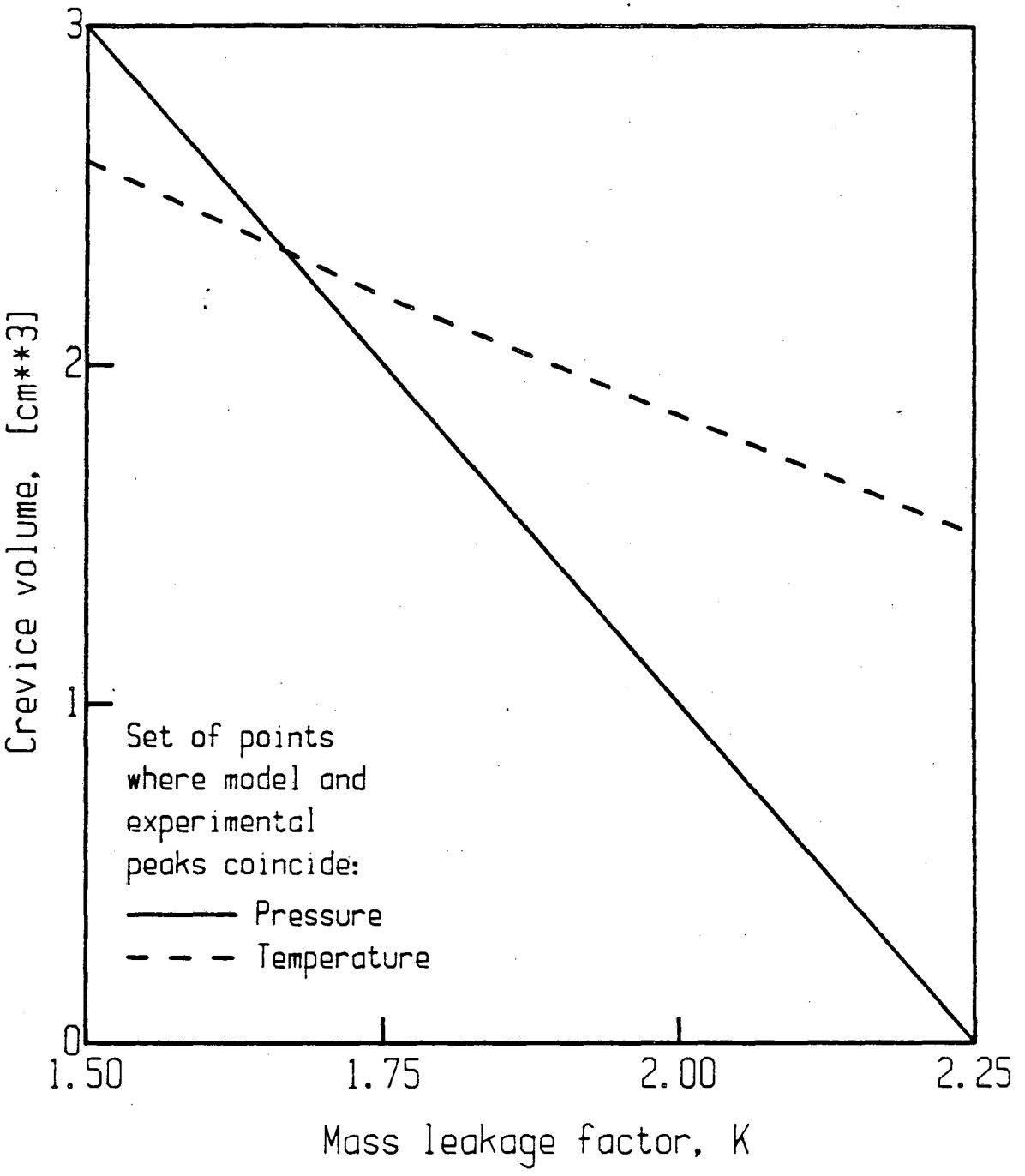

Figure 3.11. Set of solutions of crevice volume and mass leak factor matching experimental peak pressure and solutions matching experimental peak temperature plotted for case with ambient inlet conditions in 16:1 CR square piston engine simulator.

the subsequent cases at 16:1. The comparison to the experimental results is shown in Fig. 3.12.

The supercharge pressure is set at 2 atm abs. for the remaining tests. However, because a large plenum chamber or reservoir is not available on the inlet, the pressure fluctuates a significant amout due to the periodic suction of the engine intake stroke. Pressure waves are established in the inlet lines. Measurements of the inlet system pressure for a motoring cycle show a peak-to-trough variation of 0.7 atm. Thus, inlet pressures between 1.5 and 2.0 atm were modelled. Figure 3.13 shows that an inlet pressure of 1.65 atm satisfies the temperature and pressure requirements. The agreement between model and experiment is shown in Fig. 3.14.

Four cases with inlet air preheat were investigated. The fine wire thermocouple measurement at BDC of the motoring cycle (discussed in Section 3.1.1) is the initial temperature for the model calculations. Thus, for these cases, no parameters are unconstrained. Two examples of the results are shown in Figs. 3.15 and 3.16.

To attain the highest compression temperatures, the engine block is preheated by forcing 300 ° C air through the open valves. During the preheat process the fine wire thermocouple plug is replaced with a thermocouple plug in which the bead is slightly below the plug surface. The thermocouple indicates temperatures just over 100 ° C. However, the wall containing the thermocouple plug is furthest away from the valves where the heated air is introduced. Thus, the average block temperature could be considerably higher. Of the cylinder wall temperatures modelled, 150 ° C

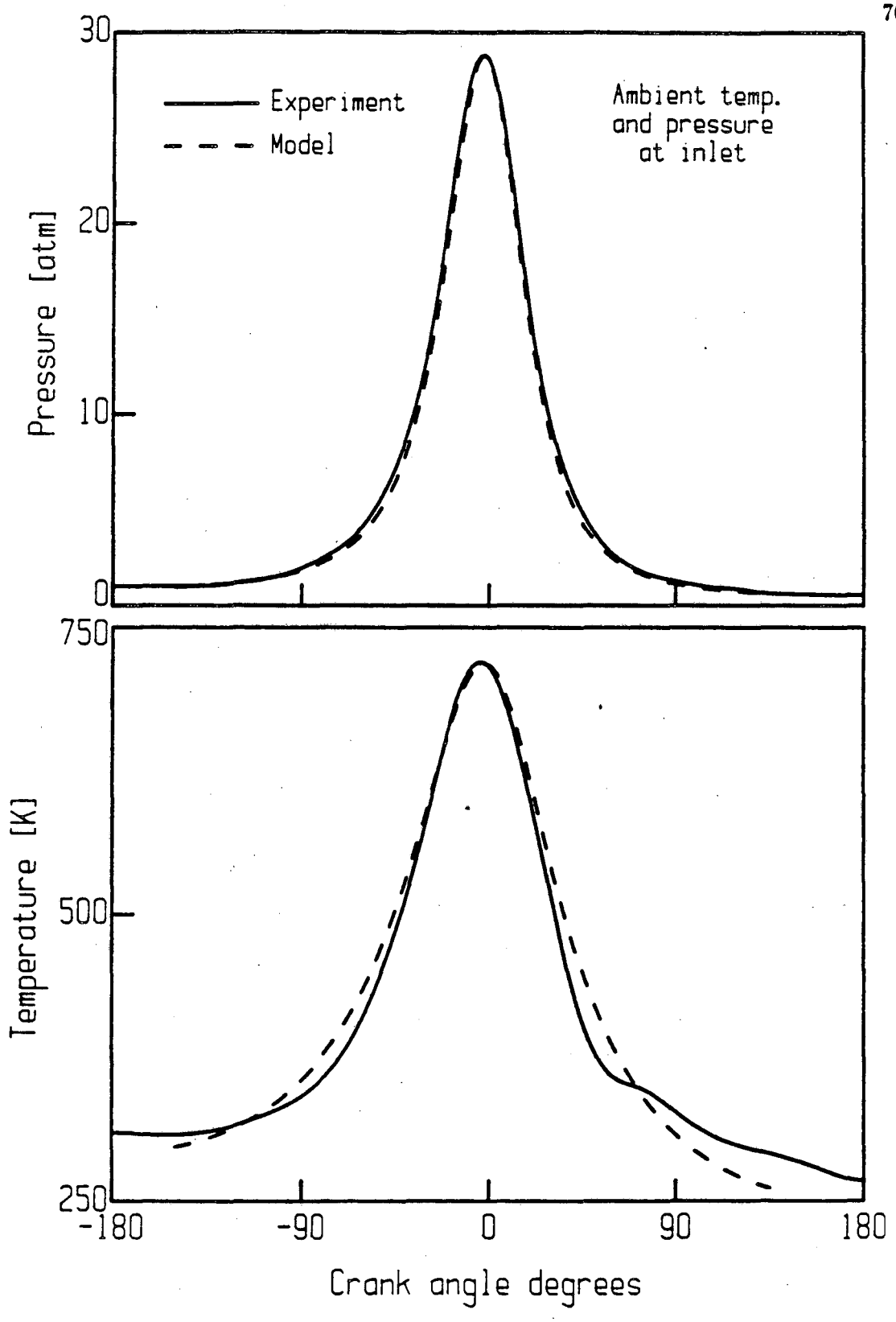

Figure 3.12. Comparison between experimental and calculated (two-zone model) temperatures and pressures for 16:1 CR, 900 rpm square piston motored engine with ambient inlet conditions.

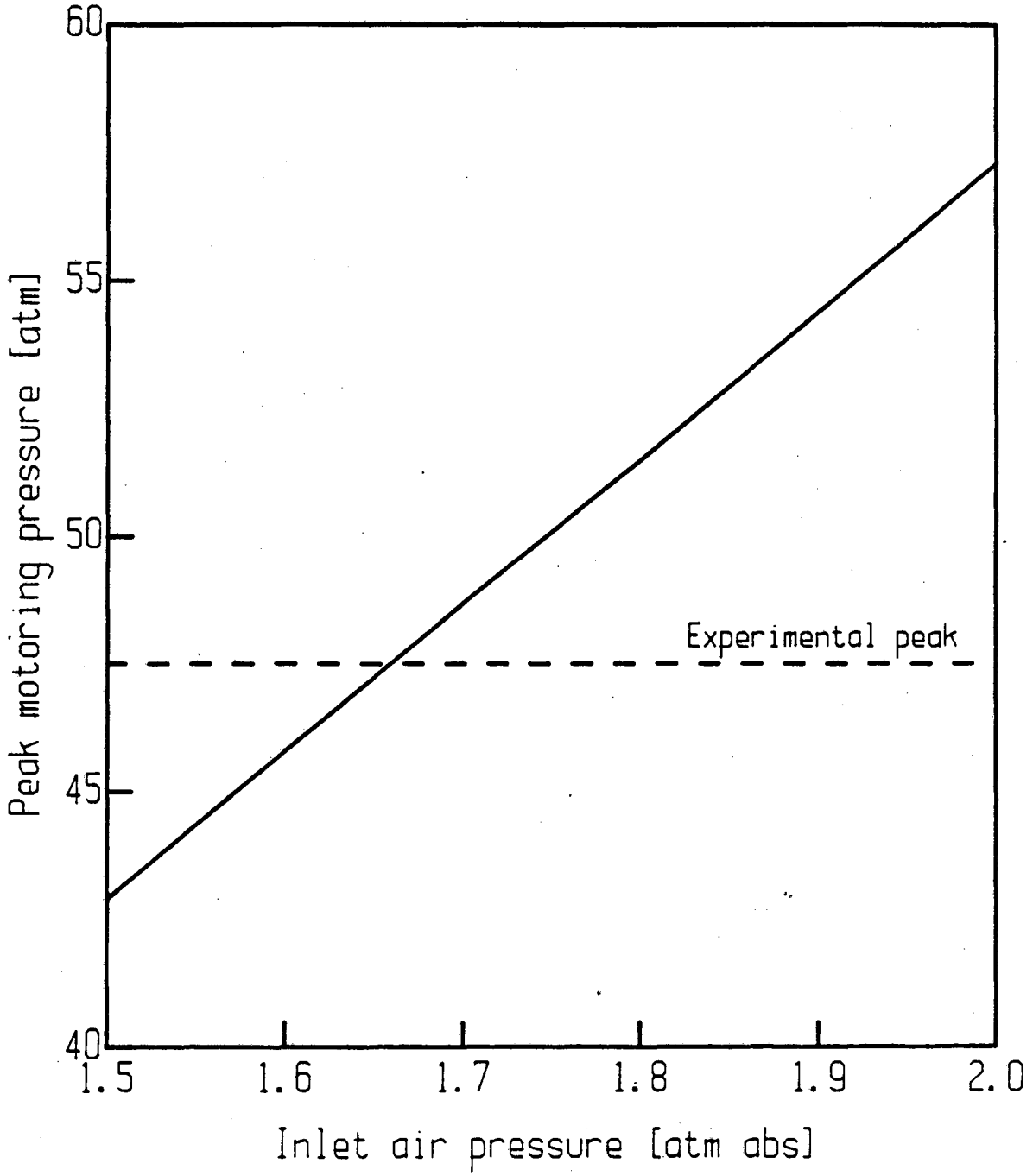

Figure 3.13. Experimental peak pressure for square piston engine with nominal 2 atm abs inlet pressure and ambient inlet temperature compared to computed peak pressure at varied inlet air pressures.

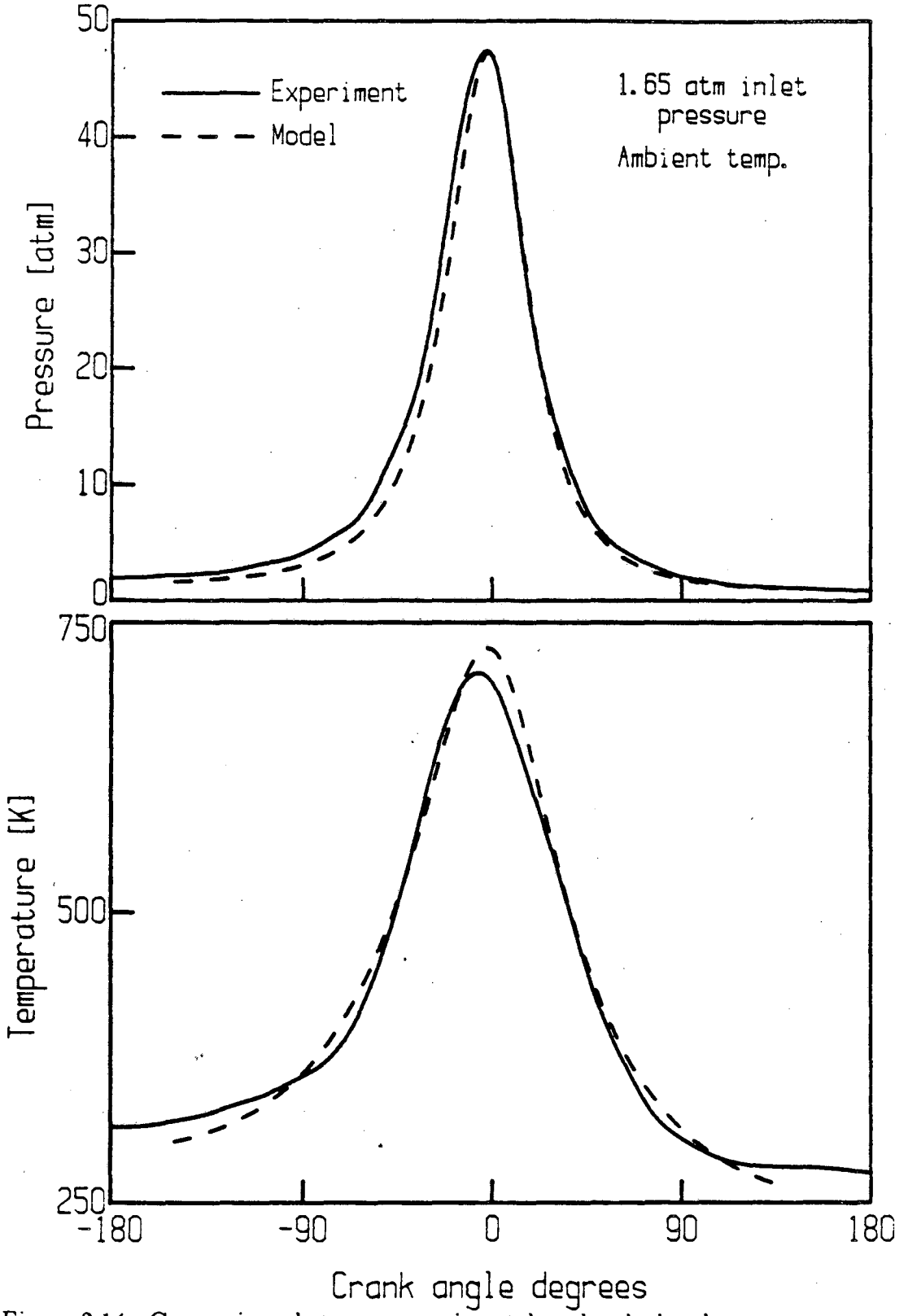

Figure 3.14. Comparison between experimental and calculated temperatures and pressures for 16:1 CR square piston engine at ambient inlet temperature and 1.65 atm abs actual pressure at IVC.

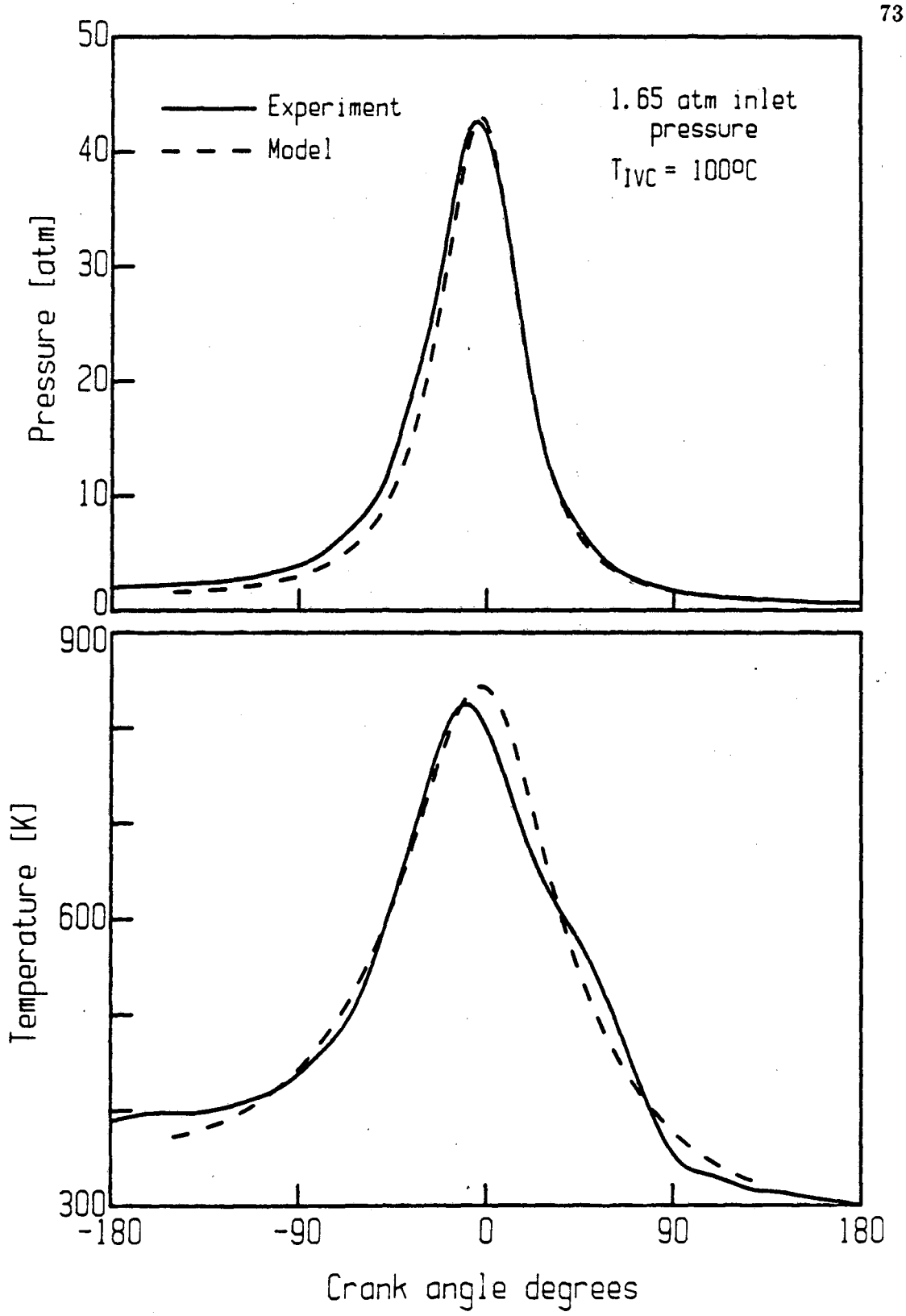

Figure 3.15. Comparison between experimental and calculated temperatures and pressures for motored square piston engine simulator with following conditions at IVC: 100 ° C, 1.65 atm abs.

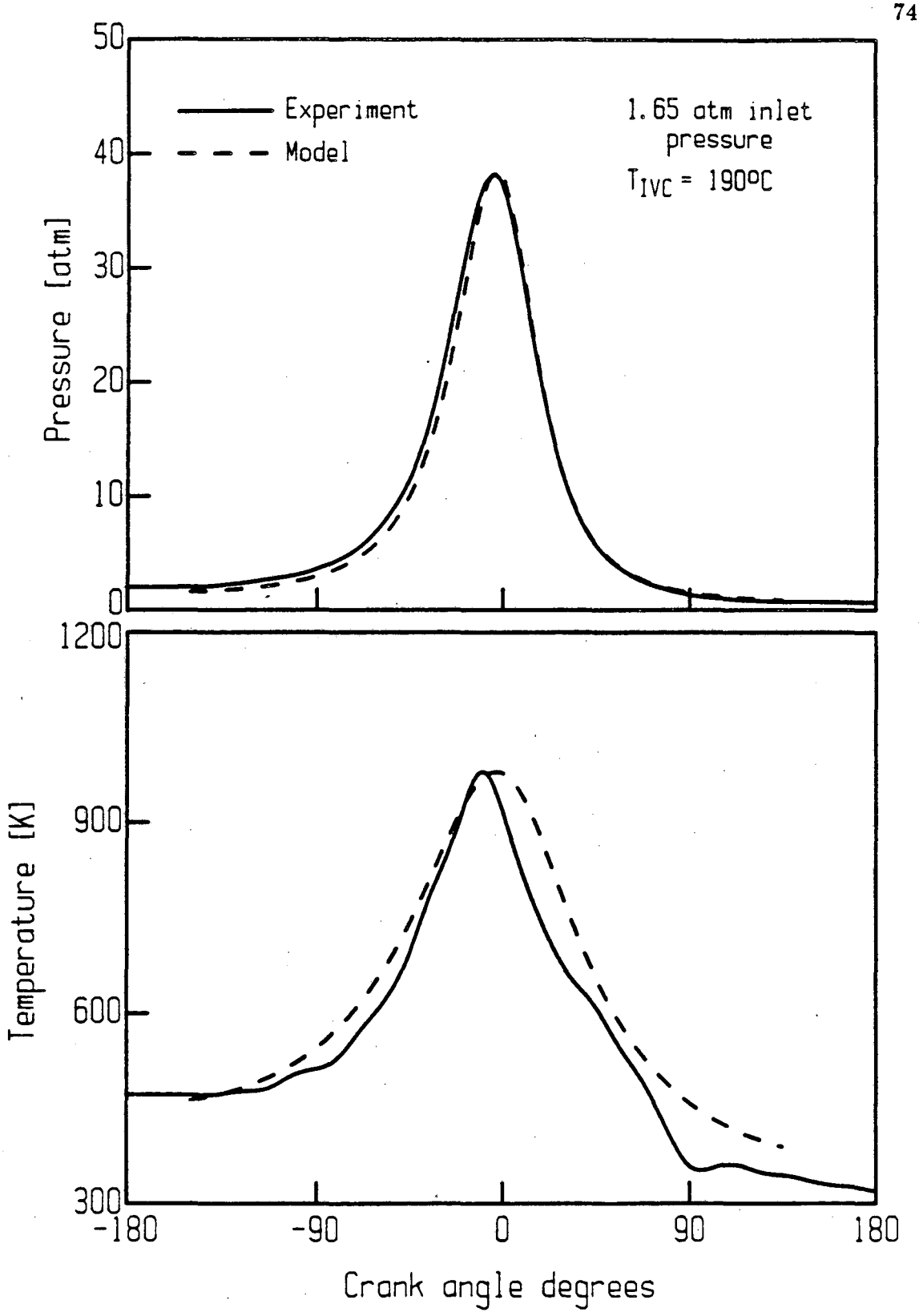

Figure 3.16. Comparison between experimental and calculated temperatures and pressures for motored square piston engine simulator with following conditions at IVC: 190 ° C, 1.65 atm abs.

provides the best compromise at fitting the temperature and pressure. The results are plotted in Fig. 3.17.

Coal/water slurry does not ignite at 16:1 compression ratio with inlet air and block preheating. Therefore, a compression ratio of 22:1 with a heated engine block is attempted. The lower surface of the thermocouple probe is located approximately 5 mm below the cylinder head. Temperatures cannot be measured at 22:1 as the clearance height is 4.0 mm. So, the model is used to estimate the motoring temperatures. Using the crevice volume of 2.4 cm^3, an inlet pressure of 1.65 atm, and mass leak factor of 1.65, the model's peak motoring pressure is significantly higher than the experimental peaks, demonstrated by the dashed and solid lines in Fig. 3.18. But, the dash-dot curve in same figure for a mass leak rate of 2.25 closely aligns with the least squares fit of the experimental data. The piston is severely scuffed (metal transfer between sliding surfaces from adhesive forces) after experiments with a preheated block. Metal particles lodge in between the top piston ring set and the groove preventing free movement. The rings stick in place and are no longer pushed out (by the leaf springs) against the walls for sealing. In light of the lower sealing capability of the piston rings after block preheating, it is reasonable to use the higher leak rate coefficient.

The temperatures for three inlet temperatures with no block heating and two temperatures with block heating are shown in Fig. 3.19. The difference in the general shape of the unheated versus heated block temperature profiles arises from the inclusion of a crevice zone in the model. At 22:1 the crevice accounts for 10% of the combustion chamber volume at TDC. Because the temperature in the

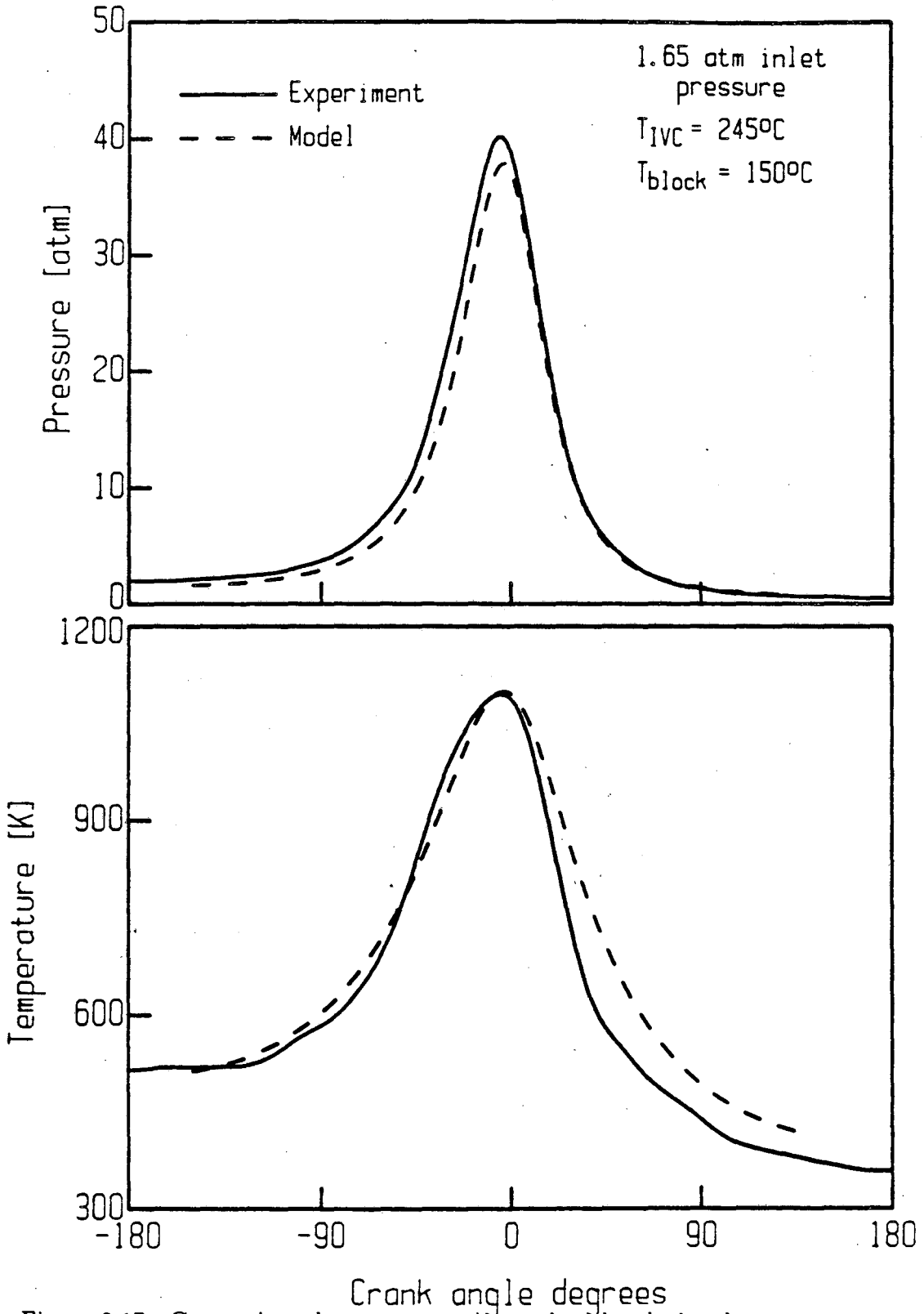

Figure 3.17. Comparison between experimental and calculated temperatures and pressures for square piston engine with block heated to 150 °C. Inlet air temperature and pressure at IVC are: 245 °C and 1.65 atm abs, respectively.

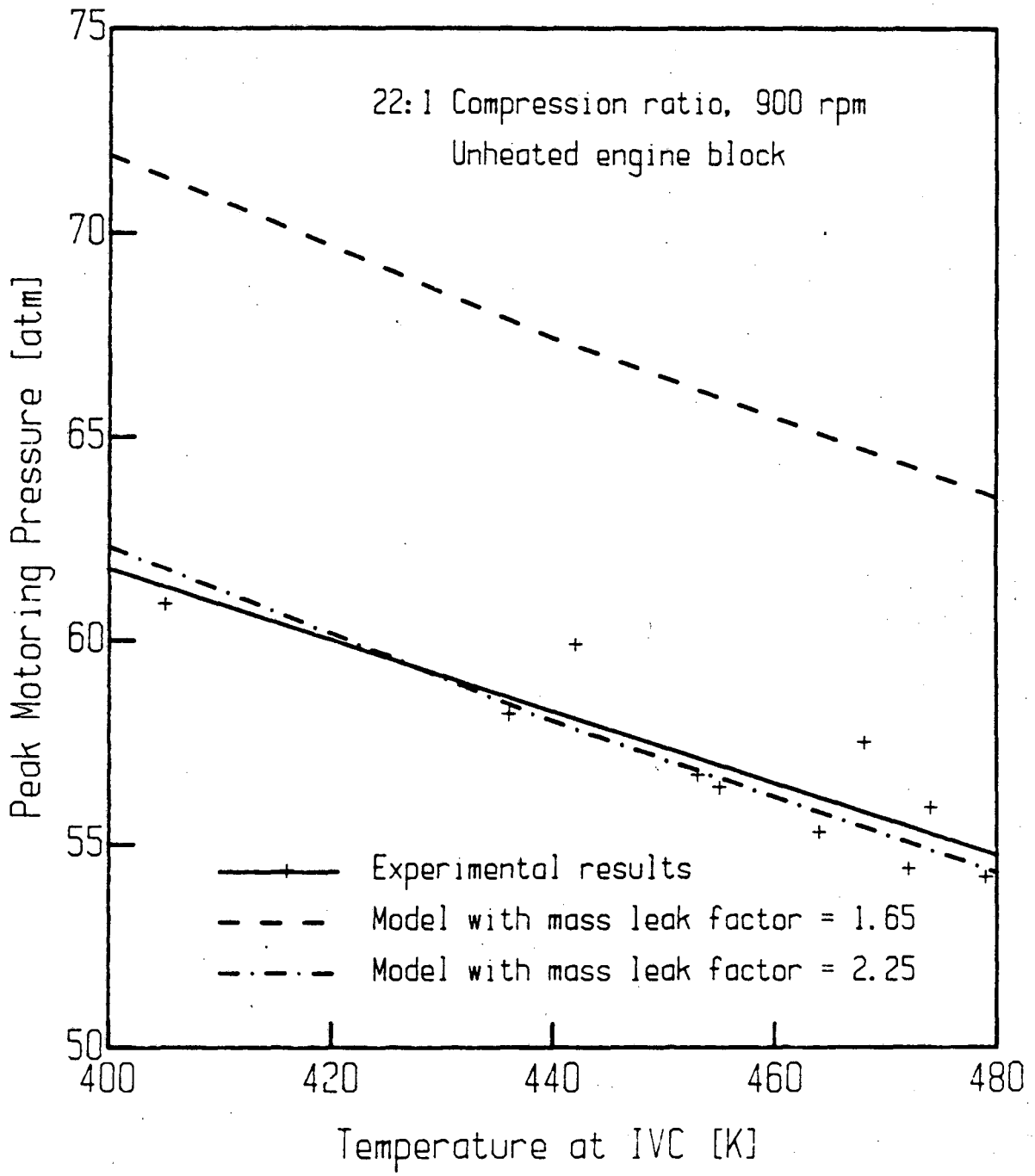

Figure 3.18. Peak motoring pressure for 22:1 CR, 900 rpm square piston engine with IVC temperatures of 400-480 °C from experimental results and two cases of computed results with mass leak factor of 1.65 and 2.25.

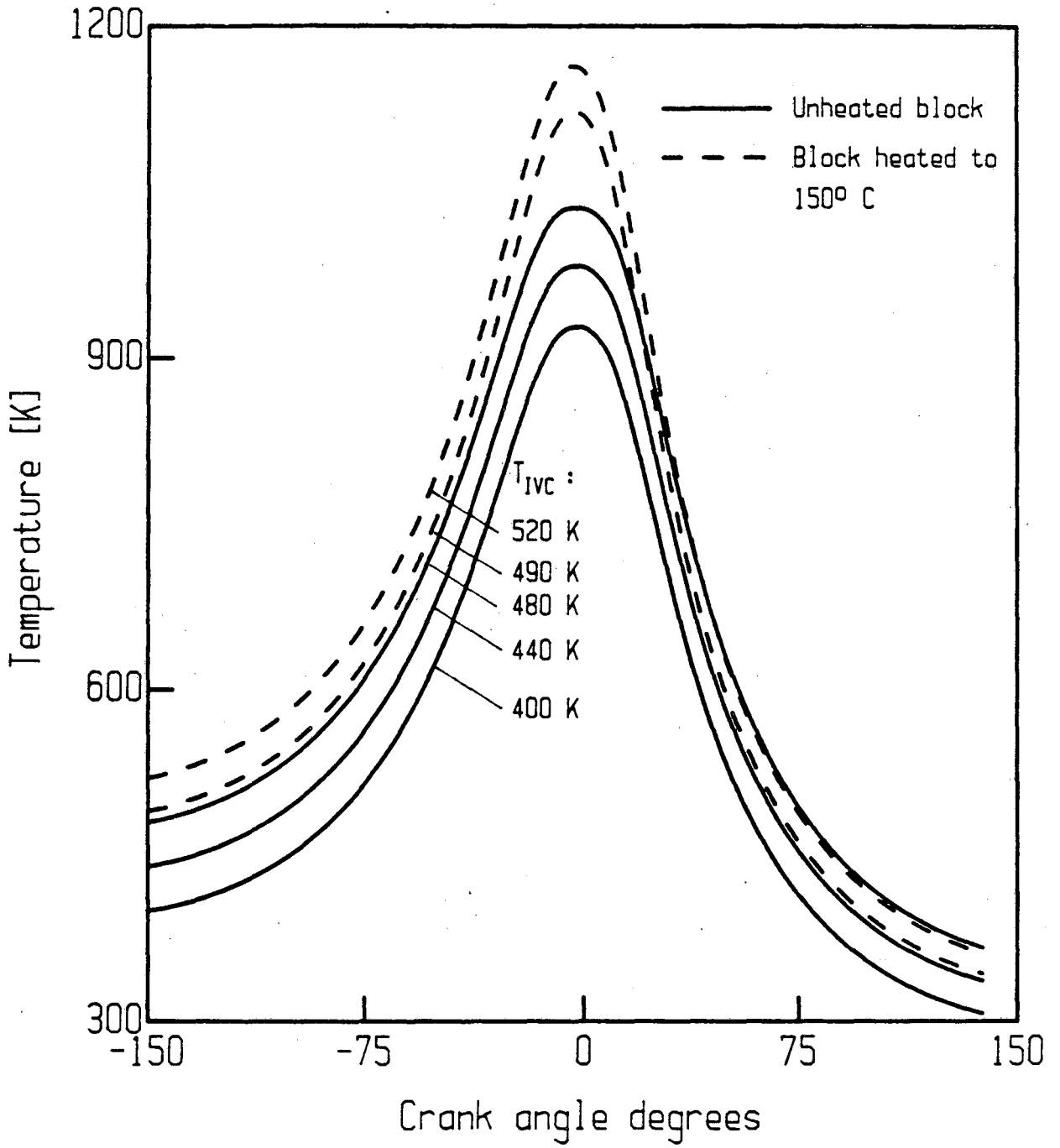

Figure 3.19. Motored square piston engine (22:1 CR) temperatures computed by two-zone model for three inlet temperatures with unheated block and two temperatures with 150 °C block. Mass leak factor is 2.25.

crevice is less than the bulk gas zone, more than 10% of the mass is in the crevice zone. An increase of the mass in the crevice affects the temperature profile similar to that of a reduction in compression ratio. The 150 ° C crevice retains less mass than the ambient crevice. Therefore, the heated block cases show steeper slopes on both sides of TDC. Also, the higher pressures with block heating result in higher mass leakage which accounts for the heated block temperatures going below unheated block temperatures on the expansion stroke. The temperatures in Fig. 3.19 are used for the Arrhenius relation computations.

The leak rate from the combustion chamber is estimated for purposes of temperature prediction. As a consequence, mass in the cylinder as a function of CAD is also known. The experimental values of temperature, pressure, and volume also give an estimate of the mass in the cylinder. Both model and experimental computations of mass are plotted in Fig. 3.20. Both experiment and model results indicate that approximately 30% of the mass is lost in each compression-expansion cycle for this case with ambient inlet conditions.

The case with ambient temperature and a nominal 2 atm of supercharge is compared in Fig. 3.21 with an adiabatic, no leak run at the same inlet conditions. The pressure is reduced by about 30% from adiabatic whereas the temperature is reduced by about 15%. The effect that the mass loss has on the temperature and pressure is modelled as an adiabatic expansion. Since the pressure ratio is raised to the power of the specific heats ratio and the temperature ratio to the specific heats ratio minus one power, the pressure drops faster than the temperature. The model

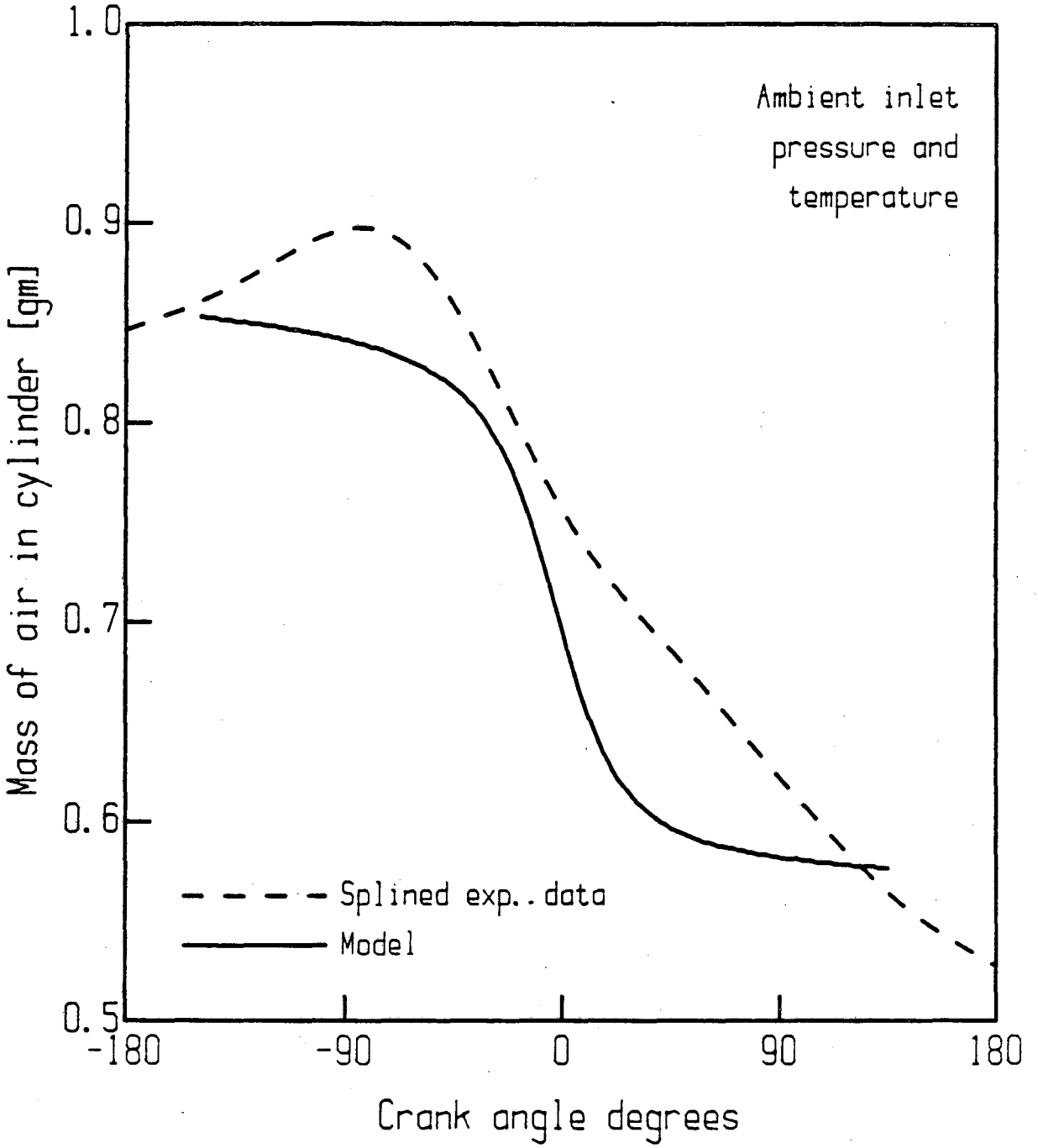

Figure 3.20. Comparison between model prediction of mass in cylinder with computations from experimental pressure, temperature, and volume values for case with ambient inlet air conditions in 16:1 CR, 900 rpm square piston engine.

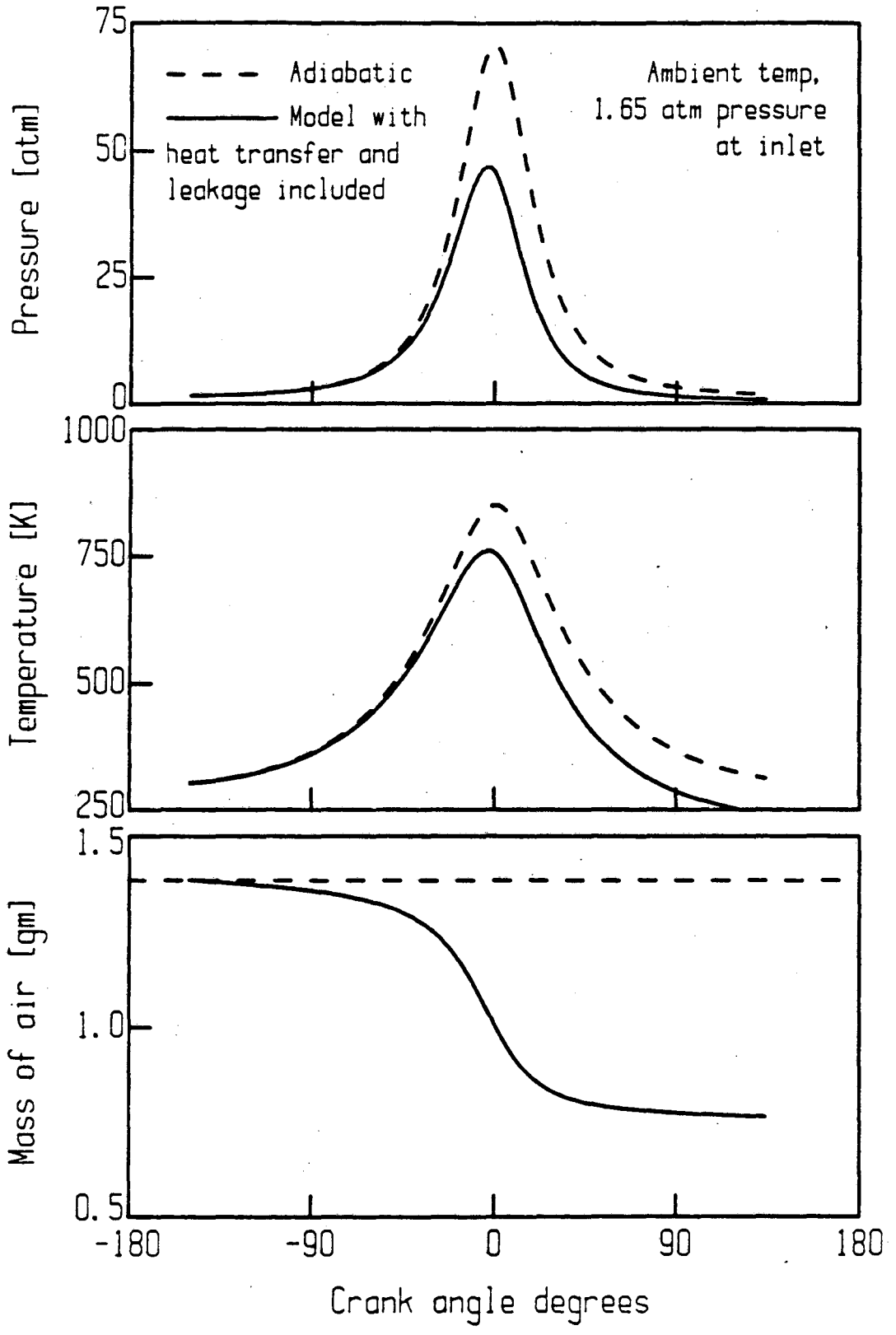

Figure 3.21. Calculated pressure temperature and mass in cylinder using two-zone model for isentropic compression-expression with no leakage and for cycle with heat transfer and leakage included. Motoring cycle of square piston engine (16:1 CR) with ambient inlet temperature and 1.65 atm actual inlet pressure.

predicts a 40% mass loss in one cycle for 2 atm inlet pressure. This is consistent with the 30% loss shown in Fig. 3.20 with no supercharge.

3.2. COMBUSTING CYCLE

The definition for ignition delay is discussed in Section 1.2. To apply Eqn. 1.1, the following quantities must be known: air temperature and pressure at the time of injection, the time of the start of injection, and the time of the start of combustion. The temperature at injection is taken from corrected thermocouple measurements for 16:1 CR and from the engine model (Section 3.1.2) for 22:1 CR. Pressure is directly measured by a piezoelectric transducer. The beginning of the ignition delay interval is defined by the injector needle opening. The end of the luminosity and pressure delay times are known by measuring the initial combustion radiation emitted and the pressure rise, respectively. The combusting pressure rise is compared to a run at the same condition without fuel injection and combustion to determine when significant pressure rise from combustion occurs. An example of the ignition delay measurements is shown in Fig. 3.22.

The analyses to compute work and rate of energy release are discussed in Section 1.2. Due to higher leak rates encountered in the square piston engine simulator compared to engines with cylindrical geometry, the work and energy release calculations are indexed by a comparable motoring cycle. That is, work is computed by subtracting motoring cycle work (always a negative quantity) from

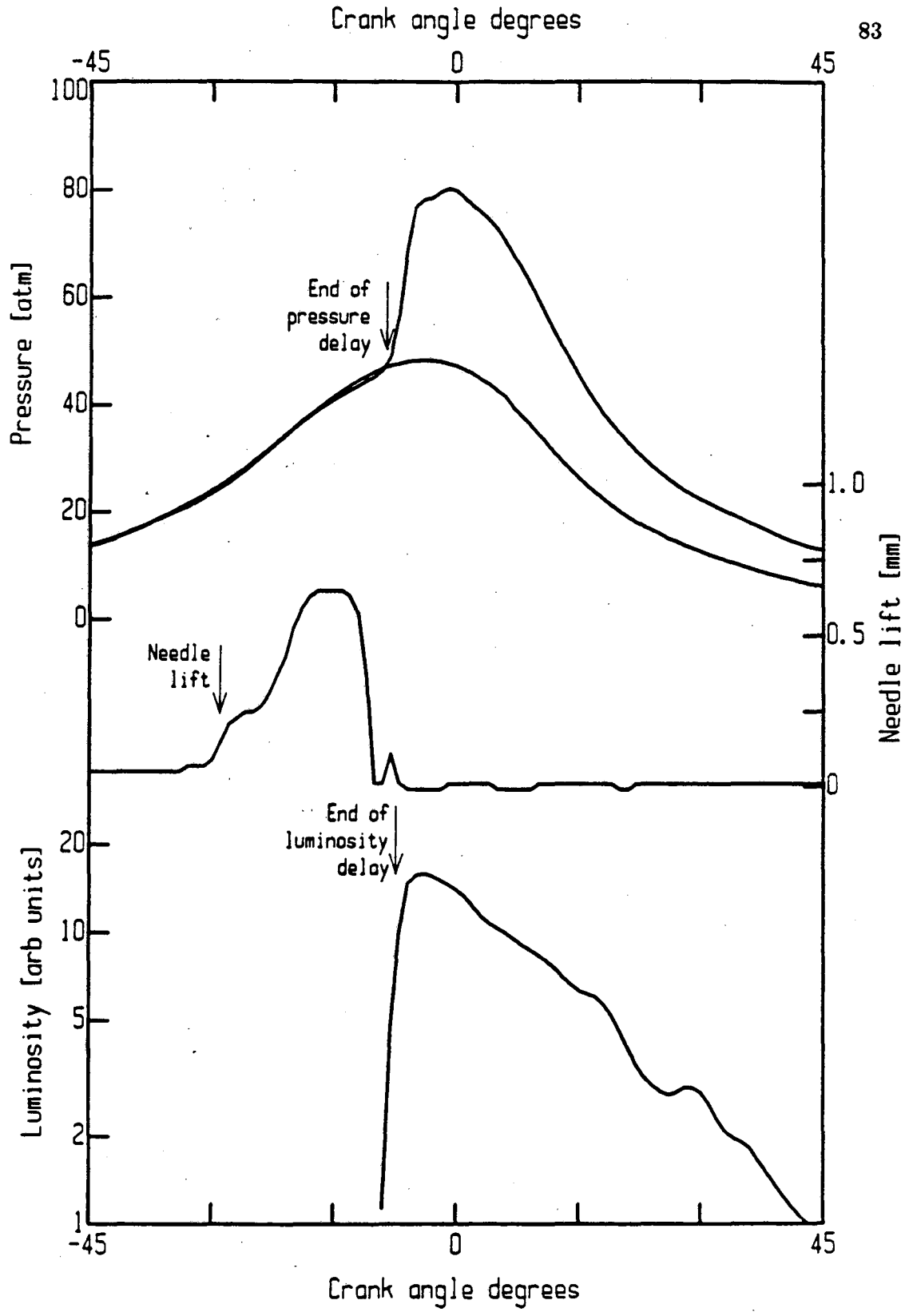

Figure 3.22. Cylinder pressure for a burning and a corresponding motoring run in the square piston engine simulator with the needle lift and luminosity traces indicating the technique for determining start of injection and start of combustion by pressure and luminosity methods.

the combusting cycle:

$$W = \int P_{comb} dV - \int P_{mot} dV \, .$$

$$\text{Also, } Q = \int \frac{dQ_{comb}}{d\theta} \, d\theta - \int \frac{dQ_{mot}}{d\theta} \, d\theta \, .$$

The same holds true for calculating the energy released as shown in the above equation.

In a conventional engine, efficiencies are measured by adjusting the injection timing and fuel delivery rate to provide a given power level and rpm. The injection timing is optimized to minimize the fueling rate without incurring diesel knock. The square piston engine simulator makes this measurement difficult because of the single event nature of the combustion. The shaft power from a conventional engine on a dynamoneter is measured continuously. The only measure for power for the square piston engine simulator is the indicated power. Indicated power is computed from the work per cycle and is greater than the shaft power by the amount of power absorbed by engine friction. The amount of fuel injected and the injection timing are measurable on the square piston engine simulator. But, they cannot be controlled to tight tolerances. Due to the 5 CAD range in injection timing and the 5 mg range in fuel rate at the same settings, the number of tests required to evaluate the true thermal efficiency at each condition is prohibitively large. Even if the efficiency is measured, the knocking limits can not be determined. Diesel knock is normally detected by listening to an engine running at steady state. Knock can also be evaluated by comparing rate of pressure rise in the cylinder to known knocking and nonknocking cases. Knocking operation is not detectable in the

square piston engine because of the highly unsteady manner of operation. Because of these difficulties, a complete analysis is not presented; sample values of the thermal and combustion efficiencies are presented in Section 4.4 below.

4. RESULTS AND DISCUSSION

4.1. FUEL INJECTION

Previous researchers report problems injecting coal slurries. Therefore, preliminary injection tests on the bench facility (Section 2.2.3, Fig. 2.8) were conducted and reported by Dickson (1983). Injection line pressure and shadowgraphs of the spray were used to evaluate the spray atomization and injection equipment reliability for the slurries. The engine block was heated for coal/water engine experiments. To determine the effect heating had on the water slurry, additional tests were conducted with a heating coil placed around the injector. The injection parameters varied were: needle opening pressure (75-200 atm), nozzle orifice diameter (0.254-0.635 mm), and rack setting (8-20 mm^3 or 5-60 mm^3). Dickson concluded that:

- the atomization improved with smaller nozzle diameter.
- the slurries frequently plugged with an orifice less than 0.33 mm diameter.
- the atomization improved with higher needle opening pressures.
- opening pressures above 200 atm damaged the orifice.
- moderate rack openings gave the best atomization.
- the atomization of coal slurries was poorer for slurries than diesel fuel as observed by shadowgraphs.
- it was not possible to inject coal/slurries when they attained temperatures above 100 ° C because they became extremely viscous.

The 0.33 mm diameter orifice and 200 atm needle opening pressure is used for all the engine studies. Also, the water slurry temperature is held below 100 ° C.

The mass of fuel injected per stroke is also measured on the bench test. A paper cup with loose cotton placed in the bottom is used to catch the fuel issuing from the nozzle. Diesel fuel and coal/diesel slurry injections into atmospheric air and into a pressure vessel at 25 atm are collected and weighed. During the engine tests, the mass of fuel is computed from the injection line pressure or the needle lift records; sample traces are shown in Fig. 4.1. (Both the pressure and needle lift have negative values in Fig. 4.1. The negative needle lift is caused by vibrations giving erroneous readings. The pressure in the injection line remains above atmospheric between tests. Piezoelectric pressure transducers do not provide an absolute measure of pressure, but, relative pressures instead. The data taking routine arbitrarily assumes the pressure at time 0 is 0 atm gauge.)

The rate of fuel injection relates to the line pressure through Bernoulli's relation. An empirical discharge coefficient, C_D, is inserted:

$$\dot{m}_f = C_D \, a \, \sqrt{2\rho \, \Delta P}$$

where m_f is the mass of fuel injected, a the nozzle area, ρ the fuel density, and ΔP the pressure difference. To compute the mass over the injection interval, integrate over time:

$$m_f = C_D \, a \, \sqrt{2\rho} \int \sqrt{\Delta P} \, dt$$

(The pressure is integrated only for the shaded region in Fig. 4.1.). Austen and Lyn (1960-61) report that the discharge coefficient for hole type nozzles is

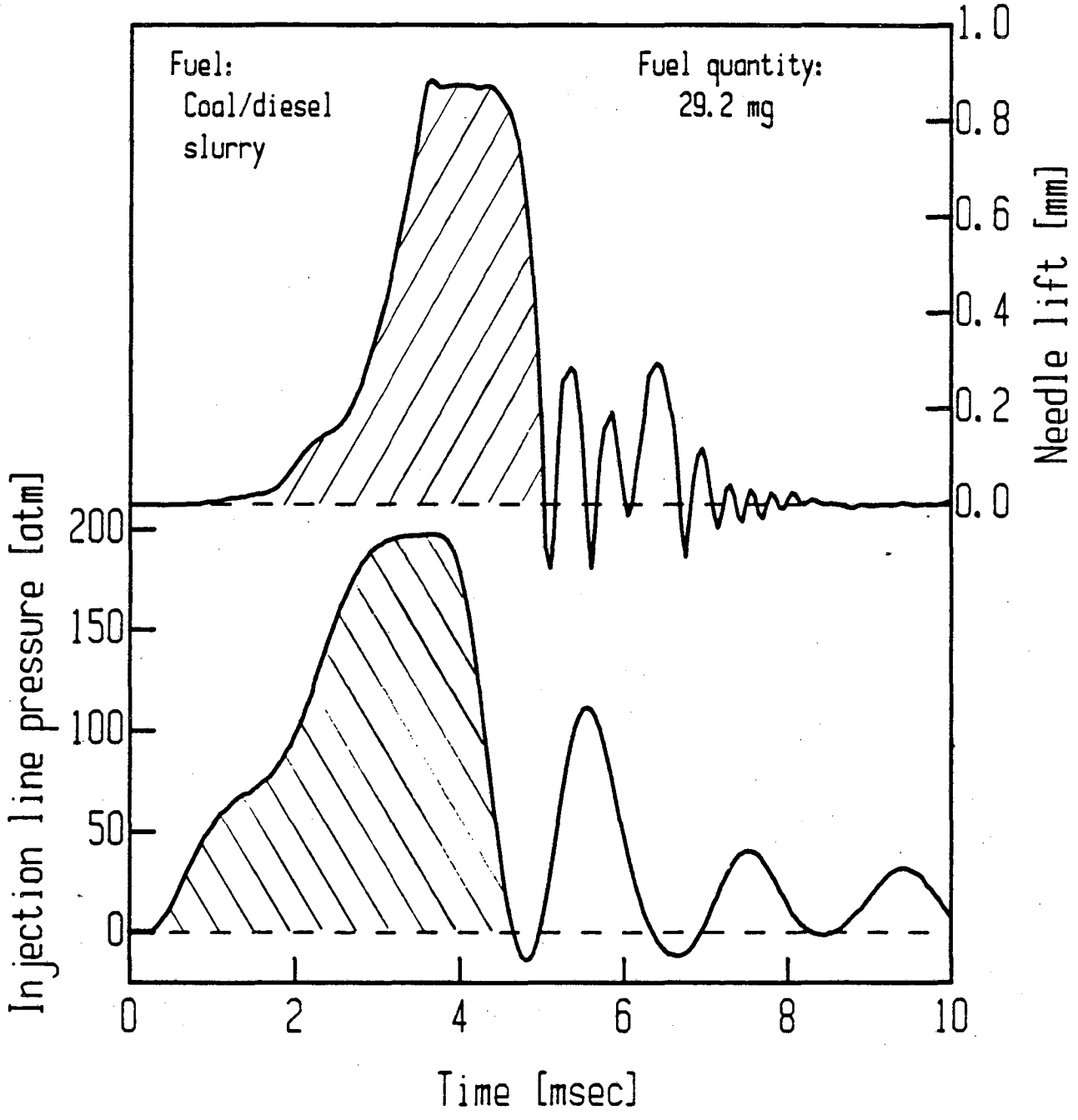

Figure 4.1. Injection line pressure and needle lift history for coal/diesel slurry injection on bench test outside of engine.

approximately 0.7. To check this value for C_D, the actual mass and the calculated mass if C_D equals one are shown in Fig. 4.2. A least squares analysis indicates that:

$$m_f = 0.57\ a\ \sqrt{2\rho} \int \sqrt{\Delta P}\ dt + 12.9\ \ [mg]\ . \tag{4.1}$$

Thus, C_D is found to be approximately 0.57. If the actual diameter of the nozzle is smaller than that measured under a stereo microscope (*eg*, due to blockage) then the computed C_D will be smaller than expected. As little deviation as 5% or 0.02 mm accounts for the discrepancy. Normally, a zero intercept in Fig. 4.2 is expected. But, in this case with a spring loaded needle pressed against the orifice, the pressure builds before fuel is injected and the needle covers the orifice before the pressure drops fully. Thus for this system, the calculated mass overpredicts by 12.9 mg.

Integrating the expression in Eqn. 4.1 above to determine the mass of fuel injected is somewhat cumbersome. Also, the injection line pressure was not measured for all the tests in the engine. Therefore, a correlation between the injector needle lift and the measured mass is desired. The needle lift integrated over time versus actual mass is shown in Fig. 4.3. (Integration is performed for the shaded area only in Fig. 4.1.) Results from three cases, diesel fuel and coal/diesel (corrected for difference in specific gravity) at atmospheric pressure and diesel fuel at 25 atm, show a strong correlation between the integrated lift and the mass injected. The correlation is very strong at the higher values of mass injected which corresponds to the majority of the cases tested in the engine. Neither the fuel type nor the pressure in the vessel affects the relationship between these quantities:

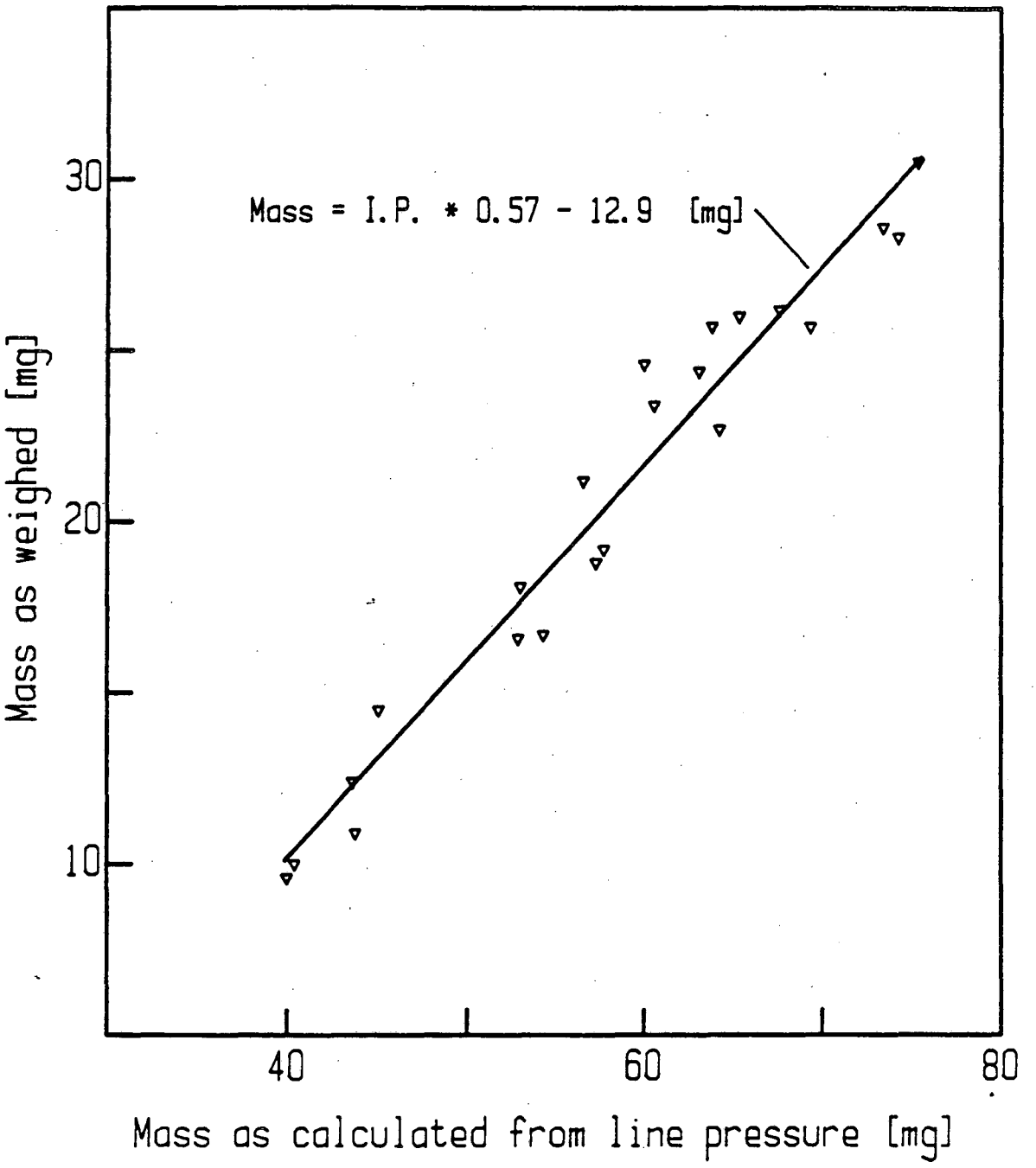

Figure 4.2. Weighed mass of fuel injected versus the computed mass from the line pressure using Bernoulli's relation for diesel No. 2 injected into atmospheric pressure.

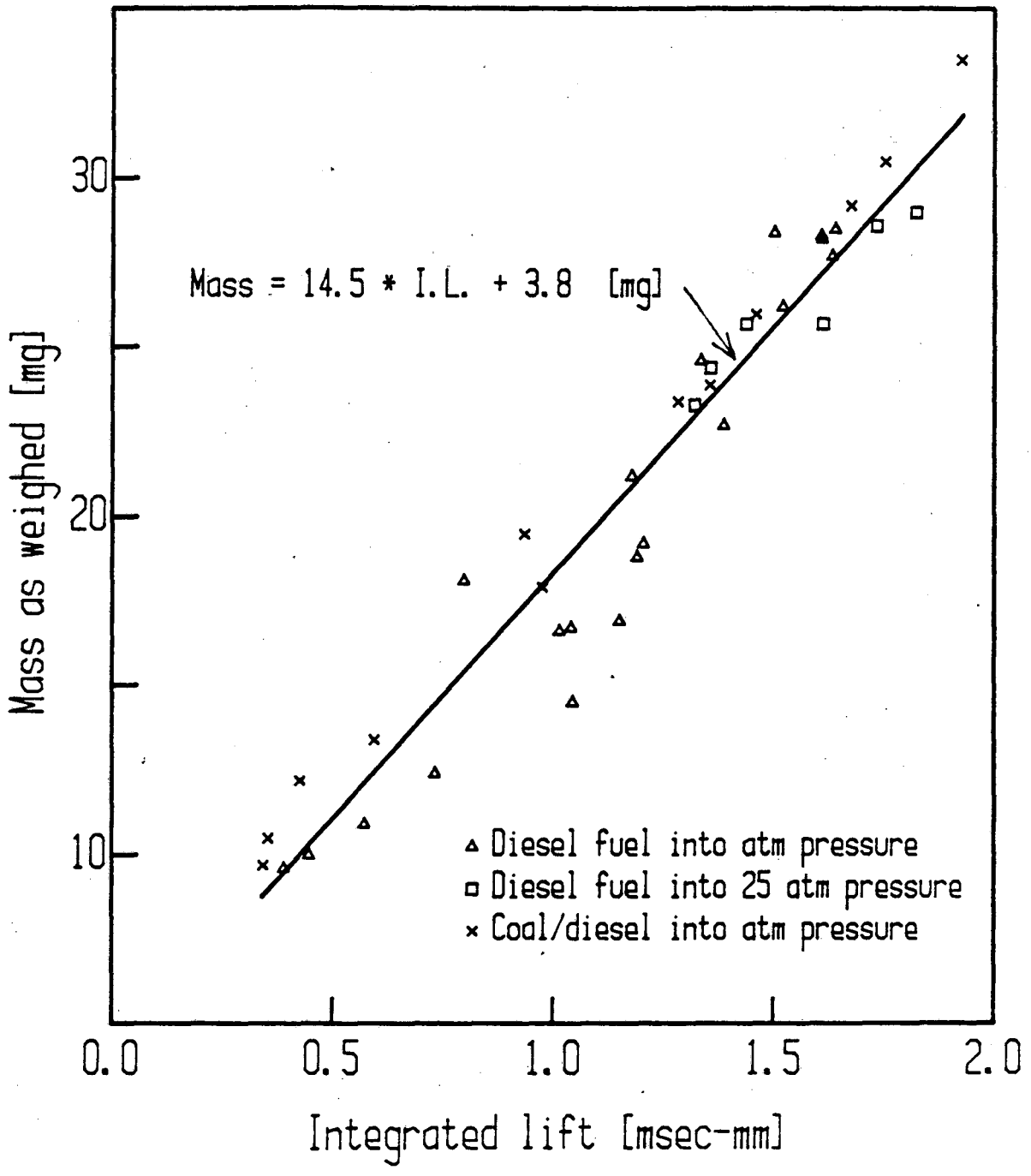

Figure 4.3. Weighed mass of fuel injected versus the computed mass from the integrated needle lift for diesel No. 2 at atmospheric and 25 atm pressure and for coal/diesel slurry.

$$m_f = 14.5\ IL + 3.8\ \ [mg]\ , \tag{4.2}$$

where IL is the needle lift integrated over time in mm-msec. Two sample traces are shown in Figs. 4.4 and 4.5: one with a small quantity and one with a large quantity of fuel injected. The weighed fuel is given along with line pressure and needle lift estimates for mass injected from the correlations of Eqns. 4.1 and 4.2, respectively. The mass of fuel injected into the engine is computed from the integrated lift equation in all cases.

4.2. CONDITIONS FOR IGNITION OF FUELS

The longest ignition delays measured in the square piston engine simulator at 900 rpm are less than 10 msec (54 CAD). For injection at about 20 °BTDC, ignition occurs as late as 35 °ATDC. After this CAD, the lower temperatures and pressures from expansion do not permit substantial chemical activity. Ignition at 35 °ATDC is not of practical significance; it does, however, provide information concerning the ignition characteristics of the fuels.

Ignition of coal/water slurry is not possible under the conditions attainable in the square piston engine facility under the current configuration, *i.e.*, up to 22:1 CR, 150 °C block temperature, and 250 °C inlet temperature at IVC. The temperatures and pressures attained at the time of coal water slurry injection for 16:1 and 22:1 CR tests are shown in Fig. 4.6. Neither pressure rise nor significant luminosity are observed at any of the these conditions in the approximately 10 msec available for combustion.

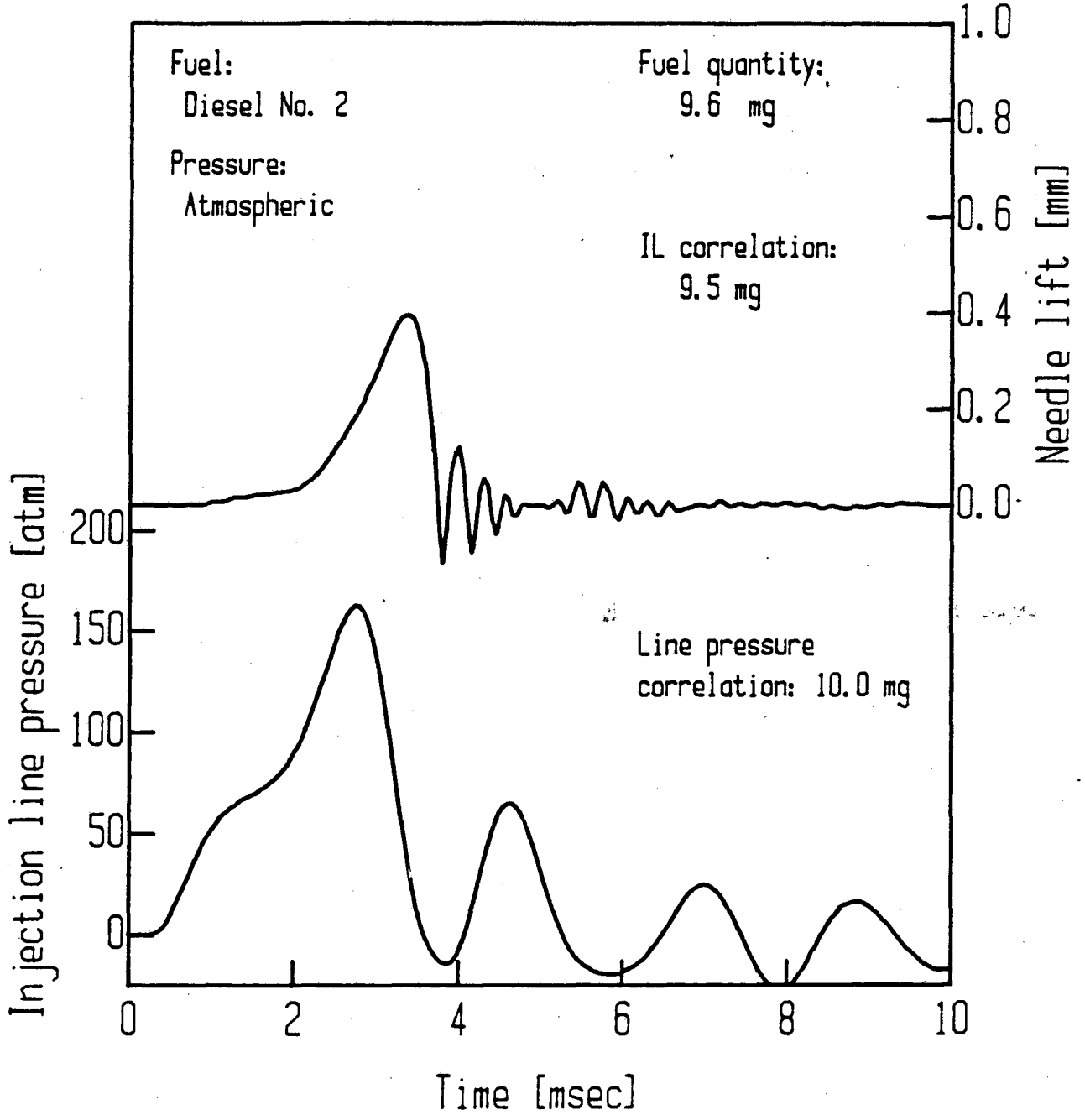

Figure 4.4. Injection line pressure and needle lift traces for diesel fuel into atmospheric pressure with comparison data for weighed mass and computed mass for the needle lift and line pressure correlations.

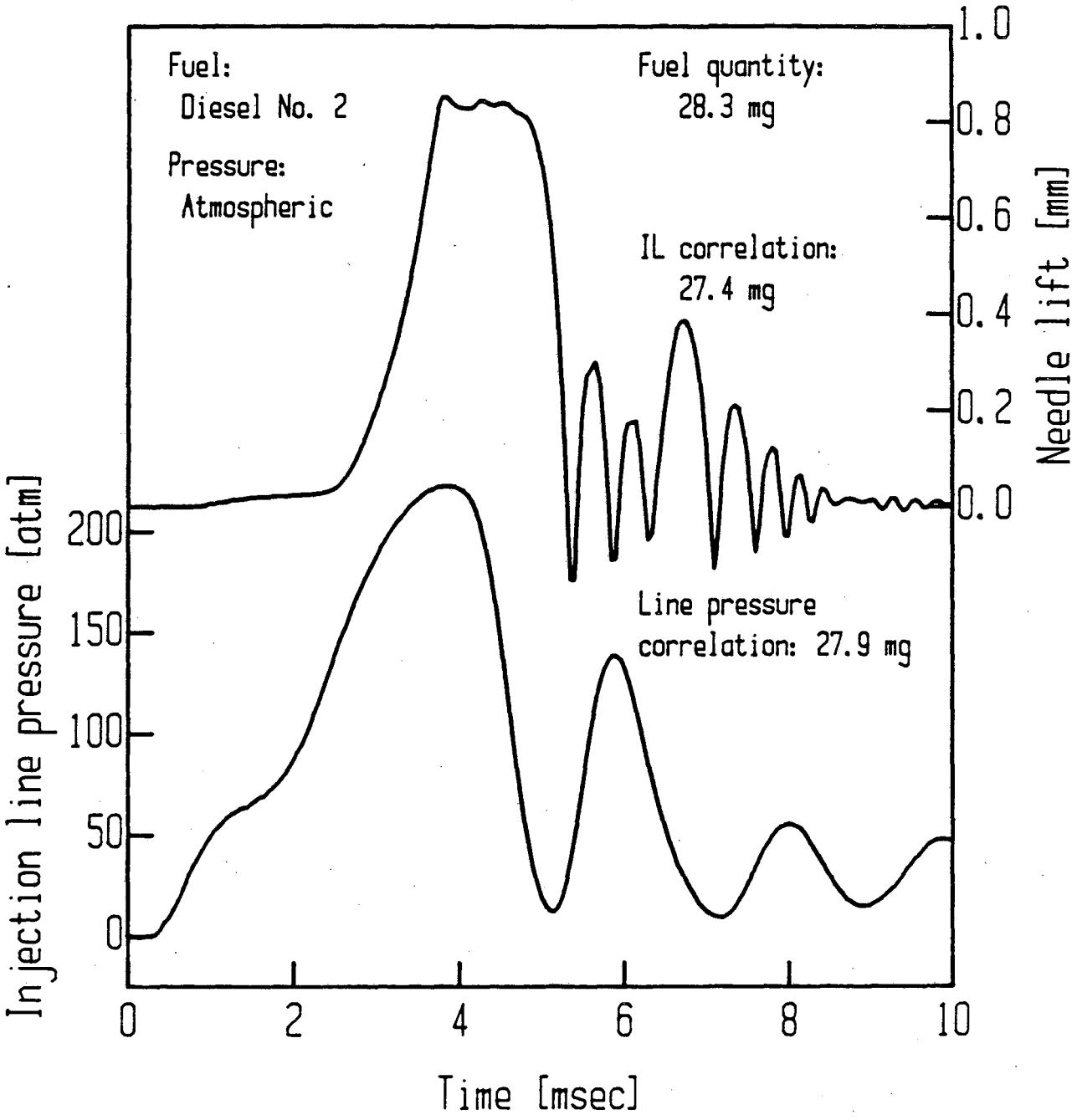

Figure 4.5. Injection line pressure and needle lift histories for diesel fuel into atmospheric pressure with comparison data for weighed mass and computed mass for the needle lift and line pressure correlations.

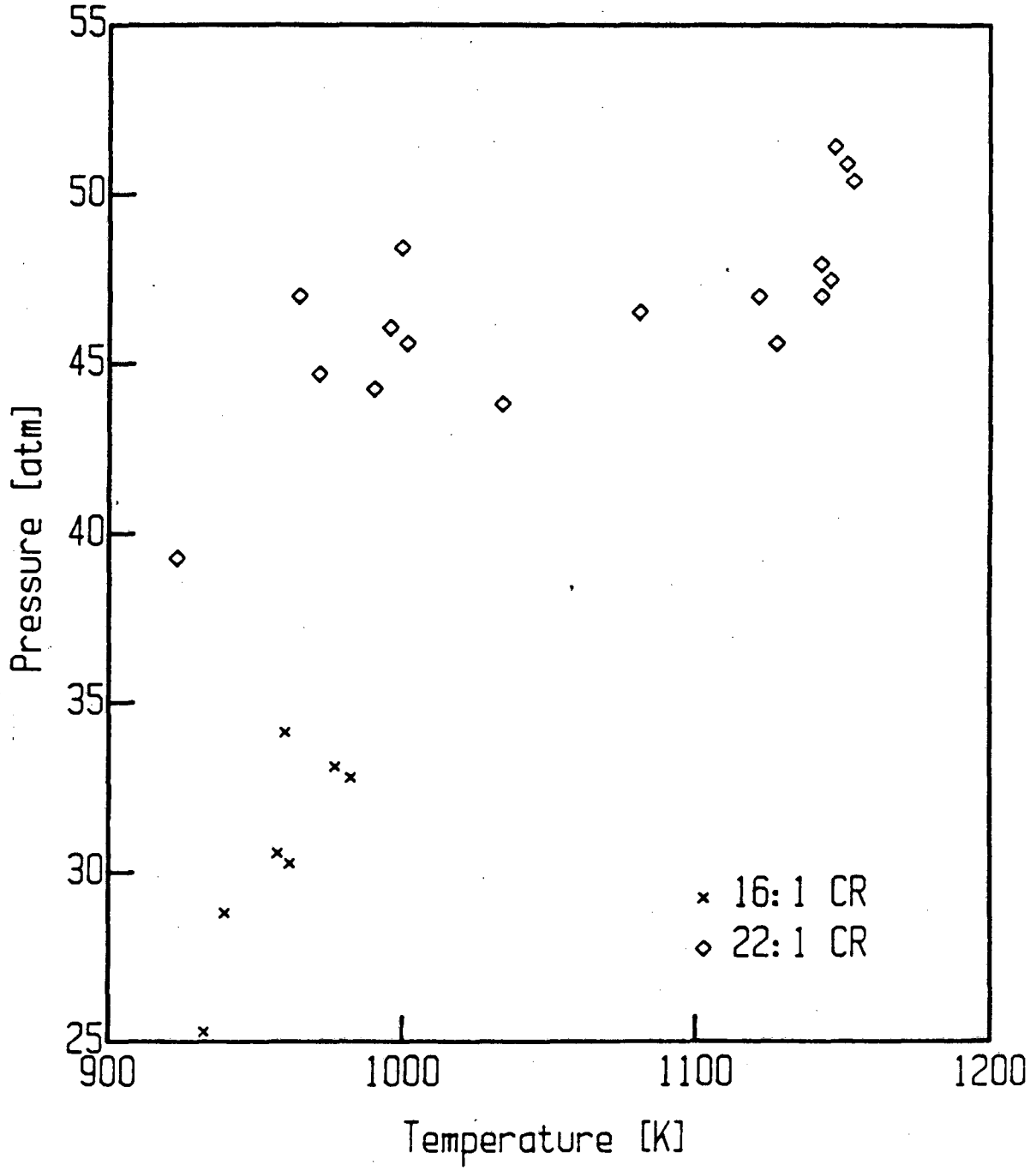

Figure 4.6. Pressure and temperature conditions at the time of injection which coal/water slurry was tested in the engine simulator.

Henein and Elias (1978) discuss using inlet air preheat to extend the cetane scale. For evaluating diesel No. 2, methanol, coal/oil, and coal/methanol slurries, the inlet air temperature is increased, per Henein and Elias, until ignition is obtained. The minimum temperatures required for combustion at 16:1 CR are (approximately 30 atm pressure at the injection timing of 20 ° BTDC):

Fuel	Temperature at IVC [K]	Temperature at time of injection [K]
Diesel No. 2	320	675
Coal/diesel	325	685
Methanol	450	825
Coal/methanol	360	725

The temperatures above are only approximate due to the errors in measurement and the unrepeatable nature of ignition near the limiting temperature.

The temperatures for coal/diesel ignition are nearly the same as those for diesel No. 2. Coal/methanol and methanol fuels both require higher temperatures than diesel fuel for ignition as expected due to the low cetane number of methanol. However, coal/methanol ignites at temperatures well below those required for neat methanol.

The autoignition of coal/methanol slurry at lower temperatures than neat methanol is either due to the additive package in the slurry or the coal. As mentioned in Section 1.2.1, coal addition to the liquid carrier increases the viscosity dramatically causing the fuel droplets injected to be larger than with neat liquid fuel. Thus, any physical effect of the coal on the autoignition is most probably detrimental. Thurgood and Smoot (1979) summarize data from 24 experiments in which the gaseous coal pyrolysis products are measured. Twenty of the reported

experiments are conducted at rapid heating rates, *i.e.*, greater than 10^4 K/sec. The products of devolatilization depend on coal type, heating rate, final temperature, and other factors. But, average values of the various components are: 3% CO_2, 15% CO, 53% H_2, 14% CH_4, 10% C_2H_6, and 5% of other C_2 molecules. The final temperatures of the coal in these experiments is 1000 K or higher. The fuel at the periphery of the spray cone injected into the square piston engine simulator experiences very high heating rates: on the order of 10^5 K/sec. However, if the temperature at the time of injection is 725 K, the final temperature is below 800 K. Kimber and Gray (1967) report that at 1050 K final temperature and a reaction time of 70 msec, less than 25% of the coal's volatile matter is removed. Therefore, it is unlikely that enough combustible gas is devolatilized during the $\sim$5 msec ignition delay to ignite the mixture. The more plausible explanation for the autoignition characteristics of coal/methanol is that the additive package contains chemicals which ignite more readily than methanol.

4.3. IGNITION DELAY

The end of the ignition delay is measured in two ways: emission of light from combustion and measurable pressure rise compared to the motoring trace. The amount of light emitted from methanol combustion is much less than that emitted from the other fuels as demonstrated by sample luminosity traces in Fig. 4.7. To obtain adequate sensitivity from the photodiode, the gain is raised by a factor of five for methanol tests. At this high gain with engine block heating and high inlet temperatures, the photodetector senses the infrared radiation from the warm

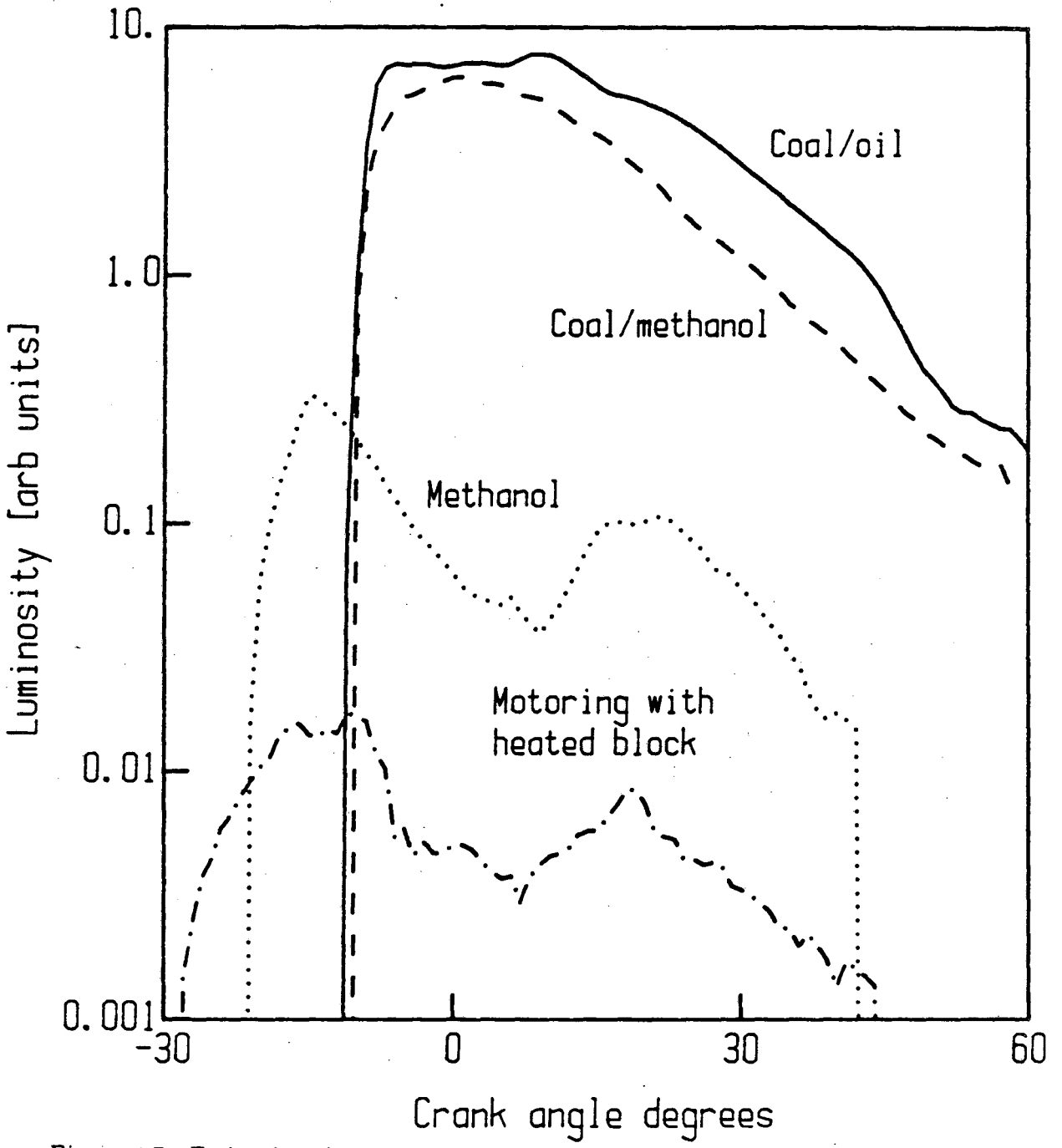

Figure 4.7. Emitted radiation from the cylinder for three fuels compared to a motoring run with heated engine block measured by a photodiode on the engine simulator at 900 rpm.

surfaces giving erroneous ignition readings. Thus, only the pressure rise determination at start of combustion is used for methanol.

The reciprocal temperature at the time of injection is shown with the corresponding pressure delay time for methanol in Fig. 4.8. By neglecting the pressure dependence of ignition delay in Eqn. 1.1, the delays at 16:1 CR are longer than at 22:1 CR. This confirms that pressure does play a role in the ignition delay times as the 22:1 CR results are at higher pressures than those at 16:1 CR. The data are plotted in Fig. 4.9 with the reciprocal temperature plotted against the log of delay time times the pressure to the 1.5 power. The data for the two compression ratios are indistinguishable. The activation temperature for methanol is 7685 K.

Methanol is compared with coal/methanol in Fig. 4.10. Coal/methanol combusts at lower temperatures than neat methanol as discussed in Section 4.2. Therefore, the coal/methanol data cover a larger interval in temperature. The actual delay times for the two fuels are similar. However, the coal/methanol activation temperature at 5330 K is much lower than that of methanol at 7685 K. A statistical analysis at the 90% confidence level indicates that the uncertainties on T_a are $\pm$ 2080 K and $\pm$ 645 K, for methanol and coal/methanol, respectively. The 90% confidence bands for the two fuels are shown in Fig. 4.11. The middle line of each set of three is the least squares fit given in Fig. 4.10. The upper and lower lines indicate bounds at 90% certainty for the ingition delay as a function of temperature. Because of the high degree of uncertainty in the methanol T_a, the differences between the two fuels in Fig. 4.10 are indicative of trends only.

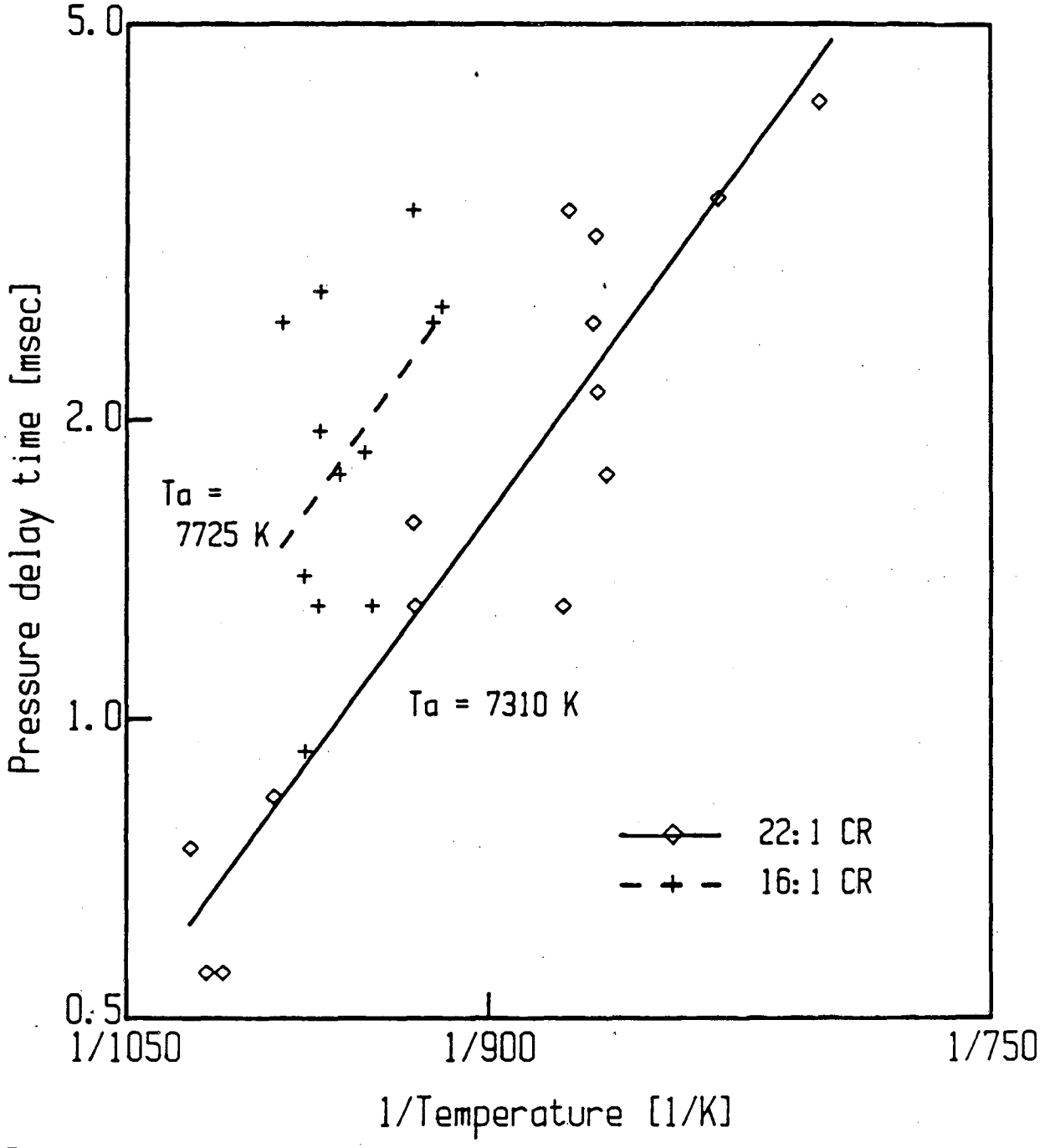

Figure 4.8. Arrhenius type plot of reciprocal temperature versus log of pressure delay time for combustion of methanol at 16:1 and 22:1 CRs in the square piston engine at 900 rpm.

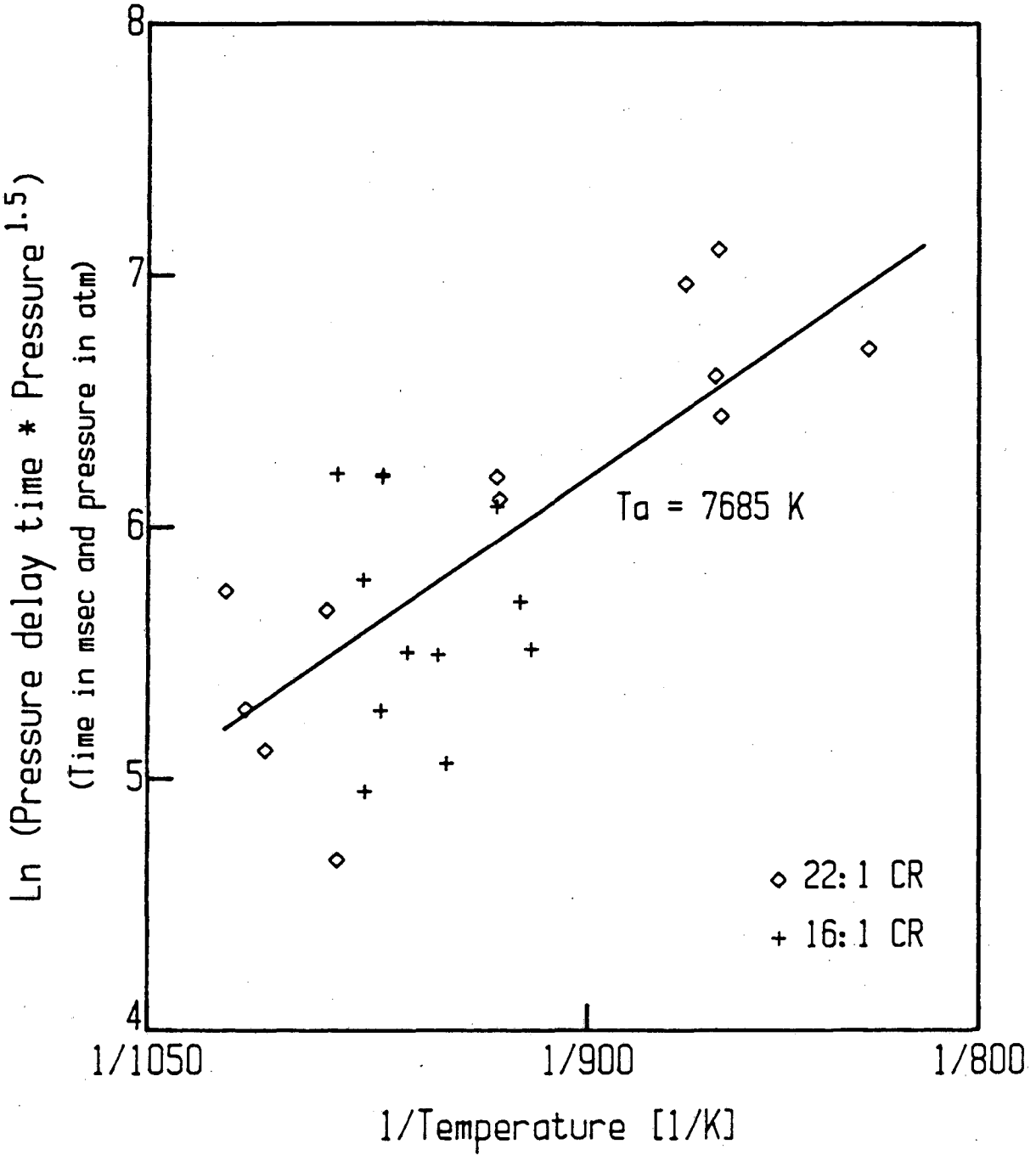

Figure 4.9. Reciprocal temperature and log of pressure delay time times the pressure to the 1.5 power plotted for methanol combustion in the square piston engine simulator.

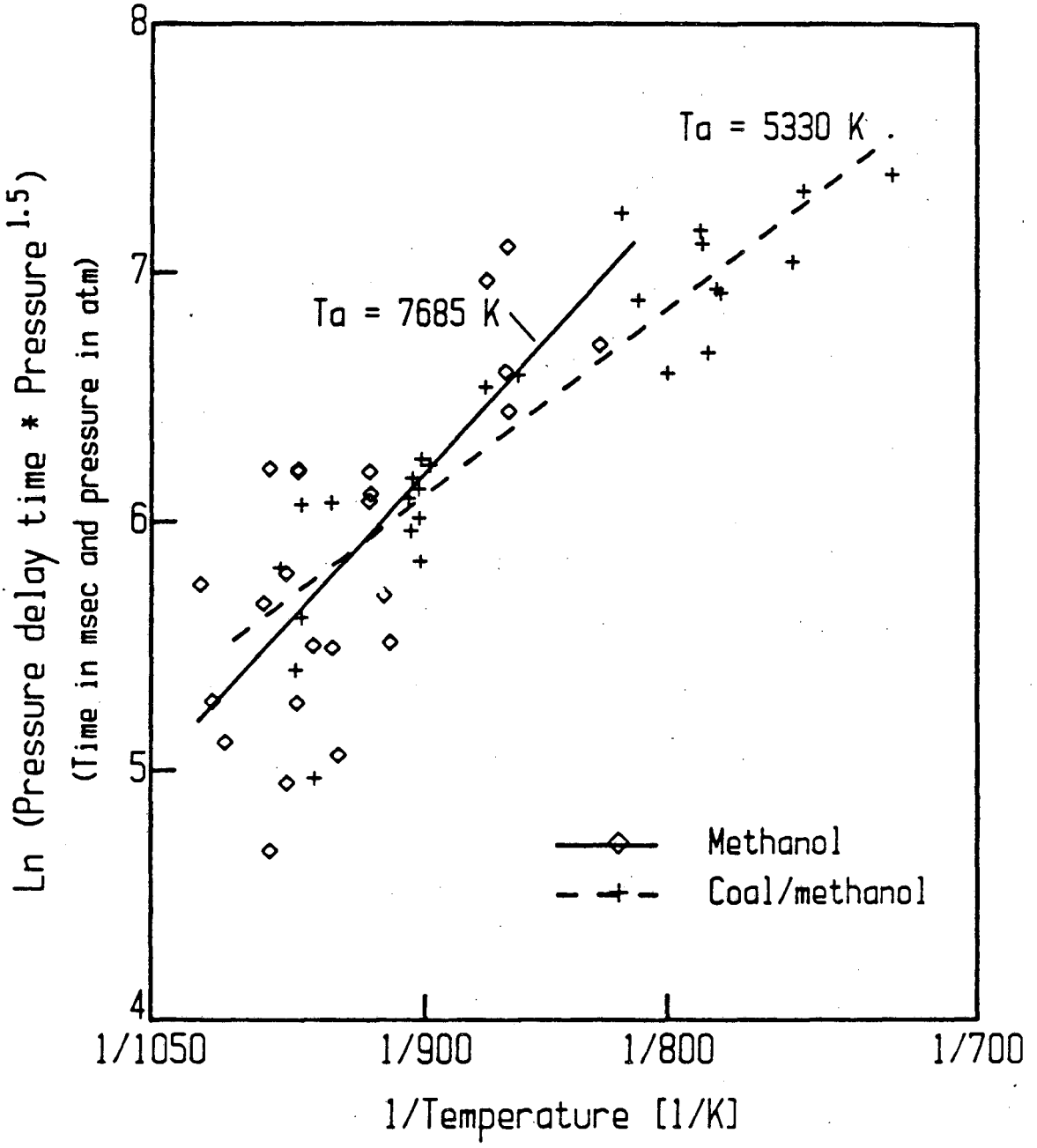

Figure 4.10. Ignition delay comparison between methanol and coal/methanol fuels based on pressure delay time.

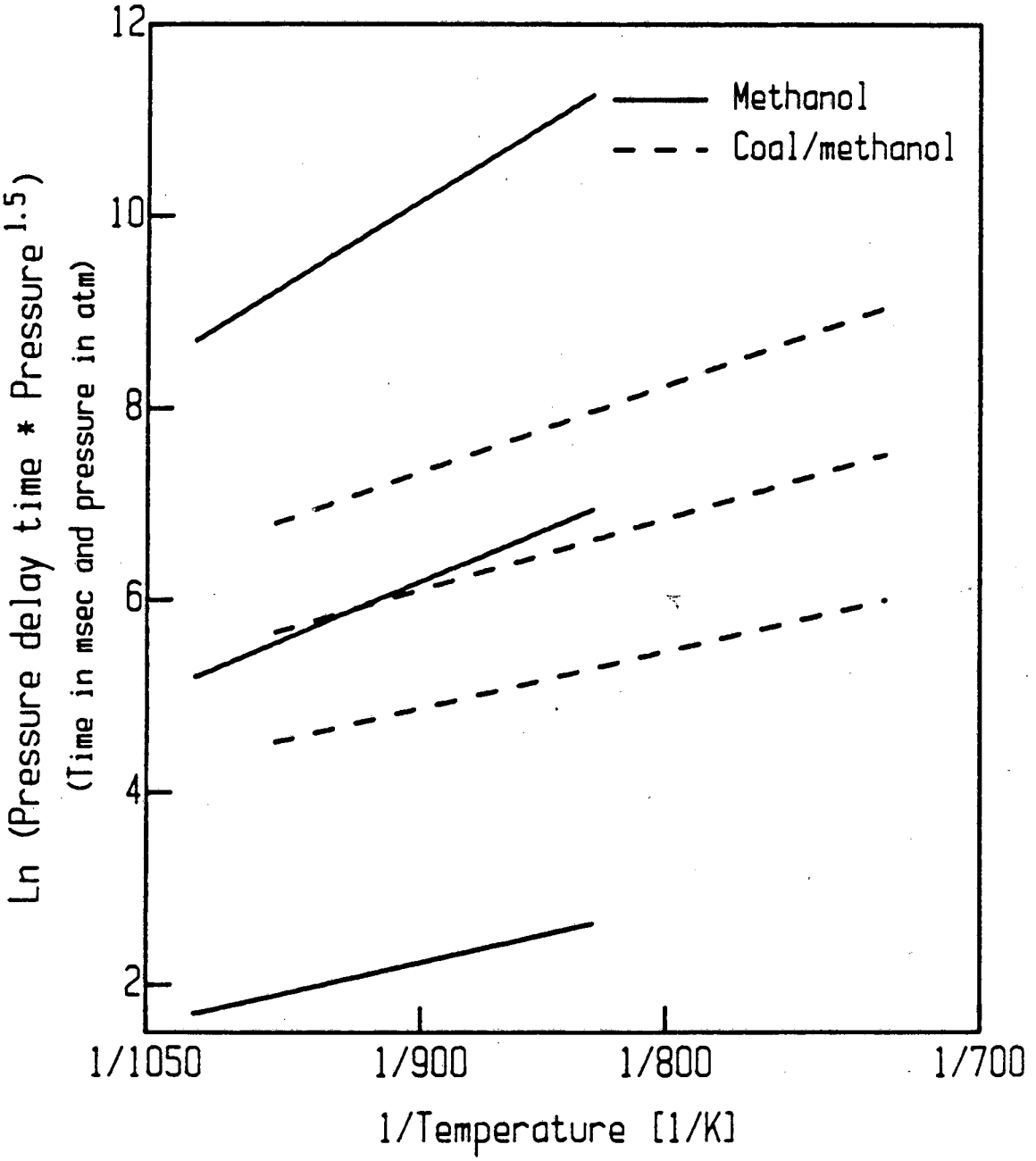

Figure 4.11. Least squares fit of reciprocal temperature versus the pressure delay time times pressure to the 1.5 power with the 90% confidence level upper and lower bounds for methanol and coal/methanol fuels.

The diesel No. 2, coal/oil slurry, and coal/methanol slurries pressure and luminosity delay results are shown in Figs. 4.12 and 4.13, respectively. The coal/methanol tests tend to give higher ignition delay throughout the temperature range. However, the 90% confidence level bands on the least squares correlation in Figs. 4.14 and 4.15 indicate no statistical difference between the delay periods for these three fuels.

The uncertainty on the activation temperatures and pre-exponential factors for the data in Figs. 4.10, 4.12, and 4.13 are contained in Table 4.1. The following differences are significant at the 90% confidence level:

- coal/diesel has a lower activation temperature than diesel No. 2, coal/methanol, and methanol fuels by the pressure delay measurement.
- coal/diesel slurry has a lower activation temperature than coal/methanol when considering the luminosity delay.

No differences between the luminosity delay and pressure delay results are found within the measurement precision of these tests.

In both the luminosity and pressure delay analyses the activation temperature for coal/diesel is lower than diesel fuel pointing to the same trend noticed in Fig. 4.10: the neat fuel has higher T_a than its coal slurry. The ignition delay interval is comprised of overlapping physical and chemical periods. El Wakil, *et al.* (1956) present calculated physical delay times for a 20 μm decane droplet in Fig. 7 of their paper. They also report that physical delay times are proportional to the

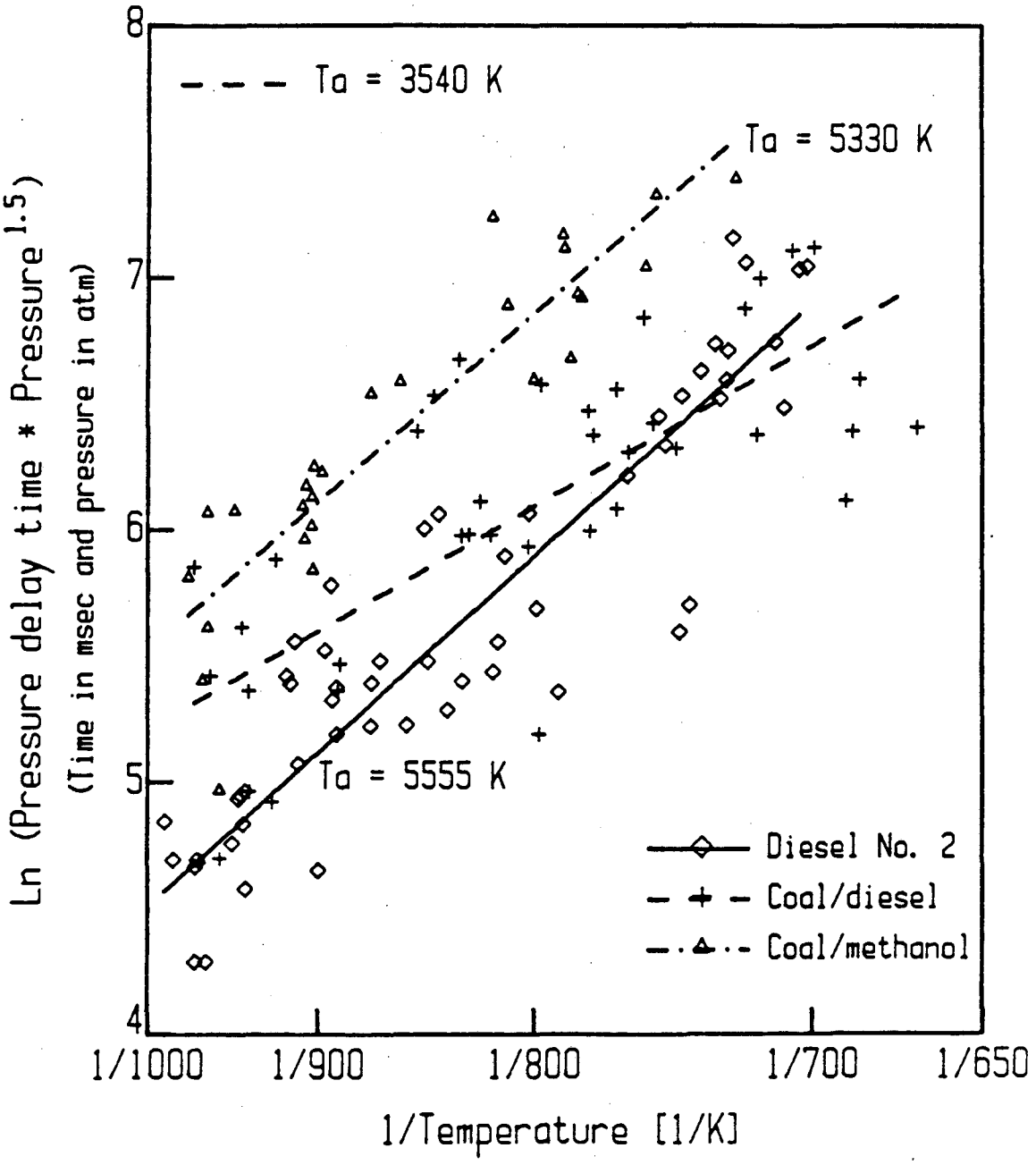

Figure 4.12. Diesel No. 2, coal/diesel, and coal/methanol ignition delay results based on pressure delay and the least squares fit indicating the activation temperature.

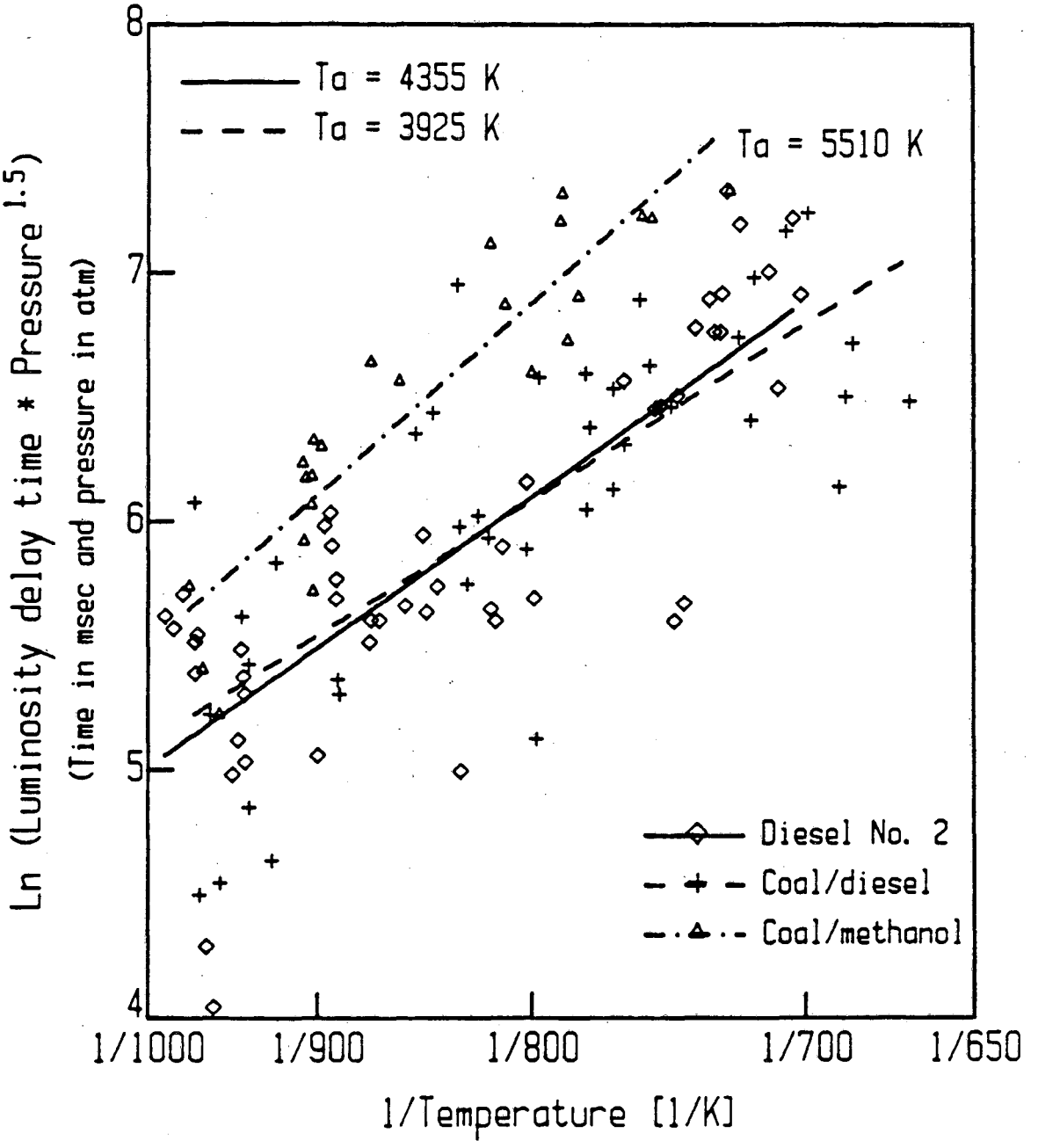

Figure 4.13. Luminosity delay measurements for diesel No. 2, coal/diesel, and coal/methanol with the activation temperature as computed from a least squares analysis.

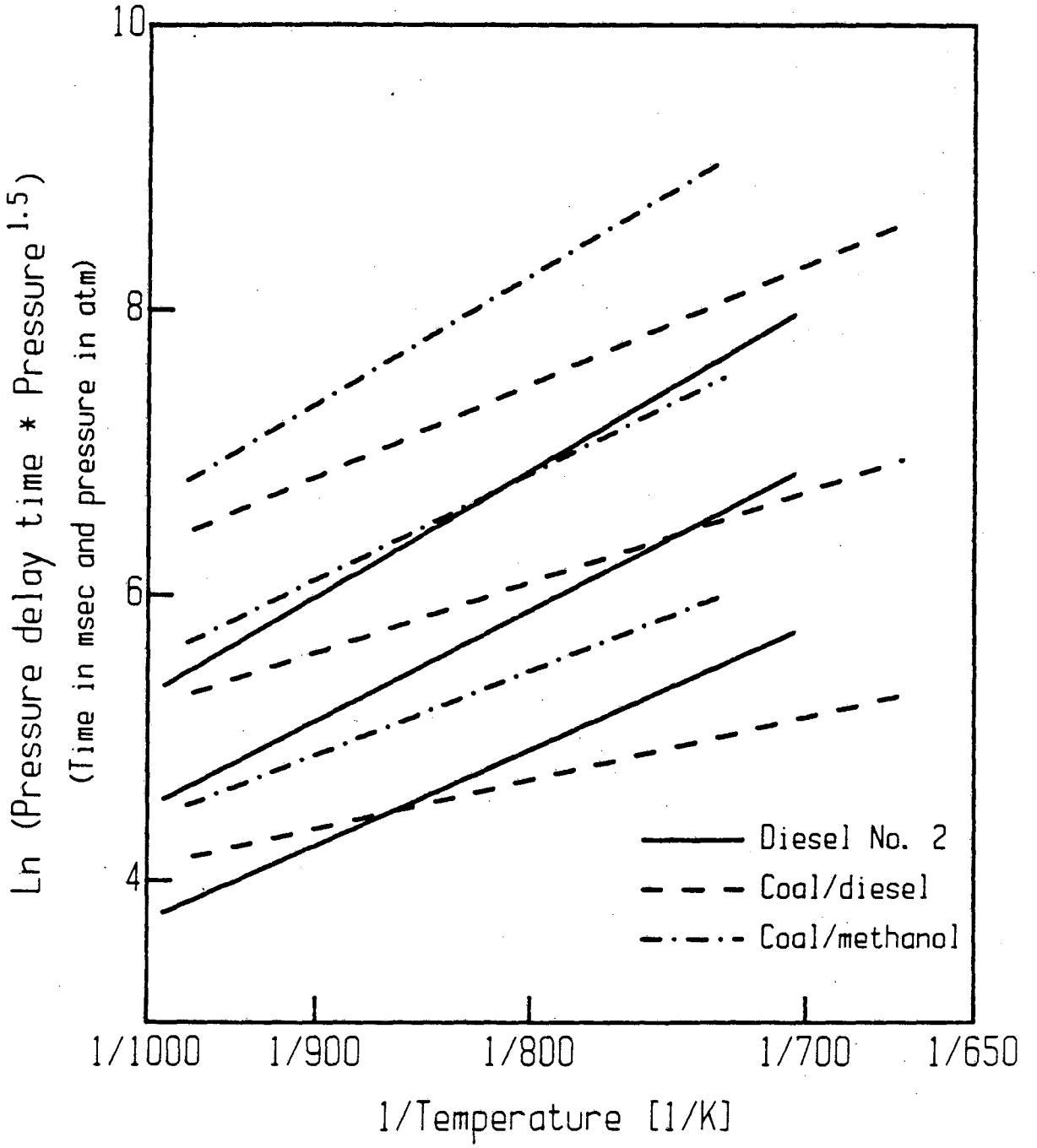

Figure 4.14. Least squares analysis on Arrhenius type plot of pressure ignition delay for diesel No. 2, coal/diesel, and coal/methanol indicating the bands of 90% confidence on the results.

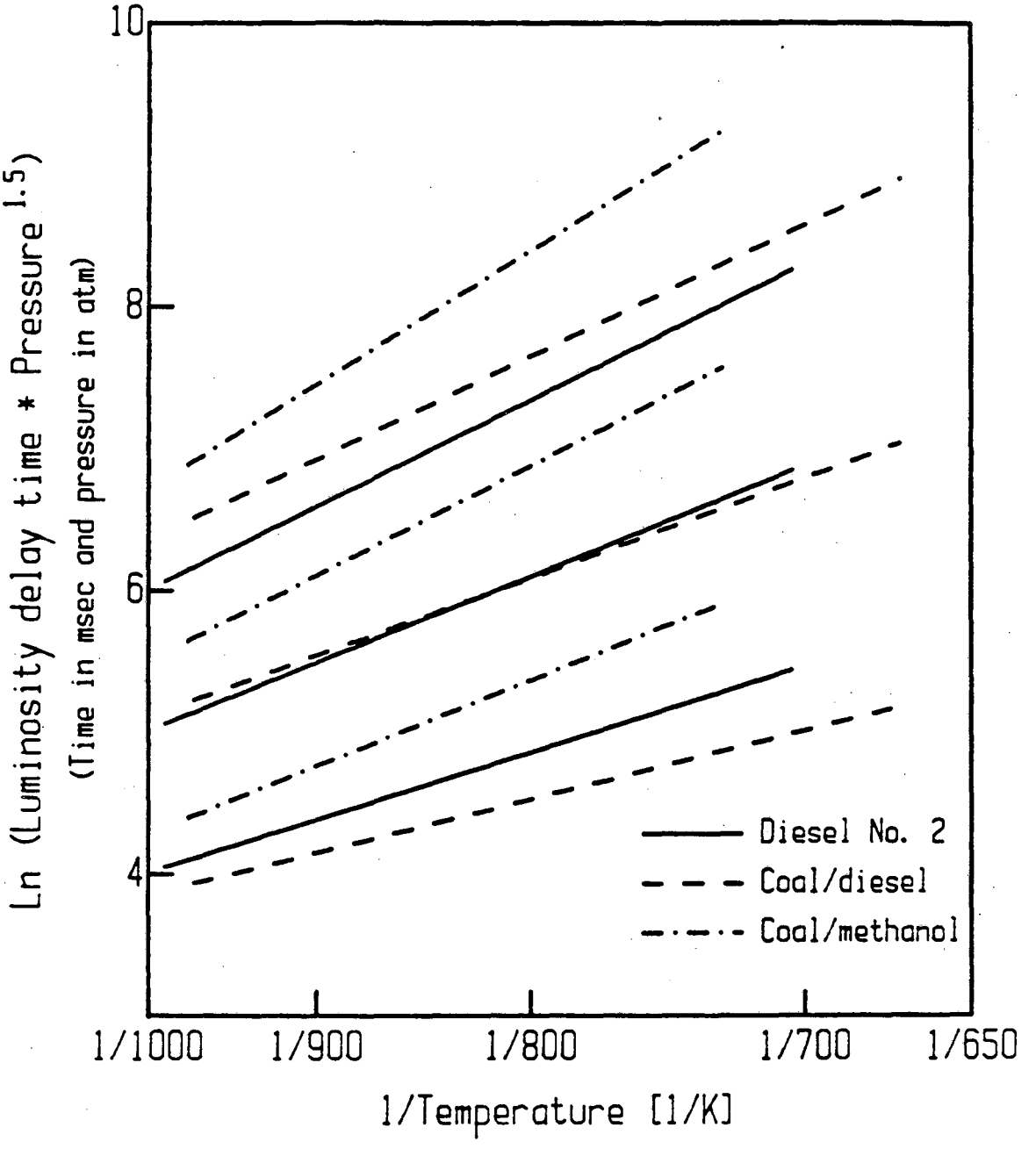

Figure 4.15. Upper and lower bounds at 90% confidence of the least squares correlation between reciprocal temperature, pressure, and luminosity delay time for diesel No. 2, coal/oil, and coal/methanol fuels.

Table 4.1 Activation temperatures and pre-exponential factors for the pressure and luminosity igntion delay periods for diesel No. 2, methanol, coal/oil slurry, and coal/methanol slurry and the uncertainties associated with the correlations at the 90% confidence level.

Fuel	n	T_a, [K] (uncertainty)	A, [msec/atm^n] (uncertainty)	Measurement technique
Diesel No. 2	1.5	5559 (5106-6012)	0.348 (0.328-0.370)	Pressure
Methanol	1.5	7685 (5605-9765)	0.097 (0.096-0.110)	"
Coal/diesel	1.5	3541 (2899-4183)	5.31 (4.86-5.80)	"
Coal/methanol	1.5	5330 (4885-5975)	1.21 (1.13-1.30)	"
Diesel No. 2	1.5	4357 (3783-4931)	0.520 (0.481-0.563)	Luminosity
Coal/diesel	1.5	3926 (3205-4647)	3.25 (2.95-3.59)	"
Coal/methanol	1.5	5510 (4810-6210)	0.988 (0.921-1.06)	"
Diesel No. 2	0	4345 (4062-4628)	0.0077 (0.0075-0.0080)	Pressure
Coal/diesel	0	3783 (3272-4294)	0.0207 (0.00193-0.0222)	"
Coal/methanol	0	5030 (4240-5820)	0.0081 (0.0075-0.0089)	"
Diesel No. 2	0	3142 (2681-3423)	0.043 (0.041-0.044)	Luminosity
Coal/diesel	0	3487 (2912-4062)	0.032 (0.030-0.034)	"
Coal/methanol	0	4375 (3493-5257)	0.019 (0.017-0.021)	"

droplet diameter to the 1.75 power. From their findings, the following table is constructed:

Physical delay time in msec				
	20 μm	50 μm	100 μm	200 μm
700 K	0.13	0.65	2.2	7.3
800 K	0.08	0.37	1.3	4.2
900 K	0.05	0.25	0.8	2.8

In Fig. 1.1, taken from Nelson, *et al.* (1985), 10% of the mass of diesel fuel droplets are contained in droplets less than 20 μm in diameter. In contrast, 10% of the mass of coal/oil droplets are found in 100 μm drop size or less. The physical delay for 20 μm droplets is almost negligible throughout the temperature range. However, at 100 μm, the physical delay interval is a sizeable portion of the total delay period. Temperature plays a less important role in determining the physical delay period compared to droplet diameter. Therefore, the lower T_a of coal/oil slurry may be due to a relatively long physical delay interval which is less sensitive to temperature than the chemical delay.

Data for n equal to 0 (n is the pressure exponent in the Arrhenius type expression, Eqn. 1.1) for diesel No. 2, coal/oil, and coal/methanol fuels are plotted in Figs. 4.16 and 4.17 and summarized in Table 4.1. Ignition delay results for n equal to 0 are computed for comparison purposes with results available in the literature (discussed in Section 4.6).

4.4. COMBUSTION ANALYSES

As discussed in Section 3.2, the square piston engine is a useful tool for testing ignition processes. However, due to its high leak rates, accurate measurement of

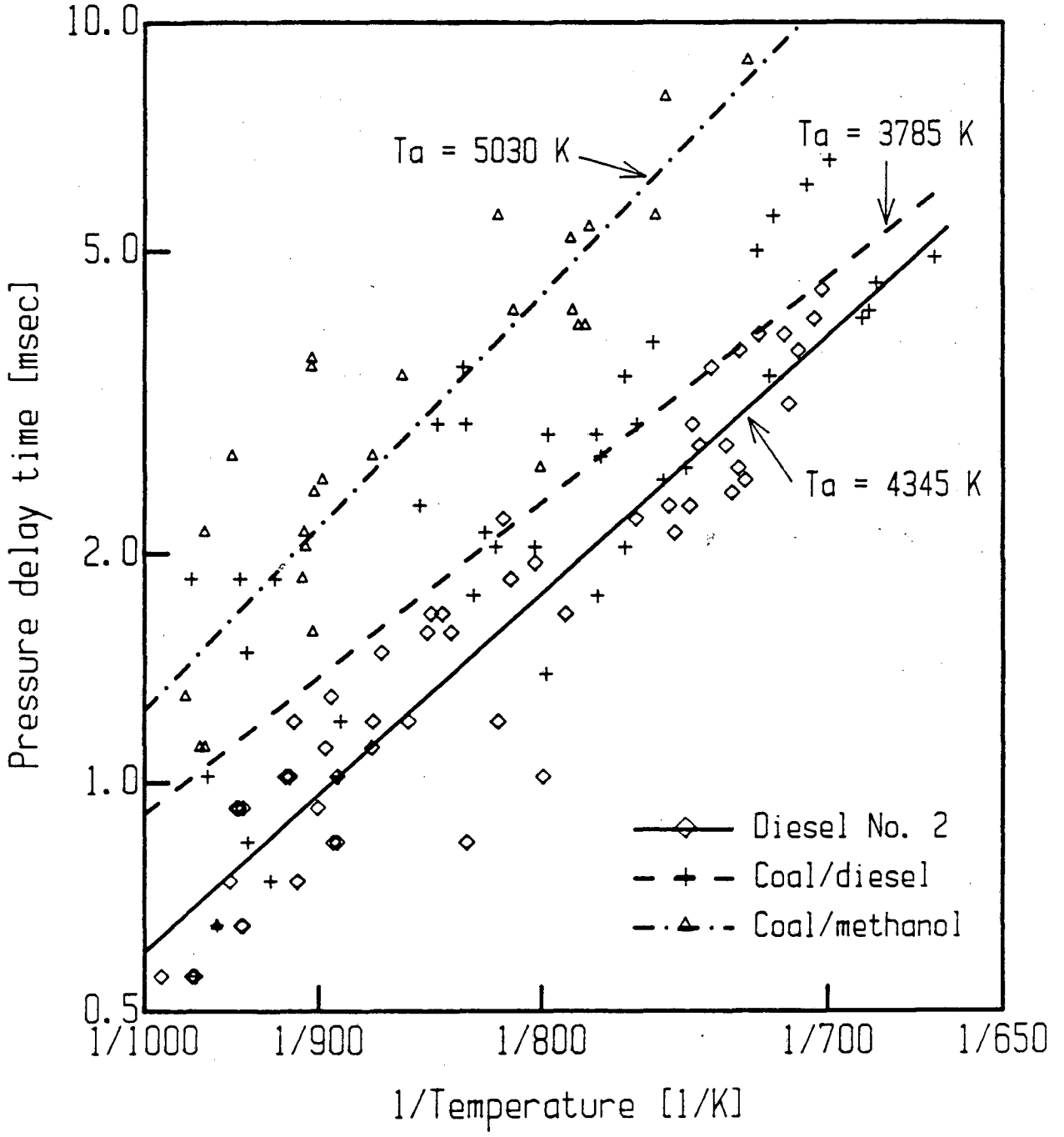

Figure 4.16. Log of pressure rise delay interval as a function of reciprocal temperature for Diesel No. 2, coal/diesel, and coal/methanol with the least squares fit indicating activation temperature.

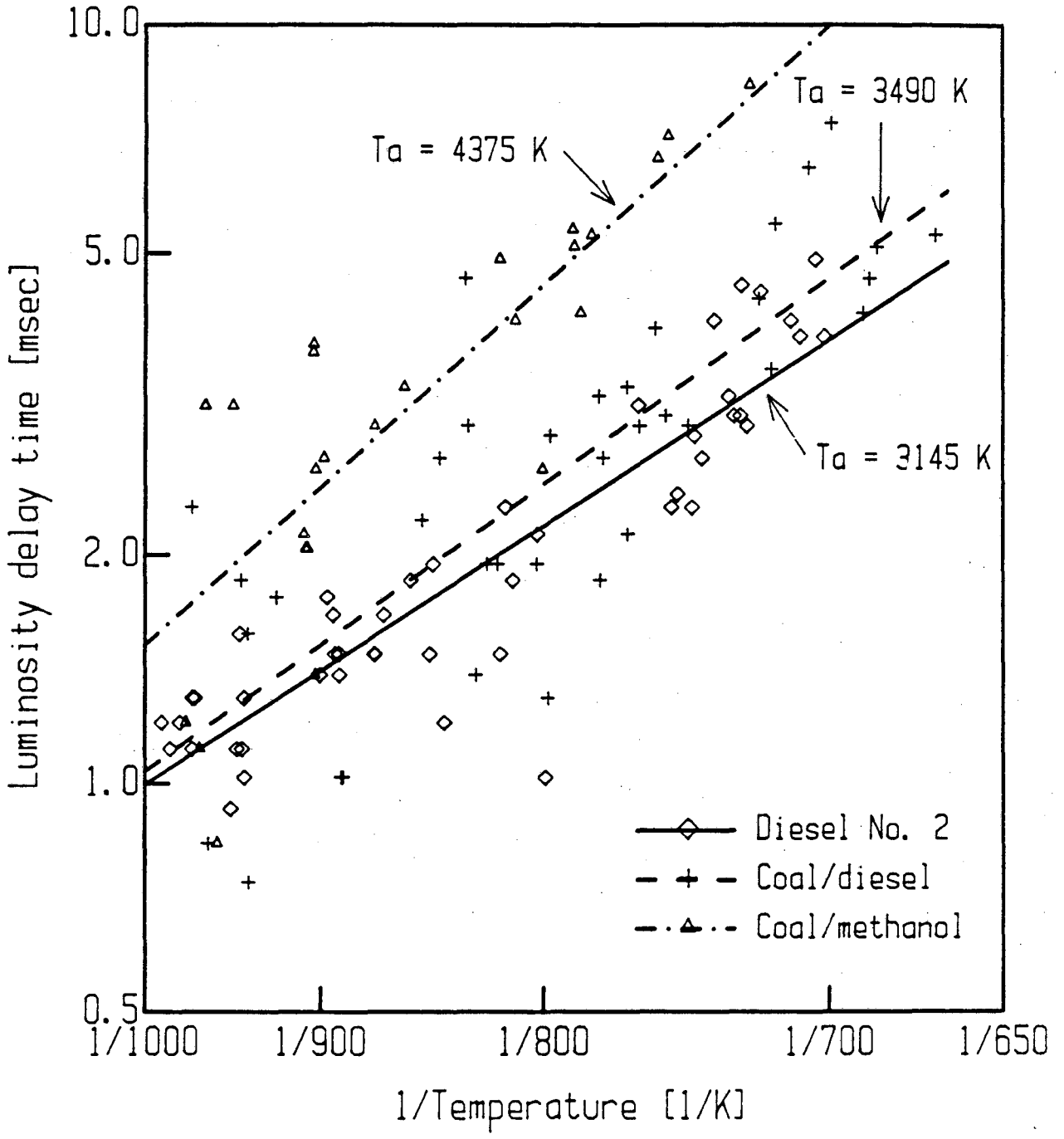

Figure 4.17. Arrhenius analysis of ignition delay measurements (based on luminosity) on diesel No. 2, coal/oil, and coal/methanol fuels.

thermal and combustion efficiencies is not possible. An estimate of the work and energy released per cycle is calculated for purposes of estimating the fraction of coal burned of the slurry fuels.

An example of a detailed accounting of the ignition and combustion for a single cycle is shown for each of the four fuels combusted: diesel No. 2 in Fig. 4.18, methanol in Fig. 4.19, coal/diesel in Fig. 4.20, and coal/methanol in Fig. 4.21. The end of the pressure delay is found by comparing the motoring and combusting pressure curves at the top of the figure. The work is computed by integrating the pressure volume curves (not plotted in the figures) and computing the difference between the combusting case and the reference motoring case. The middle curve on the figures represents the needle lift; the start of injection is taken from this trace. The rate of energy release for a motoring and combusting cycle are shown in the bottom of the figures. By integrating the combusting rate of energy release and subtracting the reference motoring energy, the energy released is computed.

As a point of comparison, Fig. 2 of Miyamoto and Muryama's (1979) paper is presented in Fig. 4.22. The shape of the rate of energy release curve is vastly different for a conventional engine than the square piston engine simulator.

In the representative cases shown in Figs. 4.18-21, the energy release is just over 50% of the estimated amount of fuel energy injected. Although it is possible that under all engine conditions and fuel types tested less than 75% of the fuel energy is consumed, it is proposed that the energy release calculations are consistently low by about 75%. An alternative explanation is incomplete burnout. For a high quality distillate fuel such as diesel No. 2, possible reasons for

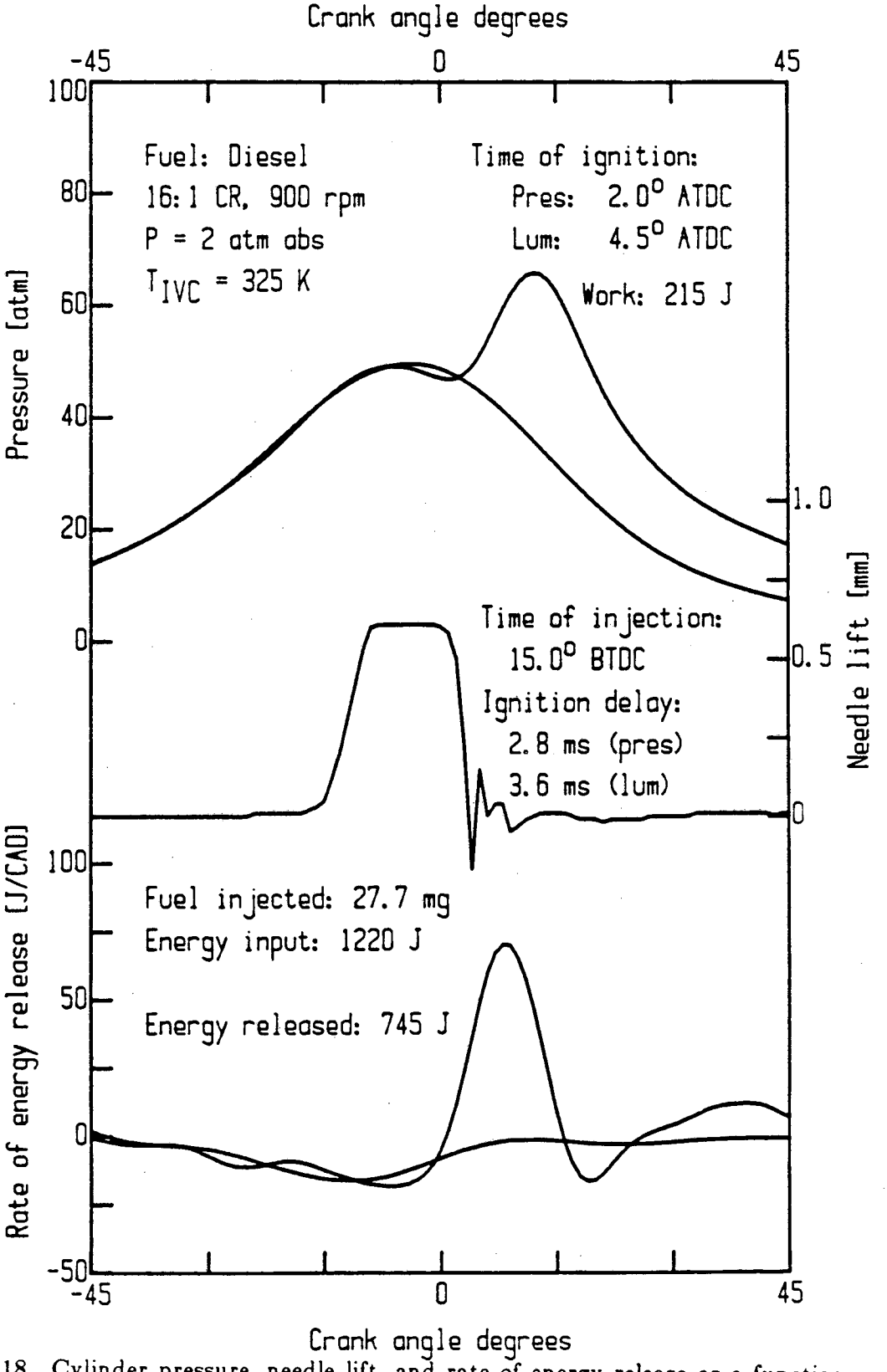

Figure 4.18. Cylinder pressure, needle lift, and rate of energy release as a function of CAD for a representative Diesel No. 2 run in the square piston engine simulator.

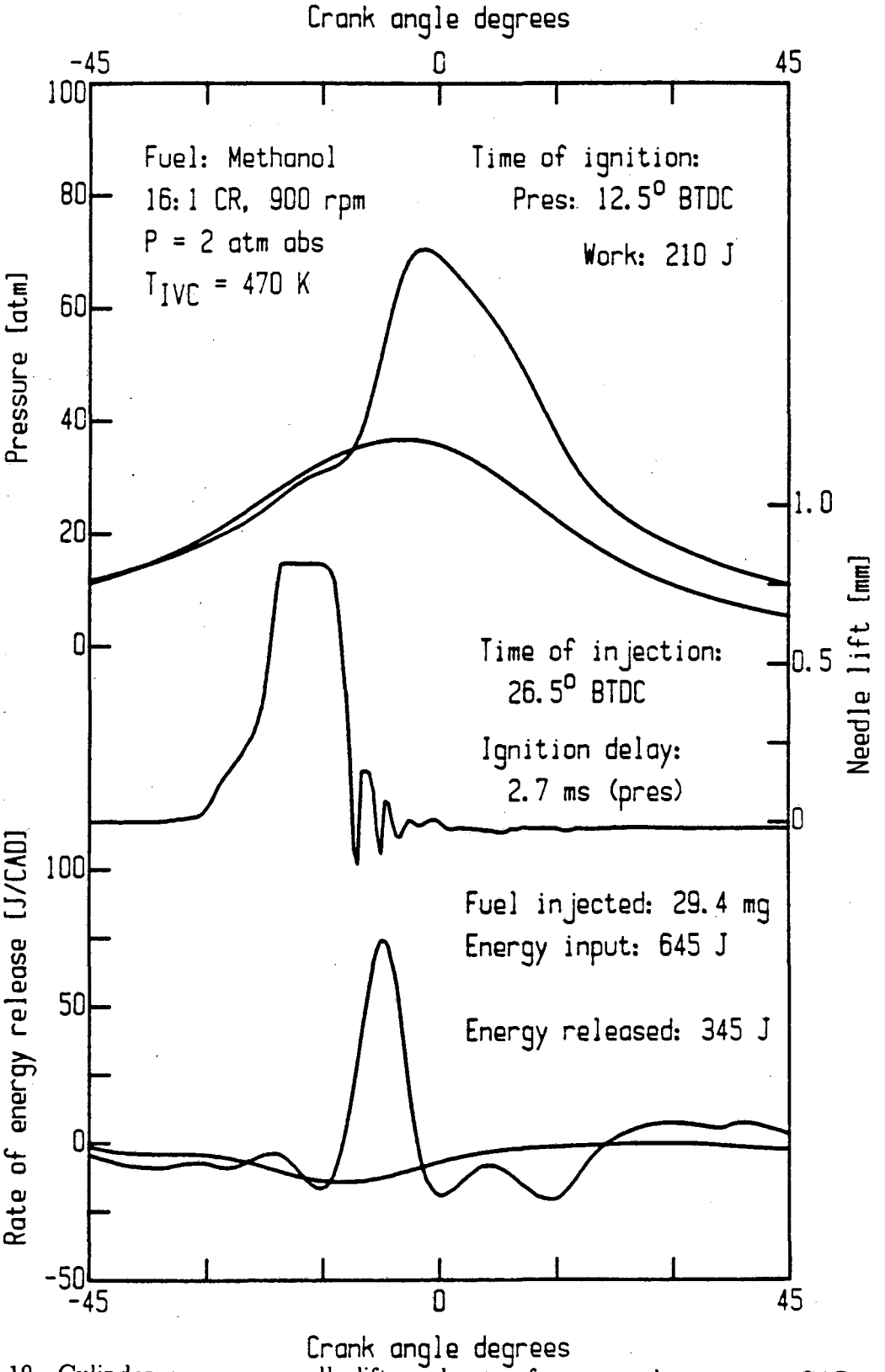

Figure 4.19. Cylinder pressure, needle lift, and rate of energy release versus CAD for combustion of methanol.

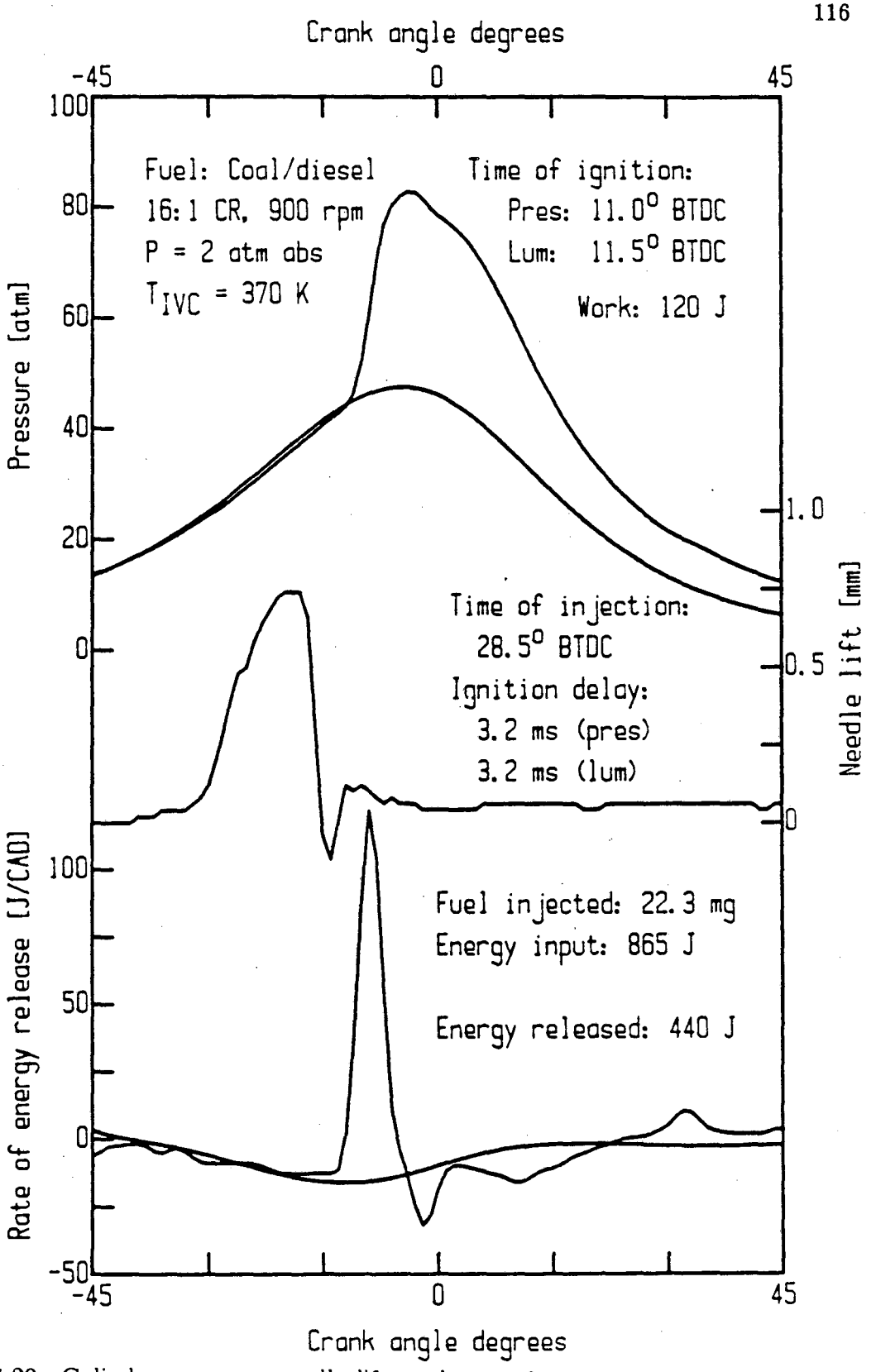

Figure 4.20. Cylinder pressure, needle lift, and rate of energy release versus CAD for a sample run with coal/oil slurry.

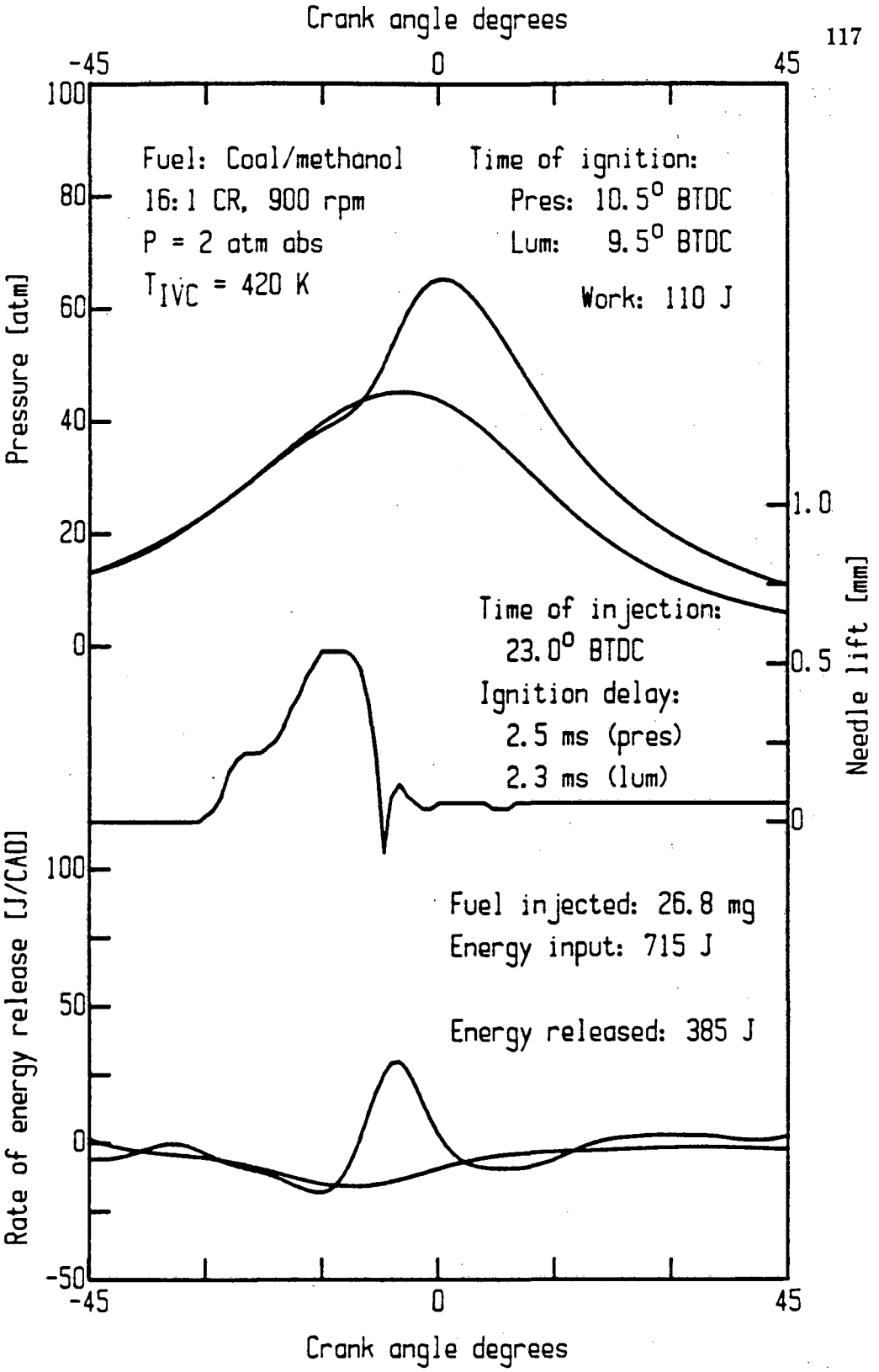

Figure 4.21. Cylinder pressure, needle lift, and rate of energy release as a function of CAD for combustion of coal/methanol slurry.

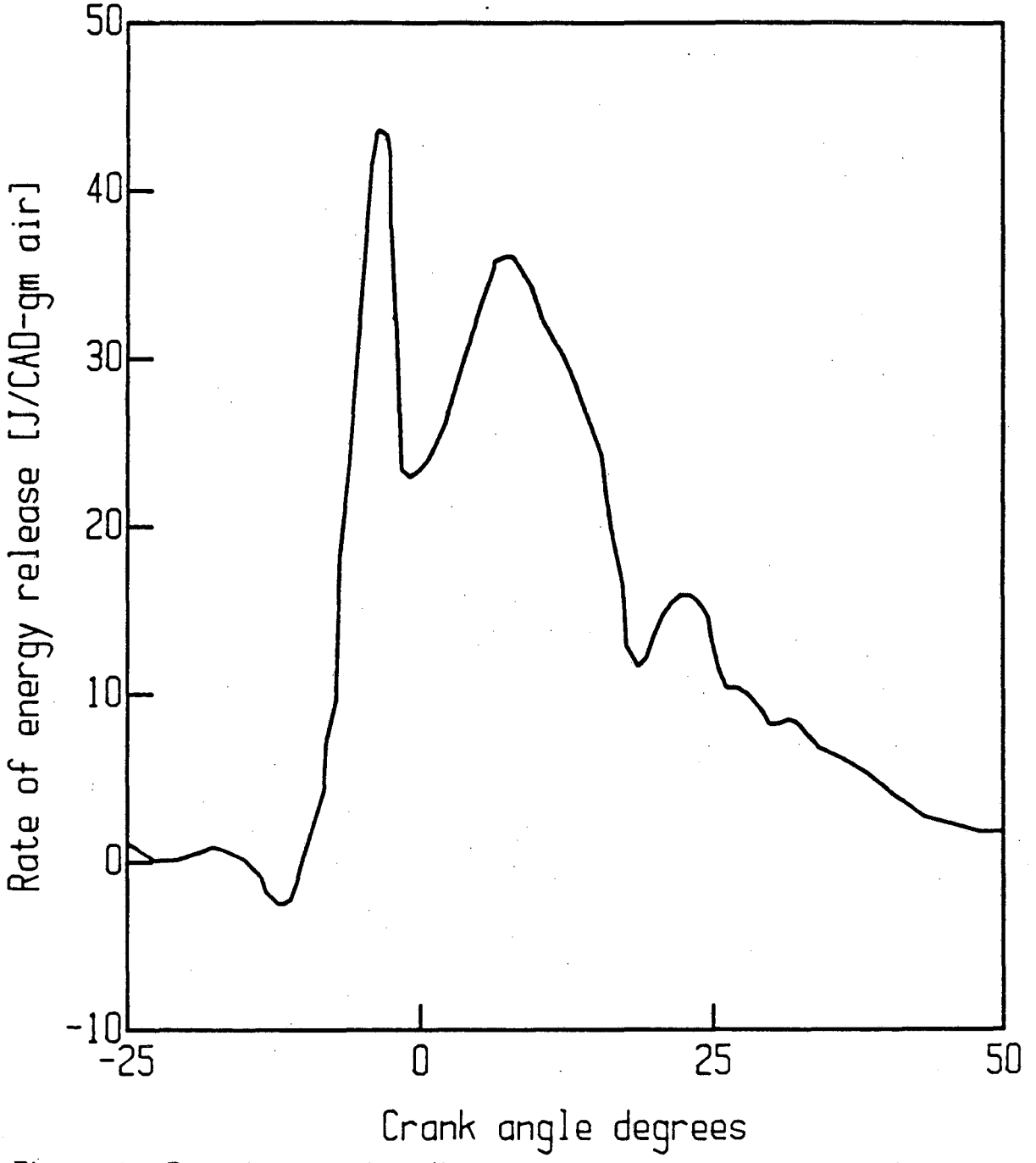

Figure 4.22. Rate of energy release (from paper by Miyamoto and Muryama(1979)) for conventional compression ignition engine fueled by Diesel No. 2.

incomplete burnout are: insufficient time at a given temperature, spray impingement on a cold combustion chamber surface, or insufficient oxygen. However, the peak temperatures attained at the higher inlet temperatures tested are certainly high enough to expect complete fuel consumption in the relatively long time interval at 900 rpm. A significant amount of fuel impingement is not observed from high speed shadowgraphic movies nor is excessive fuel buildup found on combustion chamber surfaces even after many tests. The amount of excess air in the cylinder is between 100% and 500% depending on the inlet air temperature (density), the amount of fuel injected, and the fuel enthalpy of reaction. Therefore, the overall stoichiometry is lean in all cases with excess oxygen available for complete burnout.

Analysis of the thermal efficiency provides an additional piece of evidence corroborating the conjecture that the energy release calculations are in error. The thermal efficiency is normally computed by dividing the work by the fuel enthalpy injected. But, at low combustion efficiencies (these low energy release values indicate combustion efficiencies of less than 60%), it is useful to evaluate the efficiency by comparing the work to the energy released. For the case summarized in Fig. 4.19, the overall thermal efficiency is 0.32 compared to an efficiency of 0.53 based on the energy release. The highest efficiencies attained on an optimized diesel engine are less than 0.45. Therefore, the 0.53 efficiency is in error and points to the conclusion that the energy release calculations are low.

The amount of the error in the energy release computations is postulated to be about 75%. For illustration purposes only, the data from Figs. 4.18-21 are corrected:

Fuel Type	Enthalpy of Fuel Injected [J]	Energy Released (uncorrected) [J]	Energy Released (corrected) [J]
Methanol	645	345	605
Diesel No. 2	1220	645	1130
Coal/oil	865	440	770
Coal/methanol	715	385	675

If the true value of the energy released is near the values contained in the table above, the combustion efficiencies are 90% or higher. If 90% of the slurries' energy is consumed, the worst case analysis puts the coal burnout at 75%. In any case, the combustion efficiencies for the four fuels are in the same range regardless of the argument about energy release. This also suggests that the majority of the coal in the coal/methanol and coal/oil slurries is consumed.

4.5. OBSERVATIONS FROM HIGH SPEED MOVIES

Schlieren movies of the motoring cycle were taken at atmospheric pressure and 2 atm abs. supercharge inlet pressure with temperatures between ambient and 450 K at IVC. The framing rate of 5000 frames/sec corresponds to one frame per CAD. Figures 4.23-25 are taken from a Schlieren movie of a motoring cycle with 150 ° C and 2 atm abs. inlet air conditions. The open intake valve and jet flow past the valve on the inlet stroke are seen in the upper left corner of Fig. 4.23. Capturing the large scale swirling air motion on a single still frame is impossible. Thus, even though the movie indicates vortical motion parallel to the axis of view during the compression stroke, only small structure can be identified in Fig. 4.24.

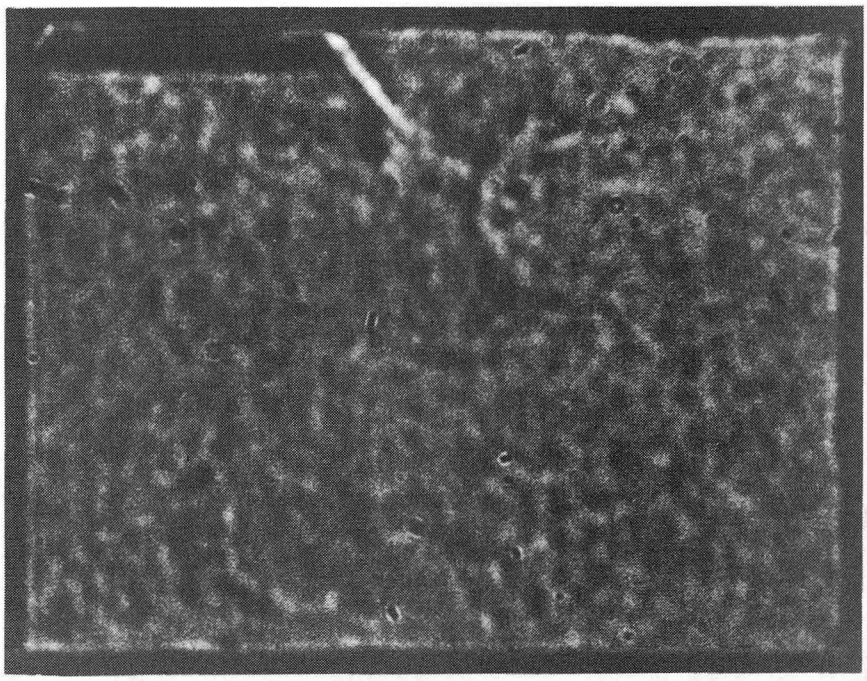

XBB 8512-10190

Figure 4.23. Schlieren photograph of square piston engine simulator during intake stroke with intake valve open.

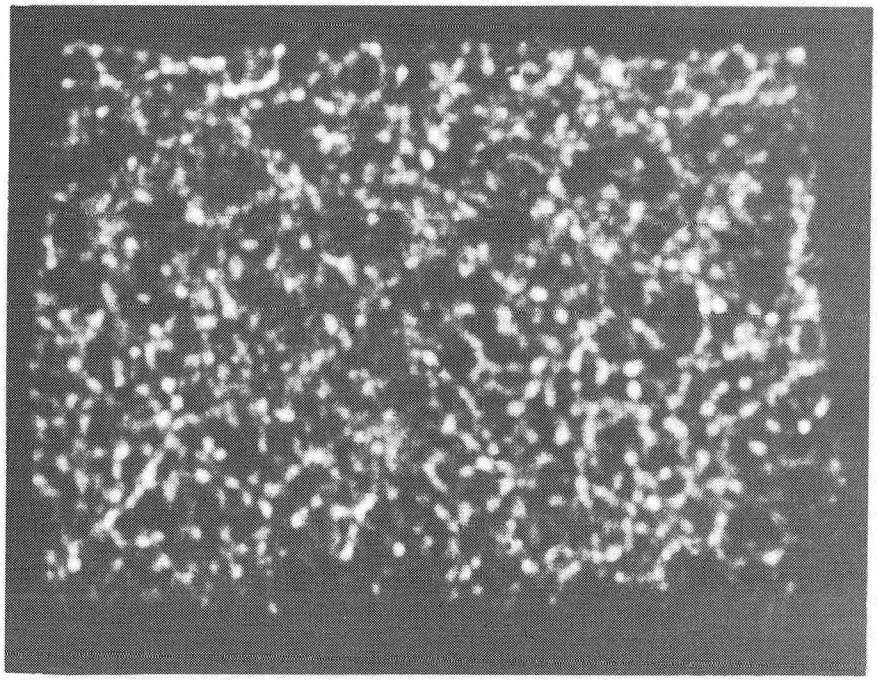

XBB 8512-10191

Figure 4.24. Schlieren photograph of square piston engine simulator early in compression stroke.

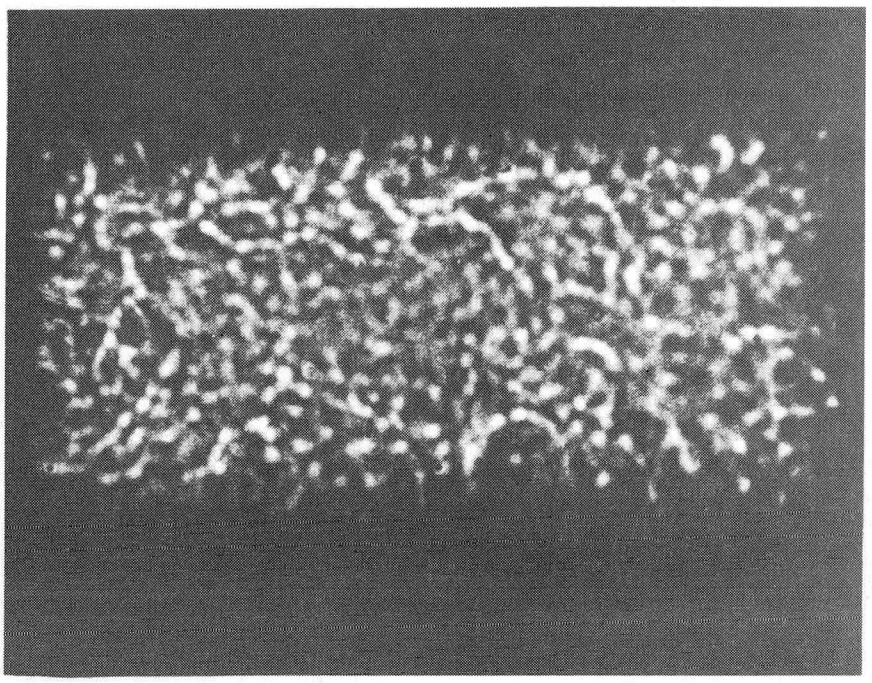

XBB 8512-10192

Figure 4.25. Schlieren photograph of square piston engine late in compression stroke.

Further into the compression stroke, the single large vortex breaks into two smaller vortices in most of the movies. As the piston compresses the gas further, the small scale density gradients become more pronounced as in Fig. 4.25. Also, the sharp difference between the dark edges of the cylinder and piston and the illuminated combustion chamber is not as discernable because the density gradients between the compressed gas and the cooler air in the boundary layer next to the walls are greater causing more light to be deflected. They are large enough at TDC to blacken the entire combustion chamber.

Both direct and shadowgraph cinematographic techniques are used to film the combustion event. Sample photographs of combustion from the movies, Figs. 4.26-28, are from direct movies with the piston and block illuminated by two flood lamps. Thus, the piston and the graphite rings appear as light and dark stripes.

The first combusting frames of coal/methanol and coal/diesel movies are shown in Fig. 4.26. In these movies and the vast majority of the movies, ignition is observed within 2 cm of the injector orifice. The larger fuel droplets penetrate further across the chamber. Conversely, the smaller droplets which ignite more readily remain closer to the nozzle tip. The flame spreads across the chamber as in the top of Fig. 4.27. Within several CAD of ignition, the entire chamber is engulfed in flame. In the lower photograph in Fig. 4.27, leakage from the combustion chamber is observed as combusting particles flowing down the piston along the crown land (right side of the photo).

The luminous combustion period persists well into the expansion stroke. The last observable frames with luminous combustion for diesel No. 2 and coal/diesel

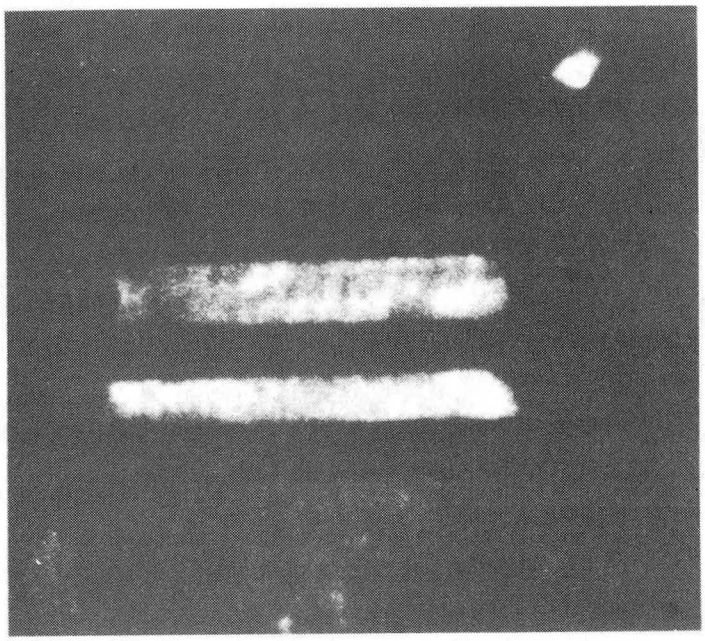

CBB 8512-10193

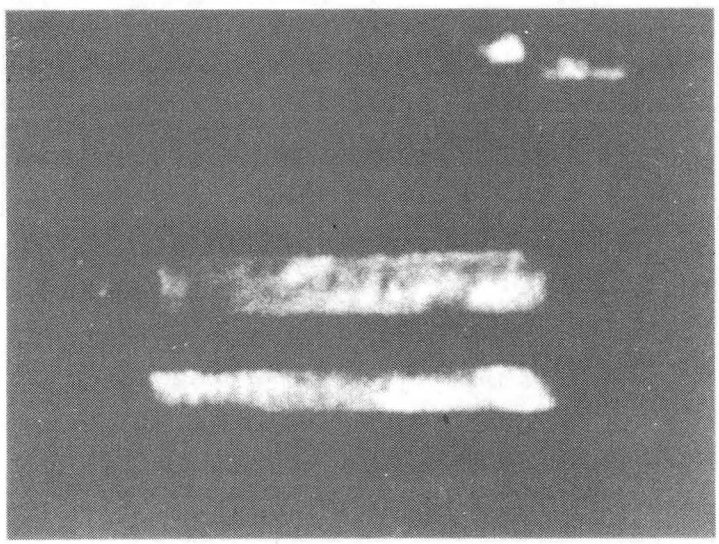

CBB 8512-10195

Figure 4.26. Photographs of coal/diesel (top) and coal/methanol (bottom) ignition in square piston engine simulator.

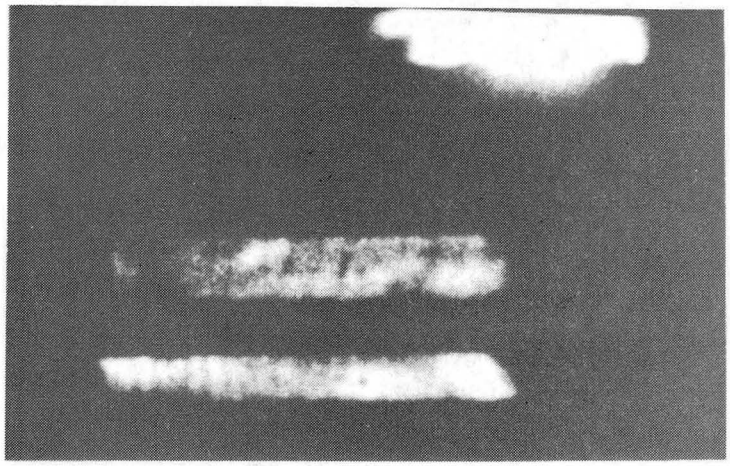

CBB 8512-10197

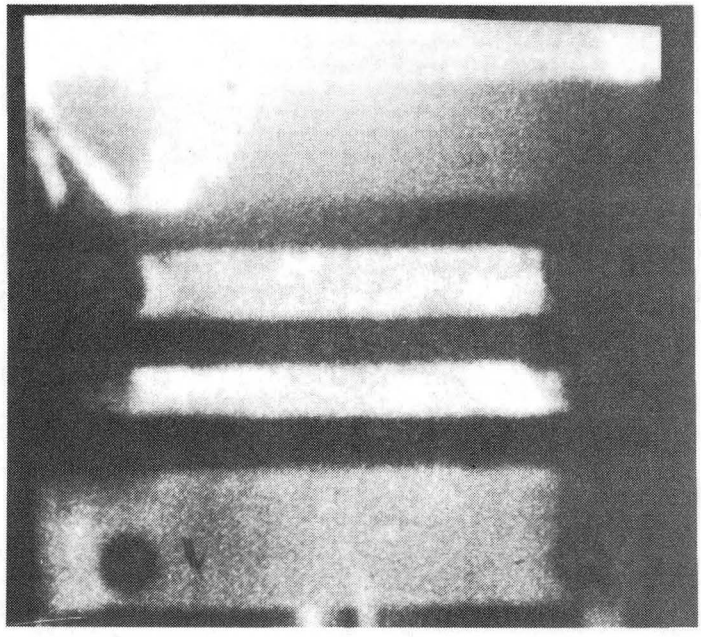

CBB 8512-10199

Figure 4.27. Photograph of coal/methanol flame progressing across combustion chamber (top). Photograph of diesel No. 2 combustion with combusting particles leaking down edge of piston (bottom).

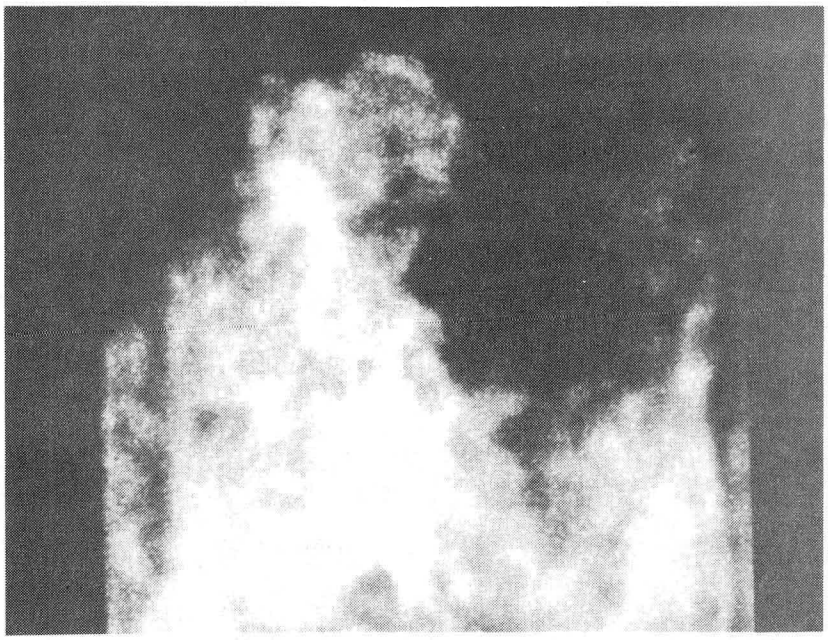

CBB 8512-10201

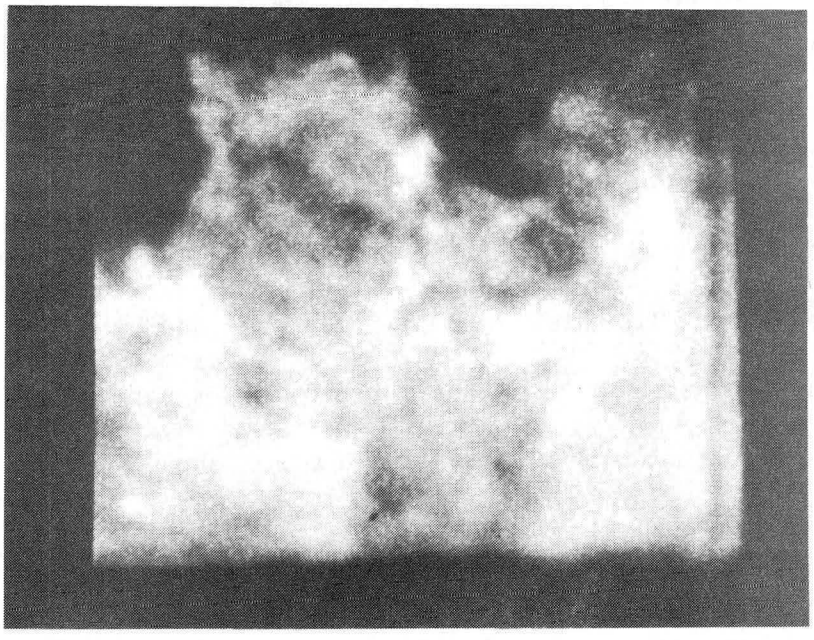

CBB 8510-10203

Figure 4.28. Photographs of the final movie frames of combustion in the power stroke for diesel No. 2 (top) and coal/diesel (bottom).

movies are shown in Fig. 4.28. The piston has retreated out of the viewing window for the diesel fuel (top of Fig. 4.28). But, the combustion does not extend as long into the expansion stroke for coal/diesel as shown in the bottom of Fig. 4.28. Coal/methanol luminous combustion ceases earlier in the expansion stroke than coal/diesel which ceases earlier than neat diesel fuel. The films of methanol combustion show less visible radiation is emitted than with the other fuels.

4.6. COMPARISON TO REPORTED RESULTS

Siebers and Dyer (1985) report ignition delay results from coal/water slurry combustion in a constant volume bomb using vitiated air (described in Section 1.2.1). They define three delays: luminosity delay, pressure recovery delay, and pressure deficit delay (the point of lowest pressure after injection before pressure rises from combustion). Their results and the least squares fit of their data are shown in Fig. 4.29. The data are replotted in Fig. 4.30 along with dotted lines demarcating the operational limits of the square piston engine simulator. The maximum temperature attainable in the engine simulator is approximately 1100 K. The maximum delay time possible in the engine simulator is 10 msec because the temperatures become too low, due to expansion, for significant reaction to occur. The delay time most relevant to the square piston engine simulator, is the pressure recovery delay. As seen in Fig. 4.30, the pressure recovery delay curve does not pass through the shaded region, *i.e.*, the conditions achievable in the engine simulator. Siebers and Dyer's results are consistent with the findings of the present

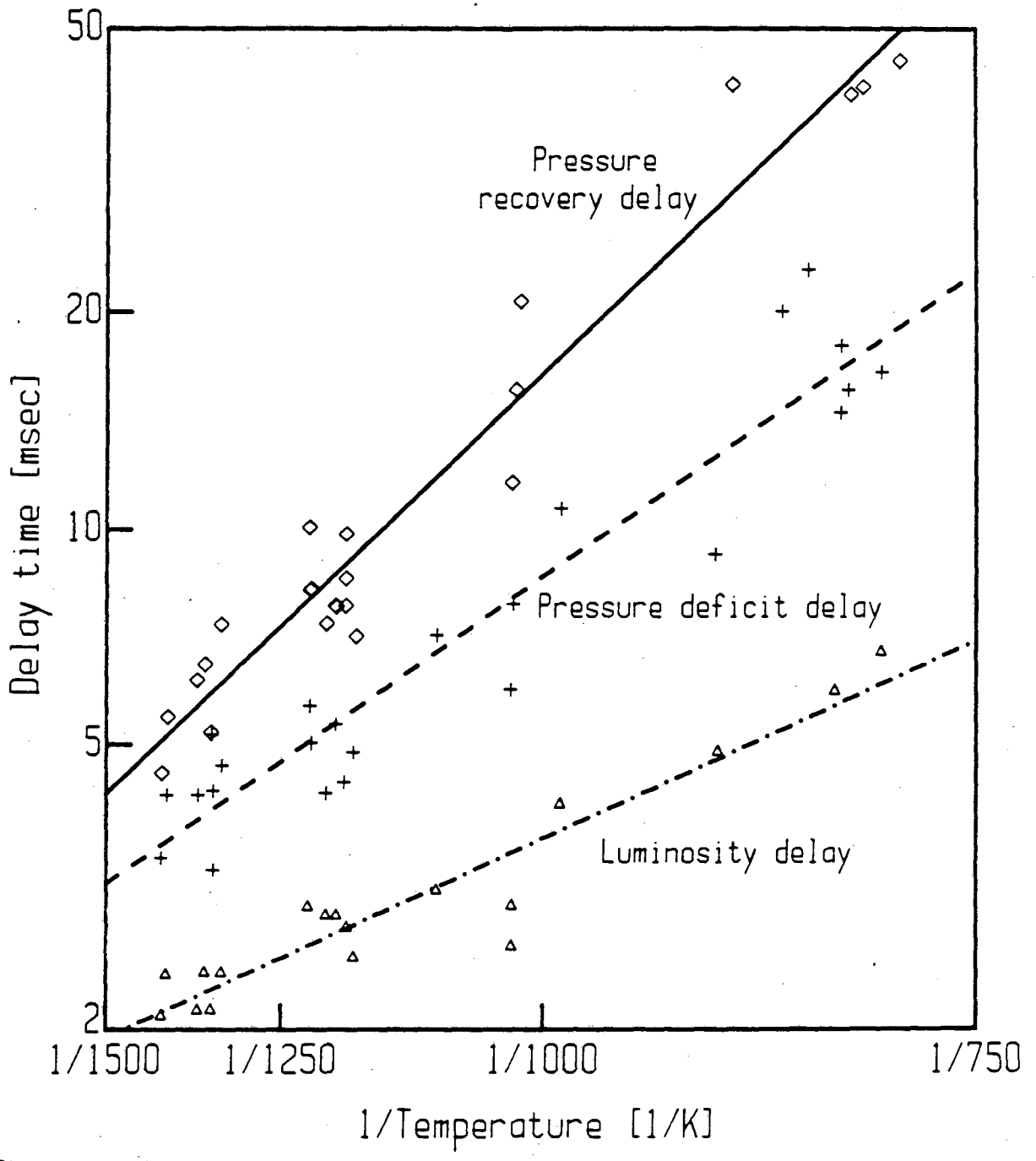

Figure 4.29. Ignition delay measurements of coal/water slurry from a constant volume bomb from paper by Siebers and Dyer (1985).

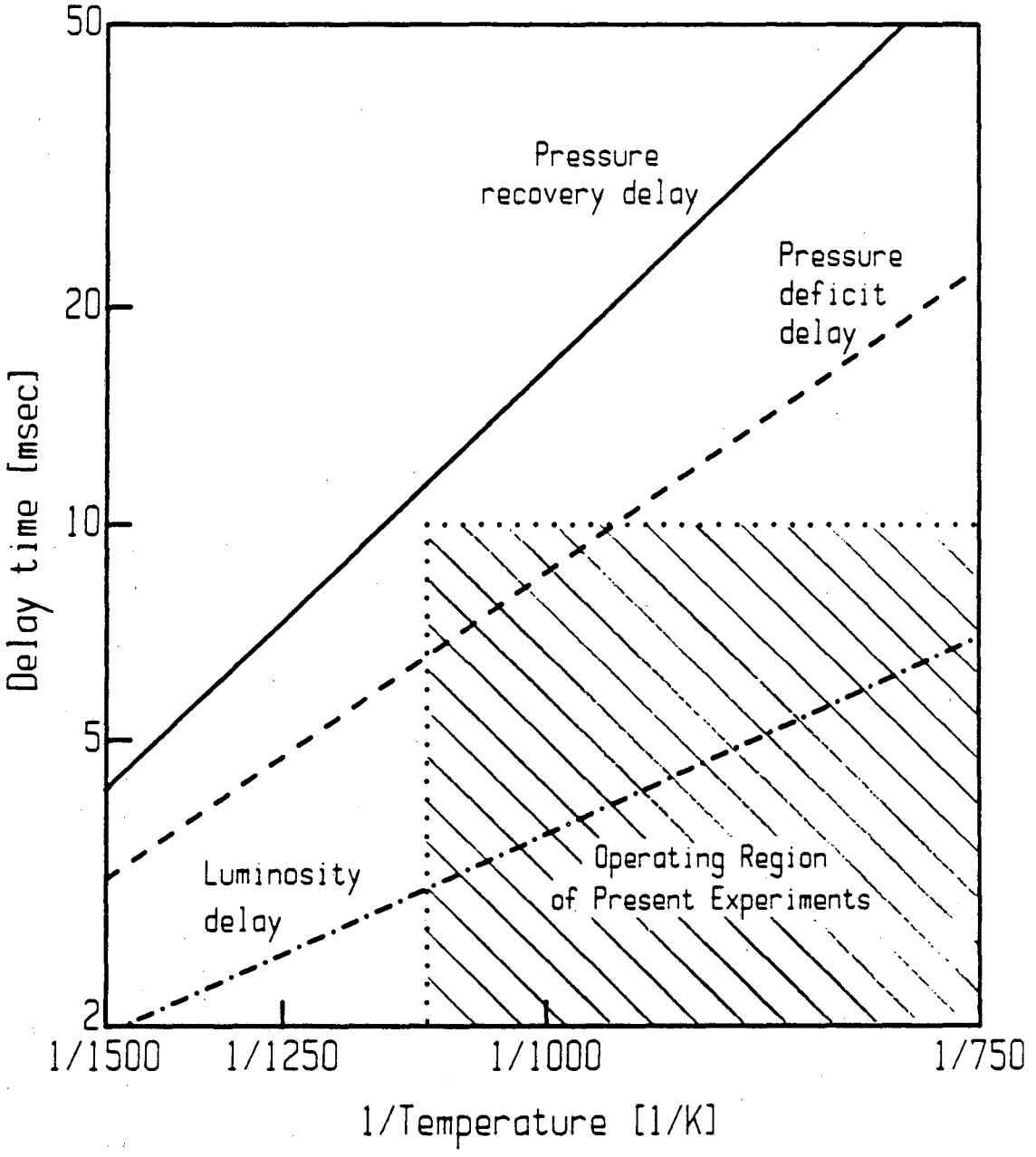

Figure 4.30. Ignition delay results on coal/water from Siebers and Dyers (1985) work with possible operating conditions in square piston engine simulator superimposed.

work that coal/water slurry ignition is not possible in the engine simulator with the current configuration.

Coal/water luminosity is not observed in the engine simulator. But, Siebers and Dyer (1985) present luminosity delay measurements for coal/water slurry in the range of conditions available in the engine simulator. The discrepancy between the present work and Siebers and Dyer's work may be due to the inability of the photodiode to discriminate between infrared radiation from hot combustion chamber surfaces and the weak radiation from coal/water slurry combustion (Siebers and Dyer's apparatus is not heated). The level of block radiation is shown in Fig. 4.7. Siebers and Dyer do not present illumination intensity comparison data for coal/water slurry and diesel fuel to confirm this conjecture. Another possible explanation is that Siebers and Dyer inject the coal/water slurry into vitiated air, *i.e.*, products of combustion of O_2 enriched, lean mixture of H_2 and air. The illumination detected could be due to radicals from the combustion before fuel injection. The difference in the luminosity delay measurements is less important than the pressure delay results from an engineering point of view because combustion luminosity without substantial energy release is of no practical use.

The exponent on the pressure in Eqn 1.1 is 1.5 for the anaylsis of Section 4.3. However, other researchers use very different values, as summarized in Section 1.2.2. To compare between the different results, a pressure of 30 atm is assumed in all the correlations eliminating the pressure dependency. In Fig. 4.31, three correlations for diesel No. 2 are compared to the present study: Tsao, *et al.* (1962) do not use an Arrhenius type expression to explain their results from an indirect

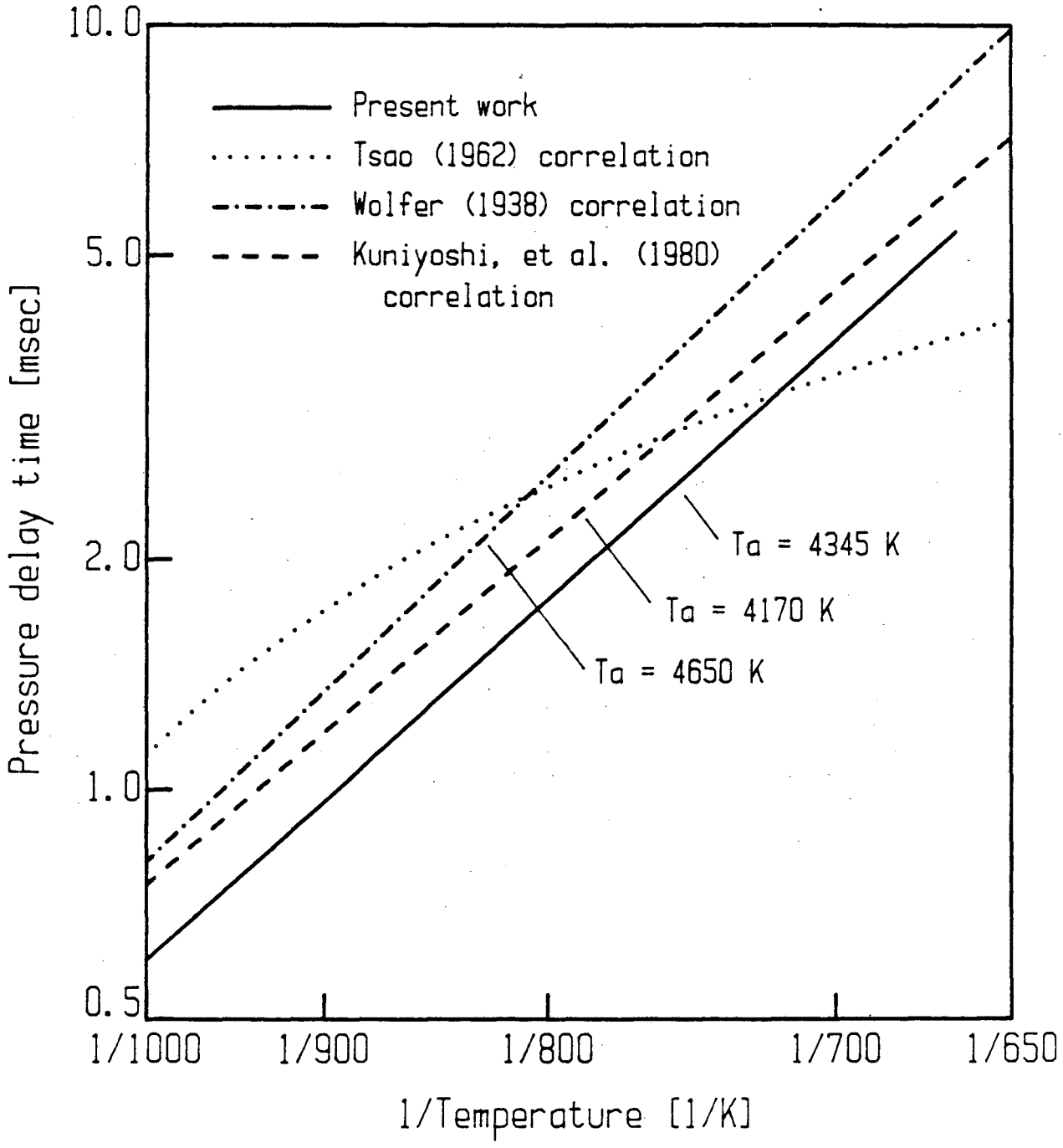

Figure 4.31. Pressure delay as a function of reciprocal temperature for diesel fuel and comparisons to work by others. (Kuniyoshi, *et al.* (1980) do not give a value for the pre-exponential factor. The slope is known; but, the magnitude of the delay times are unknown.)

injection engine; Wolfer (1938) and Kuniyoshi, *et al.* (1980) present correlations found from work in a heated constant volume bomb. Kuniyoshi and coworkers do not provide a value for the pre-exponential factor, only an activation temperature. Therefore, only the slope of the Kuniyoshi data is known in Fig. 4.31. Both the magnitude and slope of Wolfer's and the slope of Kuniyoshi's results are very similar to the square piston engine simulator results. Although the magnitude of the results from Tsao and coworkers is similar to the present work, their delay times are less sensitive to temperature than any of the others plotted in Fig. 4.31.

Luminosity delay results from Kuniyoshi, *et al.* (1980) are shown in Fig. 4.32. These measurements are in good agreement with those obtained from the square piston engine.

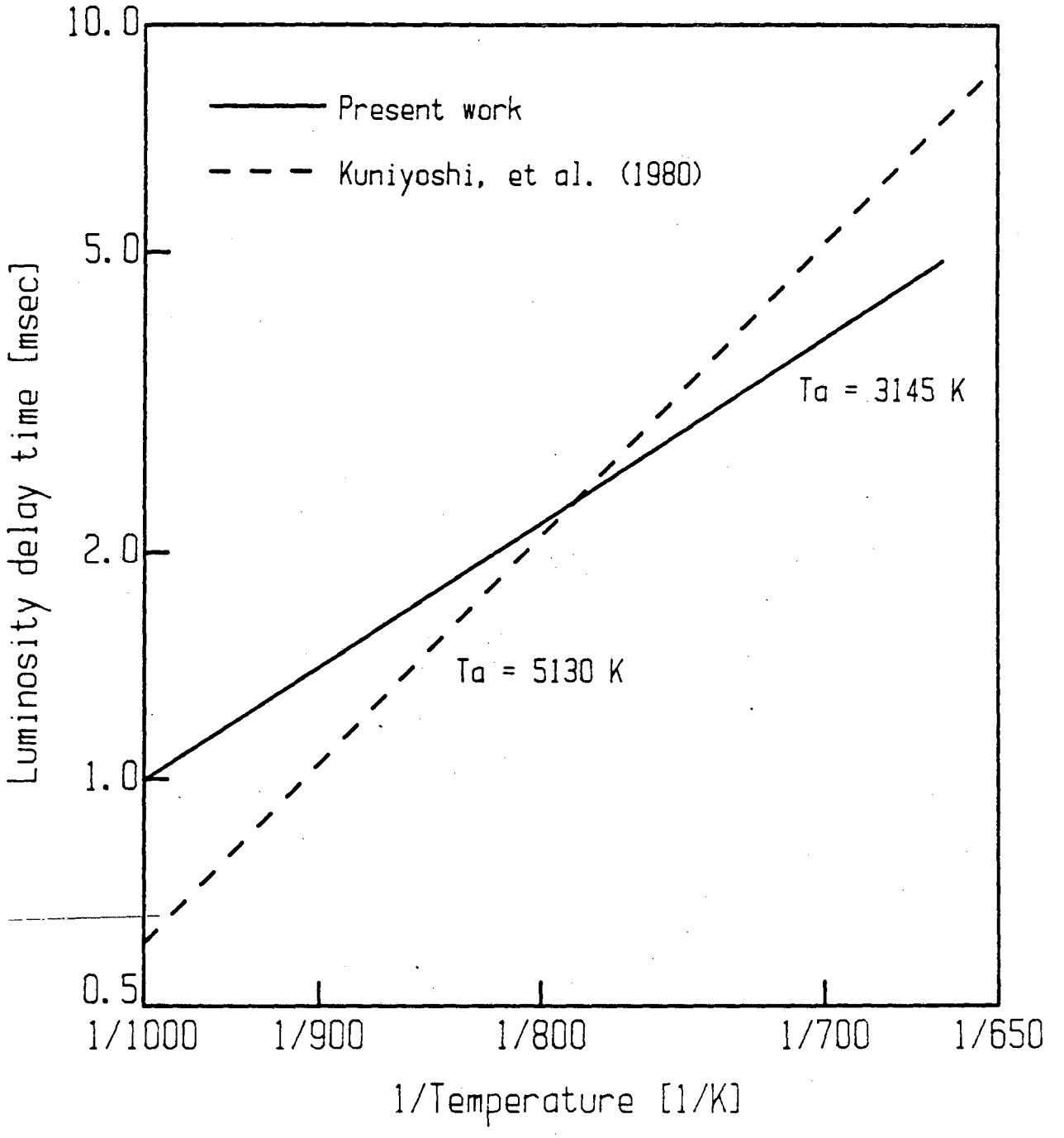

Figure 4.32 Luminosity delay versus reciprocal temperature comparisons for diesel fuel.

5. CONCLUSIONS

1.) A one-zone model of the motoring cycle in the engine simulator is inadequate for predicting the temperatures and pressures in the combustion chamber. Two zones, a bulk gas zone isentropically compressed and a crevice zone isothermally compressed, are modelled providing predictions of the cylinder conditions which agree with piezoelectric pressure transducer and fine wire thermocouple measurements.

2.) A system for injection of coal slurries is developed. The atomization of the coal slurries is noticeably poorer than for diesel fuel from shadowgraphs. Repeatable single injection performance is not provided by this system. It is suggested that a pressure accumulator type system be used for future work.

3.) The integrated needle lift is a satisfactory method for computing the mass of fuel injected.

4.) Coal/methanol slurry combusts at significantly lower inlet temperatures than neat methanol: 360 K versus 450 K.

5.) Methanol compression ignition combustion emits low levels of light making it difficult to obtain accurate luminosity delay measurements.

6.) The activation temperatures for the test fuels are:

Fuel	T_a (Lum)	T_a(Pres)
Diesel No. 2	4360 K	5560 K
Methanol	-	7685 K
Coal/diesel	3925 K	3540 K
Coal/methanol	5510 K	5330 K

The activation temperature for coal/diesel is lower than diesel and coal/methanol based on the pressure delay at the 90% confidence level.

7.) The pressure and luminosity delay intervals are not different within the precision of the measurements in the square piston engine simulator.

8.) The square piston engine simulator is a suitable tool for measuring ignition processes. Because of the high leak rates past the square piston, the combustion and thermal efficiencies cannot be determined accurately. Therefore, coal burnout can only be estimated.

9.) A rough analysis of energy release indicates that approximately 75% or more of the coal in the slurry combusts.

10.) The onset of combustion is observed near the injector in nearly all of the high speed movies.

REFERENCES

Austen, A.E.W., Lyn, W.T., "Relation Between Fuel Injection and Heat Release in a Direct-Injection Engine and the Nature of the Combustion Processes," *Proceedings of the Institution of Mechanical Engineers*, Automobile Division, 47-62 (1960-61).

Begeman, C.R., "Carcinogenic Aromatic Hydrocarbons in Automobile Effluents," SAE Paper 440C (1962).

Benson, R.S., Whitehouse, N.D., *Internal Combustion Engines*, Oxford, Pergamon Press, 164-65 (1981).

Bradley, D., Matthews, R.J., "Measurement of High Gas Temperatures with Fine Wire Thermocouples," *Journal of Mechanical Engineering Science*, **10**, 299-305 (1968).

Caton, J.A., Rosegay, K.H., "A Review and Comparison of Reciprocating Engine Operation Using Solid Fuels," SAE Paper 831362 (1983).

Clingenpeel, J.M., Gurney, M.D., Eccleston, D.B., "A Combustion and Wear Analysis of a Compression-Ignition Engine Using Coal Slurry Fuels," ASME Paper 84-DGP-8 (1984).

Dickson, E.L., "Characterization and Optimization of a Coal Slurry Fuel Injection System," Masters of Science Report, University of California, Berkeley (1983).

Edwards, C.F., Stewart, H.E., Oppenheim, A.K., "A Photographic Study of Plasma Ignition Systems," SAE Paper 850077 (1985).

El Wakil, M.M., Myers, P.S., Uyehara, O.A., "Fuel Vaporization and Ignition Lag in Diesel Combustion," *SAE Transactions*, **64**, 713-26 (1956).

Georgi, C.W., *Motor Oils and Engine Lubrication*, New York, Reinhold Publishing Corporation, 263, 344-47 (1950).

Gurney, M.D., Clingenpeel, J.M., Eccleston, D.B., "A Program to Examine the Use of Coal Slurry Fuels in Diesel Engines", ASME Paper 84-DGP-9 (1984).

Hanse, D.J., "Coal-Oil Mixture as a Diesel Fuel," Master of Science Thesis, University of North Carolina (1949).

Henein, N.A., Bolt, J.A., "Correlation of Air Charge Temperature and Ignition Delay for Several Fuels in a Diesel Engine," SAE Paper 690252 (1969).

Henein, N.A., Bolt, J.A., "Ignition Delay in Diesel Engines," SAE Paper 670007 (1967).

Henein, N.A., Elias, N.Y., "A Modified Cetane Scale for Low Ignition Quality Fuels," *SAE Transactions*, **87**, 2470-82 also SAE Paper 780640 (1978).

Kimber, G.M., Gray, M.D., qRapid Devolatilization of Small Coal Particles,.nr _F 1 q *Combustion and Flame*, **11**, 360 (1967).

Liddle, S.G., Bonzo, B.B., Purohit, G.P., Stallkamp, J.A., "Future Fuels and Engines for Railroad Locomotives," Jet Propulsion Laboratory Report 81-101 (1981).

Lyn, W.T., "The Spectrum of Diesel Combustion Research," *Proceedings of the Institution of Mechanical Engineers*, **184**, Part 3J, 1 (1969-70).

Lyn, W.T., Valdmanis, E., "The Effects of Physical Factors on Ignition Delay," *Proceedings of the Institution of Mechanical Engineers*, **181**, Part 2A, 34-59 (1966-67).

Kays, W.M., Crawford, M.E., *Convective Heat and Mass Transfer*, San Franscisco, McGraw-Hill Book Company, 102 (1980).

Marshall, H.P., Bhat, S.M., Mulvaney, S.T., Sevelli, J.F., "Performance of Diesel Engine Operating on Raw Coal-Diesel Fuel Slurries," SAE Paper 810253 (1981).

Marshall, H.P., Shelton, C., Jr., "The Coal Burning Piston Engine," Bulletin of the Virginia Polytechnic Institute, Engineering Experiment Station, **53**, 135 (1959).

Marshall, H.P., Walters, D.C., Jr., "An Experimental Investigation of Coal-Slurry Fueled Diesel Engine," SAE Paper 770795 (1977).

McBride, B.J., Heimel, S., Ehlers, J.G., Sanford, G., "Thermodynamic Properties to 6000 K for 210 Substances Involving the First 18 Elements," NASA Report SP-3001 (1963).

Miyamoto, N., Murayama, T., "Discussions on the Calculating Techniques of the Rate of Heat Release and Burning Rate in Diesel Engines and Influencing Error Factors," *Nainer-Kikan*, **18**, 9-22 (1979).

Mullins, B.P., "Studies on the Spontaneous Ignition of Fuels Injected Into a Hot Air Stream," *Fuel*, **32**, 211 (1953).

Nelson, L.P., Sampson, P.W., Seeker, W.R., "Combustion Phenomena Associated with Coal Slurries in Medium-Speed Diesel Engine," Proceedings of the First Annual Pittsburgh Coal Conference, Paper 121, 809 (1984).

Nelson, L.P., Seeker, W.R., Zimperman, R.A., "The Atomization, Ignition, and Combustion Characteristics of Coal Slurry Fuels in Medium-Speed Diesel Engines," Joint Technical Meeting of the Central and Western States Sections of the Combustion Institute, Paper 3-1A (1985).

Obert, E.F., *Internal Combustion Engines and Air Pollution,* New York, Intext Educational Publishers, 612-14 (1973).

Oppenheim, A.K., Cheng, R.K., Teichman, K., Smith, O.I., Sawyer, R.F., Hom, K., Stewart, H.E., "A Cinematographic Study of Combustion in an Enclosure with a Reciprocating Piston," from *Stratified Charge Engines,* London, Mechanical Engineering Publishing, Ltd., 127-35 (1977).

Parker, T.E., Forsha, M.D., Stewart, H.E., Hom, K., Sawyer, R.F., Oppenheim, A.K., "Induction Period for Ignition of Fuel Sprays at High Temperatures and Pressures," SAE Paper 850087 (1985).

Penner, S.S., Icerman, L., *Energy, Volume I: Demands, Resources, Impact, Technology, and Policy,* Reading, Massachusetts, Addison-Wesley Publishing Company, 35 (1981).

Raithby, G.D., Eckert, E.R.G., "The Effect of Turbulence Parameters and Support Position on the Heat Transfer from Spheres," *International Journal of Heat and Mass Transfer,* **11**, 1233-52 (1968).

Reinsch, C.H., "Smoothing by Spline Functions," *Numerische Mathematik,* **10**, 177-83 (1967).

Rich, L.L., Walker, M.L., "Pulverized Coal Burning Diesel Engine," Howard University, Office of Coal Research, R & D Report 46 (1969).

Robben, F., "Coal-Fueled Diesel Engines," SAE Paper 831747 (1983).

Roehrle, M.D., "Thermal Effects on Diesel Engine Pistons," *SAE Transactions,* **87**, 2947-63 also SAE Paper 780781 (1978).

Starkman, E., "Ignition Delay in Diesel Engines," *Transactions of the American Institute of Chemical Engineers,* **42**, 107-20 (1946).

Tataiah, K., Lestz, S.J., "Influence of MICO Fuels on Engine Performance, Exhaust Emissions, and Endurance," U.S. Army Fuels and Lubricants Research Laboratory Report 125 (1979).

Tataiah, K., Wood, C.D., "Performance of Coal Slurry Fuel in a Diesel Engine," SAE Paper 800329 (1980).

Taylor, C.F., *The Internal-Combustion Engine in Theory and Practice, Volume 1: Thermodynamics, Fluid Flow, Performance,* Cambridge, MIT Press, 119 (1977).

Taylor, C.F., Taylor, E.S., Livengood, J.C., Russell, W.A., Leary, W.A., "Ignition of Fuels by Rapid Compression," *SAE Quarterly Transactions*, **4**, 232-70 (1950).

Siebers, D.L., Dyer, T.M., "The Autoignition and Combustion of Coal-Water Slurry Under Simulated Diesel Engine Conditions," ASME Paper 85-DGP-15 (1985).

Soehngen, E.E., "Development of Coal-Burning Diesel Engines in Germany. A State-of-the-Art Review," U.S. ERDA Report FE/WAPO/3387-1 (1976).

Spadaccini, L.J., TeVelde, J.A., "Autoignition Characteristics of Aircraft-Type Fuels," *Combustion and Flame*, **46**, 283-300 (1982).

Thurgood, J.R., Smoot, L.D., "Volatiles Combustion," from *Pulverized-Coal Combustion and Gasification,* New York, Plenum Press, 169-82 (1979).

Tracy, E.W., Jr., "Feasibility Study of the Use of Powdered Coal as a Fuel for Diesel Engines," SwRI Report 8-681-1, Southwest Research Institute (1957).

Tsao, K.C., Myers, P.S., Uyehara, O.A., "Gas Temperature During Compression in Motored and Fired Diesel Engine," *SAE Transactions*, **70**, 136-45 (1962).

Ullman, T.L., Hare, C.T., Baines, T.M., "Emissions from Direct-Injected Heavy-Duty Methanol-Fueled Engines (One Dual-Injection and One Spark-Ignited) and a Comparable Diesel Engine," *SAE Transactions*, **91**, 3154-70 also SAE Paper 820966 (1982).

Wolfer, H.H., "Ignition Lag in the Diesel Engine," *VDI Forshungsheft*, **392**, 15-24 (1938).

Woschni, G., "A Universally Applicable Equation for the Instantaneous Heat Transfer Coefficient in the Internal Combustion Engine," *SAE Transactions*, **76**, 3065-83 also SAE Paper 670931 (1967).

APPENDIX A.

m2ch4.c

```
#include <stdio.h>

#define         CLKRT   10000.          /* Clock rate. */
#define         SECMIN  60.             /* 60 seconds per minute. */
#define         INERAT  0.782           /* Ratio of inertias between flywheel
                                        & motor and flywheel, motor & engine.*/
#define         OFFSET  15.             /* Offset to compensate for slow down
                                        of engine during test. */

/* M2ch4 is a data taking program for the Mark II research engine in
   Hesse Hall.  User interface and parameter setup is handled by the
   C programs:
                m2ch4.c--main controlling program
                mkst4.c-parameter setup
                input.c--I/O interface
                wr4.c--write data in output file
                look4.c---look at the maximum pressure
                draw4.c---draw data on screen

   The first thing to accomplish is setting the parameters to the right values
   using the program, markst.  Data taking is done by invoking the data
   command.  This sends the control to two assembly  language routines.
   The first routine computes the flywheel rpm during coastdown and displays
   the value on the screen.  After the desired rpm is reached, the operator
   initiates the test by starting the engine clutch brake and at the same
   time the computer is sent to the second assembly program awaiting pulses
   from the shaft encoder at the engine.  This second assembly program is
   called addat.  It takes four channels of data at one CAD intervals for
   two full revolutions.  This is done by a Data Translation A/D converter
   which runs in the DMA mode.  In addition this routine monitors and
   records the timing of the start and end of injection and combustion.
   In addition, a precise measure of engine rpm is computed. */

static char cmdtab[]="sedalowrdrhequ";
static char prompt[]="#";

double rpm = 900., comprat = 16., psc = 2.0;
double calfac[] = {20., 50., 0.254, 1000.};
char dfile[15] = "dy1:gorfit.dat";
char date[10] = "01/01/86";
int addat[2884] = 0;
int count[10] = 0;

_main()         /* Main is the controlling program which calls all the
                other subroutines.  These other subroutines are called by
                using two letter codes which are described in the help
                list. */
{
int cmd=0;
int ij, fwrpm();
float fwspeed;
FILE *fopen(), *fp;
        /* Set up forever loop and wait for commands.  The only way out
           is thru case 1 - qu = quit command.  If a return is typed it
           sits and waits for a real command, if an illegal command is
           typed it prints error message and waits for a legal command,
           if a legal command is typed it executes that command and then
           waits for the next command. */
```

```
/* Initialize the data array to zero. */
for (ij = 0; ij < 2884; ij ++)
        addat[ij] = ij;
for (ij = 0; ij < 10; ij ++)
        count [ij] = -1;

while(1)
        {
        cmd=getcmd(cmd,cmdtab,prompt);

        switch(cmd)
                {
                case 0 : break;
                case 1 : set();
                         break;
                case 2 :
        /* Compute the desired flywheel speed, compare it to the actual
        measurement.  Continue until the proper speed is obtained. */
                         fwspeed = (rpm + OFFSET) / INERAT;
                         fwrpm();
                         while ((CLKRT * SECMIN / fwrpm()) > fwspeed)
                                { printf ("%4.0f rpm.\r", CLKRT * SECMIN /
                                        fwrpm());
                                  for (ij = 0; ij < 10; ij++)
                                        fwrpm(); }
                         printf ("\n");
                         printf ("  Go for it!\n");
        /* Initialize the event array before each data run. */
                        for (ij = 0; ij < 10; ij ++)
                                count [ij] = -1;
        /* Send control to the data taking routine ad2ch4.  Two pointers
        are sent: the one for the data and the one for the event timing. */
                         ad2ch4 (addat, count);
                         printf ("\n");
                         printf("Data location in %o and events in %o octal\n",
                                addat, count);
                         break;
                case 3 : look();
                         break;
                case 4 : wr();
                         break;
                case 5 : draw();
                         break;
                case 6 : help();
                         break;
                case 7 : exit();
                         break;
                default: printf("getcmd returns bad value\n");
                         break;
                }
        }
}
```

input.c

```
#include <stdio.h>

#define MAXLINE 100

/* All subroutines that use these input routines must
   "include" input.d, which contains extern declaration
   of level and definition of nest. The include is not
   nescessary for the main program. */

int level=0;   /* level keeps track of command nesting */
static int c='a';  /* c is the last character read,
                      and must be known to all the input routines */

getcmd(cmdtab,prompt)

char *cmdtab; /* table of two letter commands */
char prompt[];   /* prompt to be printed by getcmd */

{

int j,n,i,k,l;
char curcmd[2]; /* contains current command */
int cmd;        /* numerical value of command */

/* initialize and loop until valid input found */

j=1;
while (j != 0)
       {
       /* print prompt unless line contains more input */
       if (c == ' ') level++;
       else printf("%s",prompt);

       /* read in first two letter command, eating leading
          blanks, and stopping at trailing blanks and
          newline */

       n=0;
       c=getchar();

       while (c != '\n')           /* stop at newline */
              {
              if (c == ' ') c=getchar();   /* eat blanks */
              else
                     {
                     for (l=0;l<2;l++)   /* read in command */
                            {
                            *(curcmd + l) = c;
                            c=getchar();
                            }
                     n++;
                     if (c == ' ') break;  /* stop if blank follows */
                     }
              }

       /* if first character was a newline set cmd=0,
          and set valid command flag */
```

```
        if (c == '\n' && n == 0)
                {
                cmd=0;
                j=0;
                }
        else
                {
                /* translate letter command into numerical command */

                for (i=0;cmdtab[i] != '\0';i=i+2)
                        {
                        if ((*curcmd == *(cmdtab + i)) &&
                            (*(curcmd + 1) == *(cmdtab + i + 1)))
                                {
                                cmd=(i+2)/2;
                                j=0;
                                }
                        }
                if (j != 0) printf("invalid input\n");
                }
        }
return(cmd);
}

finput(point,j)     /* float input acquisition routine */

double *point;      /* array pointer to variable to be read */
int j;              /* array size */

{
int n=0;

do      {
        /* if the input is a number, read it.
           if it is a ",", leave old value.
           if it is a return, leave old value(s).
          eat blanks and extra input */

        c=getchar();

        if (c != ',' && c != '\n' && c != ' ' && n < j)
                {
                ungetc(c,stdin);
                scanf("%lf",(point+n));
                n++;
                c=getchar();
                }
        else if (c == ',') n++;

        } while (c != '\n');
}

getstat()
{
return(c);
}

iinput(point,j)     /* integer variable input acquisition routine */

int j;          /* array size */
```

```
int *point;     /*  pointer to array to be read */

{

int n=0;

do     {
            /* if it is a number, read it.
            if it is a ",", leave old value.
            if it is a return, leave old value(s).
            eat blanks and extra input */

       c=getchar();

       if (c != ',' && c != '\n' && c != ' ' && n < j)
              {
              ungetc(c,stdin);
              scanf("%d",(point+n));
              n++;
              c=getchar();
              }
       else if (c == ',') n++;

       } while (c != '\n');
}

sinput(point)

char *point;

{

do {
        c=getchar();

        if (c != '\n' && c != ' ')
                {
                ungetc(c,stdin);
                scanf("%s",point);
                c = '\n' ;
                }
        } while (c != '\n');
}
/* This routine uses sinput to read in filenames  */

filename(name)

char name[];

{
if ( getstat() == ' ' ) sinput(name);
else
        {
        printf("filename = %s : ",name);
        sinput(name);
        }
return;
}

/*  This is a version of finput that reads data from files.  */
```

```
filefin(point,j,infp)

double *point;
int j;
FILE *infp;

{
int c;
int n=0;

do      {
        c=getc(infp);

        if ( c != ',' && c != '\n' && c != ' '  && n < j )

                {
                ungetc(c,infp);
                fscanf(infp,"%lf",(point+n));
                n++;
                }
        else if ( c == ',' ) n++;

        } while ( c != '\n' );
}

strcmp(s,t)     /* return <0 if s<t, 0 if s=t, >0 if s>t */
char *s,*t;
{
for( ; *s == *t ; s++,t++ )
        if ( *s == '\0' )
                return(0);
        return(*s-*t);
}
comment(name)

char name[];

{
FILE *fopen(),*fp;
char line[MAXLINE];

if ( (fp=fopen(name,"a")) == NULL )
        {
        printf("can't open %s !\n",name);
        return;
        }
printf(">");
while( (c=getchar() ) != '\n' )
        {
        ungetc(c,stdin);
        fgets(line,MAXLINE,stdin);
        fputs(line,fp);
        printf(">");
        }
fclose(fp);
}
```

```
        .TITLE FWRPM
        .GLOBL FWRPM
;
; This program will indirectly give the speed of the flywheel for the
; compression expansion experiment.  The positively going signal from
; the inductive pickup mounted on the flweheel is sent to bit 2 of the
; parallel port.  A loop is set up to start the clock when a high comes in.
; A following loop waits until the tick goes low.  Then, when another tick
; comes in the clock is stopped.  The contents of the counter are put into
; CKBPR where the are subsequently read by R0.
; The clock rate will be set at 10 kHz.  Thus, the flweeh rpm will be
; 10,000 (clock rate) X 60 (conversion between min and sec) / pulses in int.
;
        CKCSR = 170420          ; Clock status register.
        CKBPR = 170422          ; Clock buffer preset register.
        DRCSR = 167710          ; Parallel port status register.
        DRINBUF = 167714        ; Parallel port input address.
;
FWRPM:  NOP
        CLR @#CKCSR             ; Clear the status register.
        BIS #30, @#CKCSR        ; Clock rate is 10 kHz.
        BIS #4, @#CKCSR         ; Set up for mode 2 operation of clock.
;
ON:     BIT #4, @#DRINBUF       ; Test for a positive signal at parallel port.
        BNE ON                  ; If not, loop.
        BIS #1, @#CKCSR         ; If so, turn on clock.
LOOP:   BIT #4, @#DRINBUF       ; Wait until signal goes low.
        BEQ LOOP                ; If not, keep looping.
OFF:    BIT #4, @#DRINBUF       ; Wait for another high to turn off clock.
        BNE OFF                 ; If not, loop.
        BIS #1000, @#CKCSR      ; Set bit 9 in the status register.  It will
                                ; simulate an ST2 signal which will cause the
                                ; contents of the counter to go to BPR.
        MOV @#CKBPR, R0         ; Put the clock count in R0.
        CLR @#CKCSR             ; Turn off the clock.
        BR EXIT
;
EXIT:   RTS PC
        .END
```

```
        .TITLE AD2CH4
        .GLOBL AD2CH4
;
        DRCSR=167710            ; Parallel board status register.
        DRINBUF=167714          ; Parallel port input address.
;
        CKCSR=170420            ; KWV-11C clock status register.
        CKBPR=170422            ; KWV-11C buffer count register.
;
        ADCSR=170400            ; A/D status register.
        ADBUF=170402            ; A/D buffer register.
        DMAWCR=170404           ; DMA word count register.
        DMACAR=170406           ; DMA current address register.
psr = 177564
pdr = 177566
;
; This routine is designed for the following:
;  -A/D conversions twice at each 1/2 CAD in the auto increment mode.
;   Thus, for four channel operation at 4 conversions per crank angle degree,
;   signal 1 should be connected to inputs 0 and 4, signal 2 to inputs
;   1 and 5, signal 3 to inputs 2 and 6, and signal 4 to inputs 3 and 7.
;  -The number of conversions is for two revolutions:  2884 data points.
;  -When 2884 conversions are completed, the A/D will interrupt to exit to the
;   controlling program.
;  -The time for the injection needle opening, the beginning of ignition as
;   measured by luminosity, and the end of burning again measure by luminosity
;   will be recorded.  The clock ticks will be stored in memory for later
;   processing.
;
AD2CH4: NOP
        MOV 2(SP),@#DMACAR      ; Pop the value of the address where
                                ; the first data conversion is to go.
        MOV 4(SP),R0            ; Pop the value of the address where
                                ; the CAD occurence of needle lift and
                                ; luminosity are to go.
;
        MOV @#ADBUF, R1         ; Clear out a/d buffer by reading it.
        MOV #-2884.,@#DMAWCR    ; The A/D converter will make 2882 measmnts.
        CLR @#ADCSR             ; Clear status reg before setting bits.
        BIS #10, @#ADCSR        ;   -Auto increment mode
        BIS #40, @#ADCSR        ;   -RTC trigger enable
        BIS #3400, @#ADCSR      ;   -Start with channel 7.
        BIS #2, @#ADCSR         ;   -DMA operation
        CLR @#CKCSR             ; Clear clock status reg before setting bits.
        BIS #4, @#CKCSR         ;   -Mode 2 operation.
        BIS #30, @#CKCSR        ;   -10 kHz clock rate.
;
        MOV R0, R1              ; The address in the account array for the
        ADD #10, R1             ; number of clock ticks will be at R1.
;
LOOP:   TSTB @#ADCSR            ; Don't start clock until an A/D conversion
        BPL LOOP                ; has taken place.


        BIS #1, @#CKCSR         ; Turn on the clock.
LOOPA:  TST @#DMAWCR            ; Each of the loops will contain a check
        BPL EXIT                ; to determine if an A/D done interrupt has
                                ; occurred.  If so, exit.
        BIT #1, @#DRINBUF       ; Check for needle lift to be set high.
        BEQ LOOPA               ; If not, keep looping for another check.
```

```
        MOV @#DMAWCR, (R0)+     ; If so, store the timing in the first
                                ; location in the array, and then increment
                                ; the address.
mov #141, char
jsr PC, putchar
        BR LOOPB1
;
LOOPB1: TST @#DMAWCR            ; Check for A/D done again.
        BPL EXIT
        BIT #1, @#DRINBUF       ; Check for a low for needle lift.
        BNE LOOPC1              ; If not, check for a high in loop C1.
        MOV @#DMAWCR, (R0)+     ; If so, store the timing in the next
                                ; location in the array, increment.
mov #142, char
jsr PC, putchar
mov #61, char
jsr PC, putchar
        BR LOOPC2
;
LOOPC1: TST @#DMAWCR            ; Check for A/D done again.
        BPL EXIT
        BIT #2, @#DRINBUF       ; Check for a high on the luminosity.
        BEQ LOOPB1              ; If not go back to check needle lift detector.
        INC R0                  ; If luminosity begins before needle lift
        INC R0                  ; is over, the event timing must be put
                                ; in the proper location in the array.
        MOV @#DMAWCR, (R0)      ; If so, store event timing in array.
mov #143, char
jsr PC, putchar
mov #61, char
jsr PC, putchar
        BR LOOPB2               ; Look for needle lift signal in another loop.
;
LOOPC2: TST @#DMAWCR            ; Check for A/D done again.
        BPL EXIT
        BIT #2, @#DRINBUF       ; Check for a high on the luminosity detector.
        BEQ LOOPC2              ; If not, keep checking for a high.
        MOV @#DMAWCR, (R0)+     ; If so, store the event timing in the array
                                ; and increment the address.
mov #143, char
jsr PC, putchar
mov #62, char
jsr PC, putchar
        BR LOOPD1
EXIT:   NOP
        BIS #1000, @#CKCSR      ; Set a maintenance bit in the clk status
                                ; register so that the counter can be
                                ; indirectly read through the CKBPR.
        MOV @#CKBPR, (R1)       ; Send the number of clock ticks for the
                                ; two revolution interval into the count array.
        CLR @#CKCSR             ; Turn off clock.
        CLR @#ADCSR             ; Turn off a/d converter.
        RTS PC
;
LOOPD1: TST @#DMAWCR            ; Check for A/D done again.
        BPL EXIT
        BIT #2, @#DRINBUF       ; Check for a low on the luminosity detector.
        BNE LOOPD1              ; If not, kkeep looping.
        MOV @#DMAWCR, (R0)      ; If so, store the event timing in the array.
mov #144, char
```

```
jsr PC, putchar
mov #61, char
jsr PC, putchar
        BR LOOPEX               ; All done, go to exit loop to wait for
                                ; A/D to finish conversions.
;
LOOPB2: TST @#DMAWCR            ; Check for A/D done again.
        BPL EXIT
        BIT #1, @#DRINBUF       ; Look for a low on the needle lift detector.
        BNE LOOPD2              ; If not, look for a low on the luminosity
                                ; detector.
        DEC R0                  ; Need to get to proper address to write
        DEC R0                  ; this event.
        MOV @#DMAWCR, (R0)+     ; If so, store the event timing in the array.
                                ; Increment the address.
mov #142, char
jsr PC, putchar
mov #62, char
jsr PC, putchar
        BR LOOPD3               ; The only thing to look for is a low on
                                ; the luminosity detector.
;
LOOPD2: TST @#DMAWCR            ; Check for A/D done again.
        BPL EXIT
        BIT #2, @#DRINBUF       ; Look for low on luminosity detection.
        BNE LOOPB2              ; If not, go back to check needle lift.
        INC R0                  ; If so, increment address counter before
        INC R0                  ; storing event timing.
        MOV @#DMAWCR, (R0)      ; Store event timing.
mov #144, char
jsr PC, putchar
mov #62, char
jsr PC, putchar
        BR LOOPB3               ; Last event to detect is needle lift closing.
;
LOOPB3: TST @#DMAWCR            ; Check for A/D done again.
        BPL EXIT
        BIT #1, @#DRINBUF       ; Check for low on needle lift detector.
        BNE LOOPB3              ; If not, keep looking.
        DEC R0                  ; Get address counter to correct location
        DEC R0                  ; in array.
        MOV @#DMAWCR, -(R0)     ; Store event timing.
mov #142, char
jsr PC, putchar
mov #63, char
jsr PC, putchar
        BR LOOPEX               ; All done, go to loop to wait for A/D done.
;
LOOPD3: TST @#DMAWCR            ; Check for A/D done again.
        BPL EXIT
        BIT #2, @#DRINBUF       ; Check for a low on luminosity detector.
        BNE LOOPD3              ; If not, loop back until it is low.
        INC R0                  ; Get address counter to correct location
        INC R0                  ; in array.
        MOV @#DMAWCR, (R0)      ; Store event timing.
mov #144, char
jsr PC, putchar
mov #63, char
jsr PC, putchar
;
```

```
LOOPEX: TST @#DMAWCR            ; Check for A/D done.
        BMI LOOPEX              ; If not, keep looping.
        BR EXIT                 ; If so, exit.
;
putchar:tstb @#psr
bpl putchar
mov char, @#pdr
rts PC
;
char:   .byte   Ø
.even
        .END
```

wr4.c

```
#include <stdio.h>
#include <math.h>

#define ADCONV  0.001227        /* A/D conversion factor. */
#define CONV    -4.0            /* Conversion factor between the DMAWCR reg
                                   and the actual CAD. */
#define TWOREV  720.            /* Number of degrees in two revolutions. */
#define TICKCONV 1.2e06         /* Conversion between ticks counted at 10 kHz
                                   and rpm for the two rev sampling period. */

extern double psc, rpm, comprat, calfac[];
extern char dfile[], date[];
extern int addat[], count[];

wr()
{
        int ij, kl;
        int pmax = 0;
        float deg = 0;
        FILE *fopen();
        register FILE *fp;

        if ((fp = fopen (dfile, "w")) == NULL)
                { printf ("File not opened for writing raw data.\n");
                  return (0); }
        fprintf (fp, "# %s\n", date);
        fprintf (fp, "# Calibration factors:\n");
        fprintf (fp, "\t%4.1f\t%4.1f\t%5.3f\t%4.1f\n",
                *calfac, *(calfac + 1), *(calfac + 2), *(calfac + 3));
        fprintf (fp, "# P inlet in atm abs =\n");
        fprintf (fp, "\t%4.1f\n", psc);
        fprintf (fp, "# Rack opening and closing in CAD are at:\n");
        fprintf (fp, "\t%5.1f\t\t%5.1f\n",
                TWOREV - (float) *count / CONV,
                TWOREV - (float) *(count + 1) / CONV);
        fprintf (fp, "# Luminosity in CAD begins and ends at\n");
        fprintf (fp, "\t%5.1f\t\t%5.1f\n",
                TWOREV - (float) *(count + 2) / CONV,
                TWOREV - (float) *(count + 3) / CONV);
        fprintf (fp, "# Actual rpm =\n");
        fprintf (fp, "\t%5.0f\n", TICKCONV / (float) *(count + 4));

        for (ij = 0; ij < 721; ij++)
        {
                if (*(addat + ij * 4) > pmax)
                        {
                        pmax = *(addat + ij * 4);
                        kl = ij;
                        }
        }
        fprintf (fp, "# Max pressure of %4.1f atm at %3d deg.\n",
                (pmax - *(addat + 720)) * ADCONV * *calfac + psc, kl);
        fprintf (fp, "#\n");
        fprintf (fp, "# Integer counts at 180 CAD (in decimal).\n");
        fprintf (fp, "\t%d\t%d\t%d\t%d\n",
            *(addat + 720), *(addat + 721), *(addat + 722), *(addat + 723));

        fprintf (fp, "# Cyl pres In pres Nd lift Luminosity (in hex):\n");

        for (ij = 0; ij < 721; ij++)
                fprintf (fp, "\t%x\t%x\t%x\t%x\n", *(addat + ij * 4),
                        *(addat + ij * 4 + 1), *(addat + ij * 4 + 2),
                        *(addat + ij * 4 + 3));

        fclose(fp);
}
```

```
#include <stdio.h>

#define X0 63
#define Y0 50
#define XTIK 4
#define YTIK 16

/* ------------------------------------------------------------------ */
/*
/*  BOX(): clears screen, draws box, and puts ticks on box
/*
/* ------------------------------------------------------------------ */

bxtik()
{
int i, x, y;

fprintf (stdout, "\032\r");             /* clear screen */
vector(stdout,Y0,X0,Y0,X0+900);         /* bottom */
vector(stdout,Y0,X0 + 900,Y0 + 700,X0 + 900);   /* RHS    */
vector(stdout,Y0 + 700,X0 + 900,Y0 + 700,X0);   /* top    */
vector(stdout,Y0+ 700,X0,Y0,X0);                /* LHS    */

/* Now draw the ticks. */

for (i = 1; i < XTIK; i++)
        {
        x = X0 + i * 900 / XTIK;
        vector(stdout,Y0,x,Y0+15,x);
        }

for (i = 1; i < YTIK; i ++)             /* y-axis ticks */
        {
        y = Y0 + i * 700 / YTIK;
        vector(stdout,y,X0,y,X0+10);
        if (i == 4 || i == 8 || i == 12)
                vector (stdout, y, X0, y, X0 + 20);
        }
}

/* ------------------------------------------------------------ */
/*
/* ERASE(): clears text and graph off screen
/*
/* ------------------------------------------------------------ */

erase()
{
fprintf (stdout, "\035\033\014\036\030\r");
}
```

draw4.c

```
#include <stdio.h>
#include <input.d>

#define XBEGIN  360             /* Plot data from this number in data file. */
#define XEND    1080            /* Stop plotting at this point in data file. */
#define X0      50              /* X graph offset. */
#define Y0      50              /* Y graph offset. */
#define XMAX    900.            /* X graph size. */
#define YMAX    700.            /* Y graph size. */

extern int addat[];

static char cmdtab[] = "prinndluboerheen";
static char prompt[] = "draw>";

draw()
{
double x1, x2, y1, y2, yrange, rflev, xrange = 720.;
int cmd = 0, ij;

while(1)
{
    cmd = getcmd (cmd, cmdtab, prompt);
    switch(cmd)
        {
        case 0: break;
        case 1: /* Plot the cylinder pressure data. */
        rflev = (double) addat [720] - 82;
        yrange = 3277.;
        x1 = 0.;
        y1 = YMAX * ((double)addat[720] - rflev) / yrange;
        for (ij = XBEGIN; ij < XEND; ij = ij + 2)
                {
                x2 = x1 + 2.;
                y2 = YMAX * ((double) addat[ij * 2 + 4] - rflev) / yrange;
                vector(stdout, Y0 + (int) y1,(int) (XMAX * (X0 + x1) / xrange),
                                Y0 + (int) y2,(int) (XMAX * (X0 + x2) / xrange));
                x1 = x2;
                y1 = y2;
                }
        break;

        case 2: /* Plot the injection line pressure data. */
        rflev = (double) addat [721];
        yrange = 6553.;
        x1 = 0.;
        y1 = YMAX * ((double)addat[721] - rflev) / yrange;
        for (ij = XBEGIN; ij < XEND; ij = ij + 2)
                {
                x2 = x1 + 2.;
                y2 = YMAX * ((double) addat[ij * 2 + 5] - rflev) / yrange;
                if (y2 < 0.)
                        y2 = 0.;
                vector(stdout, Y0 + (int) y1,(int) (XMAX * (X0 + x1) / xrange),
                                Y0 + (int) y2,(int) (XMAX * (X0 + x2) / xrange));
                x1 = x2;
                y1 = y2;
                }
```

```
                break;

                case 3: /* Plot the needle lift data. */
                rflev = (double) addat [722];
                yrange = 2580.;
                x1 = 0.;
                y1 = YMAX * ((double)addat[722] - rflev) / yrange;
                for (ij = XBEGIN; ij < XEND; ij = ij + 2)
                        {
                        x2 = x1 + 2.;
                        y2 = YMAX * ((double) addat[ij * 2 + 6] - rflev) / yrange;
                        if (y2 < 0.)
                                y2 = 0.;
                        vector(stdout, Y0 + (int) y1,(int) (XMAX * (X0 + x1) / xrange),
                                        Y0 + (int) y2,(int) (XMAX * (X0 + x2) / xrange));
                        x1 = x2;
                        y1 = y2;
                        }
                break;

                case 4: /* Plot the luminosity. */
                rflev = (double) addat [723];
                yrange = 4095.;
                x1 = 0.;
                y1 = YMAX * ((double)addat[723] - rflev) / yrange;
                for (ij = XBEGIN; ij < XEND; ij = ij + 2)
                        {
                        x2 = x1 + 2.;
                        y2 = YMAX * ((double) addat[ij * 2 + 7] - rflev) / yrange;
                        vector(stdout, Y0 + (int) y1,(int) (XMAX * (X0 + x1) / xrange),
                                        Y0 + (int) y2,(int) (XMAX * (X0 + x2) / xrange));
                        x1 = x2;
                        y1 = y2;
                        }
                break;

                case 5: bxtik();
                        break;
                case 6: erase();
                        break;
                case 7: drhelp();
                        nest
                        break;
                case 8: return;
                        break;
                default:printf ("getcmd returns bad value\n");
                        break;
                        }
                }
}
```

```
#include <stdio.h>

/* ------------------------------------------------------------------ */
/*
/* VECTOR(): draws a line on screen between specified points
/*
/* ------------------------------------------------------------------ */

vector(fp,y1,x1,y2,x2)

FILE *fp;
int y1,x1,y2,x2;

{
putc('\035',fp);
putc( y1 / 040 +  040 ,fp);
putc( y1 % 040 + 0140 ,fp);
putc( x1 / 040 +  040 ,fp);
putc( x1 % 040 + 0100 ,fp);
putc( y2 / 040 +  040 ,fp);
putc( y2 % 040 + 0140 ,fp);
putc( x2 / 040 +  040 ,fp);
putc( x2 % 040 + 0100 ,fp);
fprintf(fp,"\037\030\r");
}
```

```
r link
dy1:m2ch4=dy1:m2ch4/B:7500,//
dy1:mkst4
dy1:input
dy1:look4
dy1:wr4
dy1:ad2ch4
dy1:fwrpm
dy1:bxtik4
dy1:vectr
dy1:draw4
dy1:help4
chdr
phil
clib//
```

```
#include <stdio.h>

help()
{
printf("*** Help list for Mark II data acquisition program ***\n");
printf("\n");
printf("    Legal options are:\n");
printf("\n");
printf("    se = enter set mode\n");
printf("    da = take data\n");
printf("    lo = look at maximum cylinder pressure\n");
printf("    wr = write raw data in a file\n");
printf("    dr = draw any of the four quantities on screen\n");
printf("    er = erase the screen\n");
printf("    he = print this list\n");
printf("    qu = quit main program\n");
}

sehelp()
{
printf("Help list for SET, legal commands are:\n");
printf("\n");
printf("rp = set rpm\n");
printf("cr = set compression ratio\n");
printf("cf = set calibration factors\n");
printf("df = set data file name\n");
printf("da = set date\n");
printf ("pr = set the supercharge pressure in atm abs\n");
printf("he = prints this list\n");
printf("en = returns to main level\n");
printf("\n");
}

drhelp()
{
printf ("bo = draw box and ticks\n");
printf ("pr = draw cylinder pressure (80 atm f.s.)\n");
printf ("in = draw injection line pressure (400 atm f.s.)\n");
printf ("nd = draw needle lift (0.8 mm f.s.)\n");
printf ("lu = draw luminosity (arbitrary units)");
printf ("er = erase screen\n");
printf ("he = print this list\n");
printf ("en = return to main level commands\n");
}
```

APPENDIX B.

inject.c

```
#include <stdio.h>

#define   SAMPLES   2400          /* Number of data points to take. */
#define   ADCONV    0.001221      /* Volts per integer count. */
#define   CALFAC1   100.          /* Atm per volt for inj line charge amp.*/
#define   CALFAC2   0.254         /* Millimeters per volt for proximity
                                     detector. */
#define   FREQ      0.025         /* The clock frequency is 40 kHz making
                                     the conversion between clock
                                     ticks and 0.025 msec. */
#define   XPLOT     400           /* The number of data points plotted. */

int adconv[2500] = 0, event[10] = 0;

main()
{
        int rflev1, rflev2, ijsave;
        char dfile [15];
        FILE *fopen(), *fp, *fq;
        int ij, cd, de = 'y';

while (de == 'y' || de == 'Y')
        { /* Before taking data initialize variables. */
        rflev1 = 0;     rflev2 = 0;
        ijsave = 0;
        for (ij = 0; ij <= SAMPLES; ij ++)
                adconv [ij] = 0;
        for (ij = 0; ij <= 10; ij++)
                event [ij] = 0;

        /* Take the data. */
        inj (adconv, event);

        /* Find the interesting portion of the data by locating
           the pressure rise.  The A/D board is flaky so the first
           data points can be erroneous so start looking at point 100.*/
        ij = 100;
        while (ij <= 2300 && ijsave == 0)
              { if ((adconv[ij + 20] - adconv [ij]) > 250)
                        ijsave = ij;
                ij++; }
                ijsave = ijsave - 10;
        /* Find reference levels on both channels well before data
           taking begins. */
        rflev1 = (adconv [ijsave - 50] + adconv [ijsave - 48]) / 2;
        rflev2 = (adconv [ijsave - 49] + adconv [ijsave - 47]) / 2;

        /* Draw the data.  (Draw only the first half of written data.) */
        erase();
        if ((fq = fopen("tt:", "w")) == NULL)
                { printf ("File not opened for drawing.\n");
                  exit(0); }
        bxtik (fq);

        for (ij = ijsave; ij <= XPLOT + ijsave; ij = ij + 2)
                drawd (fq, ij, rflev1, ijsave, ijsave + XPLOT / 2);
        for (ij = ijsave + 1; ij <= ijsave + XPLOT; ij = ij + 2)
                drawp (fq, ij, rflev2, ijsave, ijsave + XPLOT / 2);
```

```
        fclose (fq);

printf ("Write results? y or n\n");
scanf ("%s", &cd);
if (cd == 'y' || cd == 'Y')
      { printf ("Data file name for writing results?\n");
        scanf ("%s", dfile);

        if ((fp = fopen (dfile, "w")) == NULL)
                { printf ("File not opened successfully.\n");
                  exit(0);}

        ij = 0;
        while (event[ij] != 0 && ij < 10)
                { fprintf(fp, "# Needle opens at %d, %4.1f msec.\n",
                  event[ij] + SAMPLES - ijsave,
                  (double) ((event[ij] + SAMPLES - ijsave) * FREQ));
                  ij++;
                  fprintf (fp, "# Needle closes at %d,%4.1f msec.\n",
                  event[ij] + SAMPLES - ijsave,
                  (double) ((event[ij] + SAMPLES - ijsave) * FREQ));
                  ij++; }
        fprintf (fp, "#\tTime\tPressure Position\n");
        fprintf (fp, "#\t(msec)\t (atm)\t  (mm)\n");
        for (ij = ijsave; ij <= ijsave + XPLOT; ij = ij + 2)
                fprintf (fp, "\t%5.2f\t%5.1f\t%7.3f\n",
                  ((ij - ijsave) / 40.),
                  (adconv[ij] - rflev1) * ADCONV * CALFAC1,
                  (adconv[ij + 1] - rflev2) * ADCONV * CALFAC2);
        fclose (fp); }
        printf ("Take more data?  y or n\n");
        scanf ("%s", &de);
        }
}
```

```
inj.mac

        .TITLE INJ
        .GLOBL INJ
;
        CKCSR = 170420          ; Clock control status register.
        CKBPR = 170422          ; Buffer/preset register address.
;
        DRCSR = 167710          ; Parallel port status register.
        DRINBUF = 167714        ; Parallel port input address.
;
        ADCSR = 170400          ; A/D status register.
        ADBUF = 170402          ; A/D buffer register.
        DMAWCR = 170404         ; DMA word count register.
        DMACAR = 170406         ; DMA current address register.
;
;
; Inj is the program which collects data for the injection bench
; rig outside of the engine.  It runs in the following way:
;       a.)  The operator enables the signal conditioning box so that
;       a pulse from the inductive pickup on the cam pulley triggers
;       the injection control box.  This pulse is also detected by the
;       ST2 of the clock board on the computer.
;       b.)  Data taking is delayed for 30 msec as the injection occurs
;       on the next revolution.
;       c.) Data taking commences after the delay.
;       d.)  The clock will be run in mode 1 to produce a pulse train.
;       The clock frequency will be 1 MHz.  A clock overflow will occur
;       every 25 counts (-25 will be loaded into the buffer preset reg).
;       e.) Data conversions will be taken at each clock overflow pulse.
;       Two channels will be sampled over the 60 msec test period.
;       Thus, 2400 samples total (1200 on each channel) will be taken.
;       e.)  At bit #1 the needle lift open and close will be detected.
;       Look for a high when it is open and a low when it is closed.
;       The clock count will be read into memory when these things occur.
;       g.)  Similarily, bit #0 will be sampled to detect the inductive
;       pickup pulse.  The needle opening and closing will be judged
;       relative to this marker.
;
INJ:    NOP
        MOV 2(SP), @#DMACAR     ; The starting address for the data
                                ; conversions is passed via the stack.
        MOV 4(SP), R0           ; The address for the array for the event
                                ; timing measurements comes off the stack.
;
        MOV #-300., @#CKBPR     ; The time delay from TDC on the motor and
                                ; when data will be taken is 30.0 msec.
        CLR @#CKCSR             ; Clear clock before setting up:
        BIS #20000, @#CKCSR     ;  -ST2 go enable. (#20000)
        BIS #30, @#CKCSR        ;  -10 kHz clock rate. (#30)
                                ;  -Mode 0 operation. (#0)
;
        CLR @#ADCSR             ; Clear A/D register before setting bits.
        BIS #40, @#ADCSR        ; Set bit for RTC trigger enable.
        BIS #2, @#ADCSR         ; Set bit for DMA enable.
        BIS #10, @#ADCSR        ; Autoincrement mode.
        MOV @#ADBUF, R2         ; Read buffer to clear it out.
        MOV #-2400., @#DMAWCR   ; Take 2400 data points, 1200 on each chan.
;
DELAY:TSTB @#CKCSR              ; Test clock overflow for end of delay
```

```
                                    ; period.
        BPL DELAY                   ; If not, keep looping.
        CLR @#CKCSR                 ; Reset clock for the following:
        BIS #2, @#CKCSR             ; Mode 1 operation.
        BIS #10, @#CKCSR            ; 1 MHz rate.
        MOV #-25., @#CKBPR          ; Only every 25th clock pulse will cause
                                    ; an A/D conversion.
        BIS #1, @#CKCSR             ; Turn on the clock.
;
OPEN:   TST @#DMAWCR                ; Test for A/D overflow.
        BPL EXIT                    ; If so, exit.
        BIT #2, @#DRINBUF           ; Look for a low on the needle lift
                                    ; transducer.
        BEQ OPEN                    ; If not, keep looping.
        MOV @#DMAWCR, (R0)+         ; If so, write the address into the array.
                                    ; Then, increment the address.
;
CLOSE:TST @#DMAWCR                  ; Check again for A/D done.
        BPL EXIT                    ; If so, exit.
        BIT #2, @#DRINBUF           ; Look for a high on the needle lift
                                    ; detector.
        BNE CLOSE                   ; If not, keep looping.
        MOV @#DMAWCR, (R0)+         ; If so, store the timing.
;
OPENX:TST @#DMAWCR                  ; Check again for A/D done.
        BPL EXIT                    ; If so, exit.
        BIT #2, @#DRINBUF           ; Look for a low on the needle lift
                                    ; detector.  Looking for bounce.
        BEQ OPENX                   ; If not, keep looping.
        MOV @#DMAWCR, (R0)+         ; If so, write the address into
                                    ; the array.
;
CLOSEX:TST @#DMAWCR                 ; Check again for A/D done.
        BPL EXIT                    ; If so, exit.
        BIT #2, @#DRINBUF           ; Look for a high on the lift detector.
        BNE CLOSEX                  ; if not, keep looping.
        MOV @#DMAWCR, (R0)+         ; If so, store the timing.
        BR OPENX                    ; Look for more bounces.
;
EXIT:   NOP
        CLR @#ADCSR                 ; Turn off A/D.
        CLR @#CKCSR                 ; Turn off clock.
        RTS PC
        .END
```

bxtik.c

```
#include <stdio.h>

#define x0 200
#define y0 150
#define XTIK 4
#define YTIK 15

bxtik(fp)

FILE *fp;

{
int i, x, y;

fprintf(fp,"\032\r");                    /* clear screen */
vector(fp,y0,x0,y0,x0+700);              /* bottom */
vector(fp,y0,x0+700,y0+600,x0+700);      /* RHS    */
vector(fp,y0+600,x0+700,y0+600,x0);      /* top    */
vector(fp,y0+600,x0,y0,x0);              /* LHS    */

/* Now draw the ticks. */

for (i = 1; i < XTIK; i++)
        {
        x = x0 + i * 700 / XTIK;
        vector(fp,y0,x,y0+15,x);
        }

for (i = 1; i < YTIK; i ++)              /* y-axis ticks */
        {
        y = y0 + i * 600 / YTIK;
        vector(fp,y,x0,y,x0+10);
        if (i == 5 || i == 10)
                vector (fp, y, x0, y, x0 + 20);
        }
}

erase()
{
FILE *fopen(), *fp;

if ((fp = fopen ("tt:", "w")) == NULL)
        { printf ("Open file error.\n");
          return; }
fprintf (fp, "\035\033\014\036\030\r");
fclose(fp);
}
```

indrw.c

```
#include <stdio.h>

#define X0      200             /* X graph offset. */
#define Y0      150             /* Y graph offset. */
#define XMAX    700.            /* X graph size. */
#define YMAX    700.            /* Y graph size. */

extern int adconv[];

drawd (fp, ij, rflev1, xmin, xmax)

FILE *fp;
int ij, rflev1, xmin, xmax;

{               /* draw pressure data */
double x1, x2, y1, y2, xrange, yrange;

xrange = xmax - xmin;
yrange = 2458.;
x1 = (int) ((ij - xmin) / 2);
x2 = (int) ((ij - xmin) / 2) + 1;
y1 = adconv [ij] - rflev1;
y2 = adconv [ij + 2] - rflev1;
vector (fp, Y0 + (int) (YMAX * y1 / yrange),
        X0 + (int) (XMAX * x1 / xrange),
        Y0 + (int) (YMAX * y2 / yrange),
        X0 + (int) (XMAX * x2 / xrange));
}

drawp (fp, ij, rflev2, xmin, xmax)

FILE *fp;
int ij, rflev2, xmin, xmax;

{       /* draw needle lift data */
double x1, x2, y1, y2, xrange, yrange;

xrange = xmax - xmin;
yrange = 4840.;
x1 = (int) ((ij - xmin) / 2);
x2 = (int) ((ij - xmin) / 2) + 1;
y1 = adconv [ij] - rflev2;
y2 = adconv [ij + 2] - rflev2;
vector (fp, Y0 + (int) ((YMAX * y1) / yrange),
        X0 + (int) ((XMAX * x1) / xrange),
        Y0 + (int) ((YMAX * y2) / yrange),
        X0 + (int) ((XMAX * x2) / xrange));
}
```

vectr.c

```
#include <stdio.h>

vector(fp,y1,x1,y2,x2)

FILE *fp;
int y1,x1,y2,x2;

{
```

```
putc('\035',fp);
putc( y1 / 040 +  040 ,fp);
putc( y1 % 040 + 0140 ,fp);
putc( x1 / 040 +  040 ,fp);
putc( x1 % 040 + 0100 ,fp);
putc( y2 / 040 +  040 ,fp);
putc( y2 % 040 + 0140 ,fp);
putc( x2 / 040 +  040 ,fp);
putc( x2 % 040 + 0100 ,fp);
fprintf(fp,"\037\030\r");
}
```

```
inject.tkb

r link
dy1:inject=dy1:inject/B:4000,//
dy1:inj
dy1:bxtik
dy1:vectr
dy1:indrw
chdr
phil
clib//
```

LAWRENCE BERKELEY LABORATORY
TECHNICAL INFORMATION DEPARTMENT
UNIVERSITY OF CALIFORNIA
BERKELEY, CALIFORNIA 94720